Alma Mater Studiorum – Università di Bologna

DOTTORATO DI RICERCA IN

Scienze Biochimiche e Biotecnologiche

Ciclo XXVII

Settore Concorsuale di afferenza: 05/E1

Settore Scientifico disciplinare: BIO/10

ROLE OF (R)-9-HYDROXYSTEARIC ACID IN ZEBRAFISH DEVELOPMENT

Presentata da: Federica Naso

Coordinatore Dottorato	**Relatore**
Chiar.mo Prof. Santi Mario Spampinato	Chiar.ma Prof.ssa Natalia Calonghi

Esame finale anno 2014/2015

TABLE OF CONTENTS

1   Abstract

9-hydroxystearic acid (9-HSA) belongs to a class of lipid peroxidation products identified in several human and murine cell lines. These products are greatly diminished in tumors compared to normal tissues and their amount is inversely correlated with the malignancy of the tumor.

 9-HSA activity has been tested in cancer cell lines, where it showed to act as a histone deacetylase 1 (HDAC1) inhibitor. In particular, in a colon cancer cell line (HT29), its administration resulted in an inhibition of proliferation together with an induction of differentiation.

In this thesis the effect of (R)-9-hydroxystearic acid has been tested in vivo on cell proliferation and differentiation processes, in the early stages of zebrafish development.

The final aim of this work was to elucidate the role of (R)-9-HSA in the control of cell differentiation and proliferation during normal development, in order to better understand its molecular control of cancerogenesis.

The molecule has been administered via injection in the yolk of zebrafish embryos. The analysis of the histone acetylation pattern showed a hyperacetilation of histone H4 after treatment with the molecule, as detectable in HDAC1 mutants.

(R)-9-HSA was also demonstrated to interfere with the signaling pathways that regulate proliferation and differentiation in zebrafish retina and hindbrain. This resulted in a reduction of proliferation in the hindbrain at 24 hours post injection (hpi), and in a hyperproliferation at 48 and 72 hpi in the retina, with a concomitant inhibition of differentiation.

Finally, (R)-9-HSA effects were evident on proliferation of stem cell located in the ciliary marginal zone (CMZ) of the retina. The presence of

ROS and 4-hydroxynoneal in the CMZ of wild-type embryos supports the hypothesis that oxidative stress could regulate stem cells fate in zebrafish retina.

The data collected during this project have strengthened our knowledge about (R)-9-HSA giving a scenario of its activity *in vivo* whereby zebrafish turned out to be a reliable and useful model to investigate (R)-9-HSA effects in a whole organism. In addition, the data on the oxidative state of retinal stem cells suggested that the regulation of reactive oxygen species generation could be an important factor to influence stem cell fate during development, but this hypothesis has to be deeply investigated in the future.

2 Introduction

2.1 Oxidative stress

Oxidative stress is the result of an imbalance between the endogenous physiological production of reactive oxygen species (ROS) and the counteraction of the antioxidant defense system.

ROS are produced inside the cell during normal energy metabolism as will be thoroughly discussed in paragraph 2.1.1. In normal conditions their production and consumption are balanced due to the activity of enzymatic and non-enzymatic scavengers, so that they can to act as secondary messengers in cell signaling.

The antioxidant system is for the most part constituted by enzymatic scavengers such as: superoxide dismutase, catalase, and glutathione peroxidase. All the antioxidant enzymes act by removing free radical intermediates, and therefore by inhibiting oxidation reactions. SOD converts superoxide to hydrogen peroxidase, catalase and glutathione peroxidase convert hydrogen peroxidase to water.

In addition to these enzymatic antioxidants, there are other non-enzymatic molecules with scavenger properties, such as ascorbate, flavonoids and carotenoids.

The imbalance between ROS production and the antioxidant defense results in an excessive intracellular amount of these highly reactive molecular species that can easily react with proteins, lipids, and DNA [1].

This ROS mediated modifications of cellular structures have been implicated in several pathological states, such as carcinogenesis, neurodegenereation, atherosclerosis, diabetes and aging [2,3].
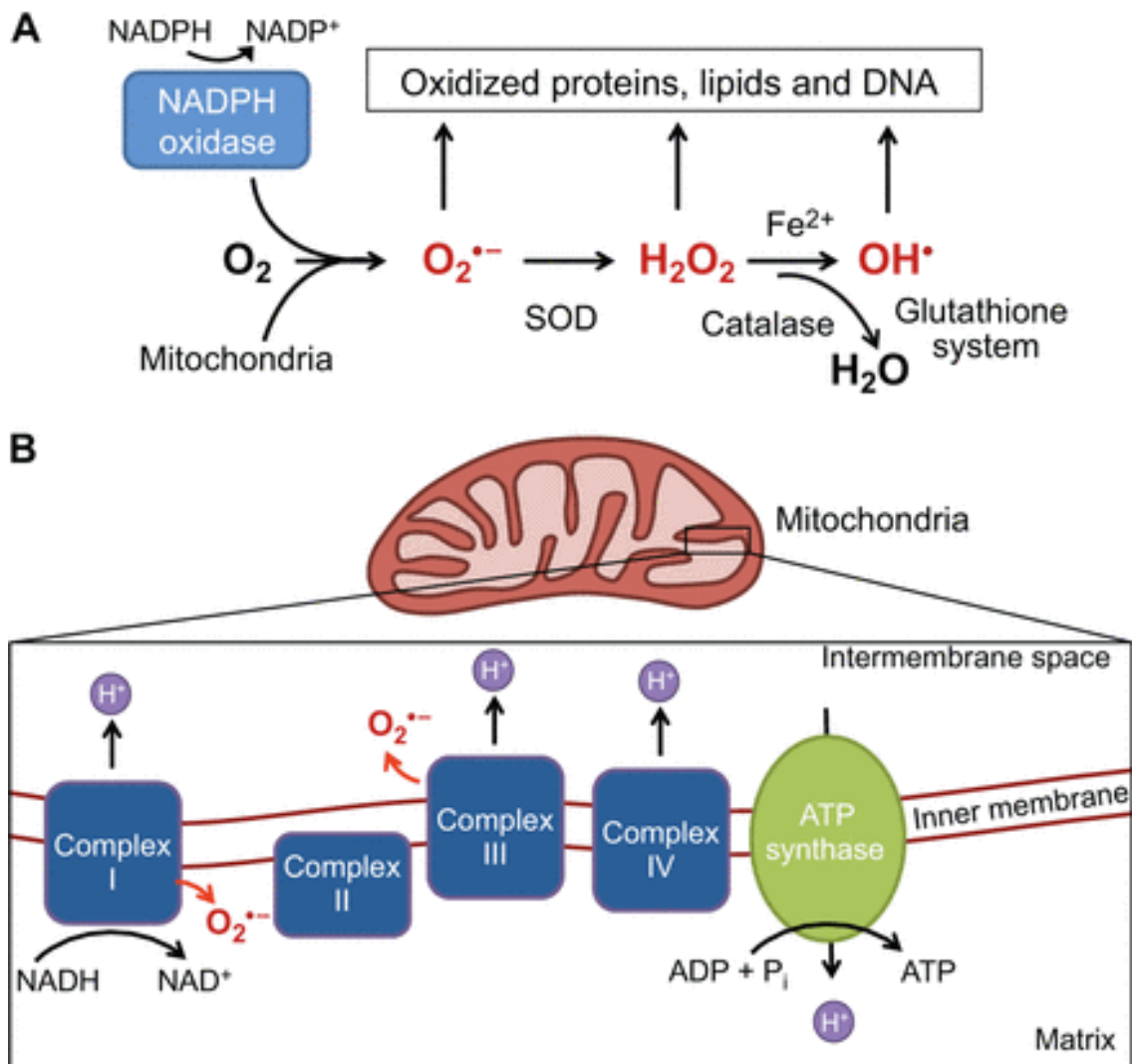
Fig. 2.1 ROS generation and scavenging. (A) Reactive oxygen species (ROS) include superoxide ($O_2^{\cdot-}$), hydrogen peroxide (H_2O_2) and the highly reactive hydroxyl radical ($OH^{\cdot}$). $O_2^{\cdot-}$ is generated from complexes I and III (shown in B) or through the oxidation of NADPH by NADPH oxidases. Figure has been reproduced from [4].

2.1.1 Reactive oxygen species

With the terminology reactive oxygen species (ROS) we usually refer to chemical species, such as superoxide anion (O_2^-), hydrogen peroxide (H_2O_2), and hydroxyl radical ($\bullet HO$) that contain radical or non-radical oxygen. [4]

The majority of the endogenously generated ROS is derived from the mitochondria, during oxidative phosphorylation.

Two are the complexes responsible for the production of ROS during mitochondrial respiration: complex I (NADH dehydrogenase), and complex III (ubiquinone-cytochrome c reductase) [1].

The electron transport chain promotes the ATP synthesis trough the generation of a proton motive force at the level of the mitochondrial membrane. The proton motive force is generated by the presence of a membrane potential at the interphase of mitochondrial membranes; this potential is coupled with the extrusion of protons (H+) generated from NADH in a series of redox reactions and protons of the matrix.
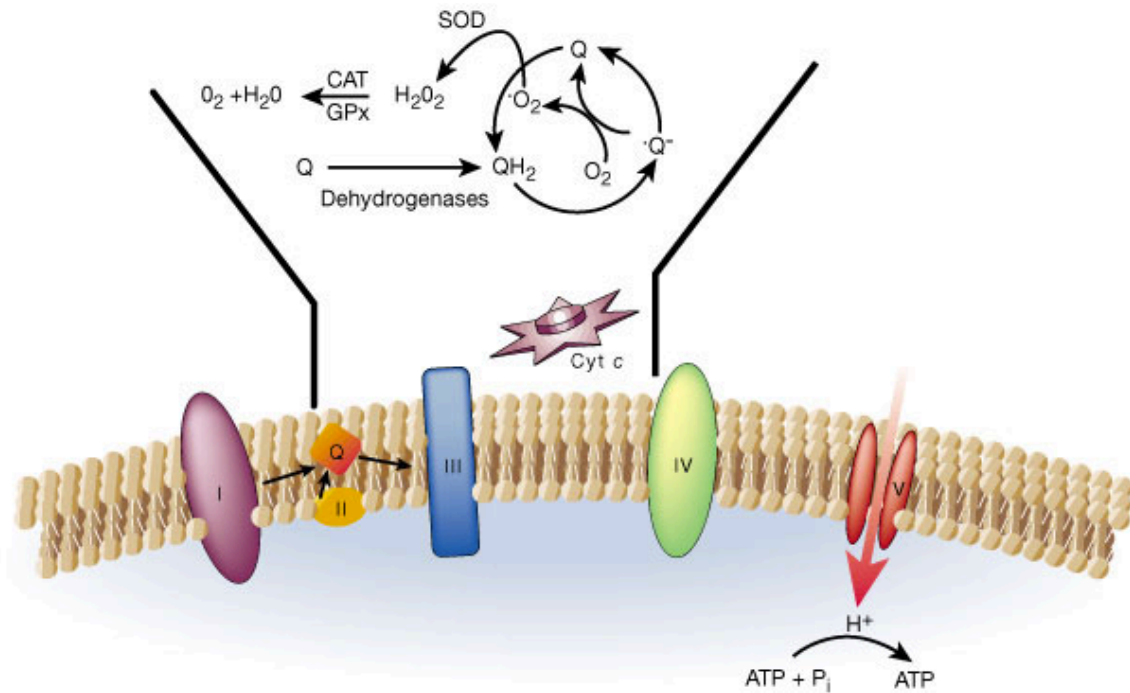
Fig. 2.1.1 Mitochondrial ROS production from complex III. Figure has been reproduced from [1].

Another source of ROS in the mitochondria is the membrane-bound protein NADPH oxidase (NOX) that consumes NADPH to generate O_2^- and H_2O_2.

Differently from the established belief that ROS are just harmful byproducts of our metabolism, it is now demonstrated their involvement, as second messengers, in the signal transduction in different signalling pathway [5,6].

Among the signaling pathways that can be activated by the formation of oxidants are: signal-regulated kinase (ERK), c-Jun amino-terminal kinase (JNK), p38 mitogen-activated protein kinase (MAPK), the phosphoinositide 3-kinase (PI (3) K/akt pathway, the nuclear factor (NF)-kB signaling system, p53 activation and the heat shock response [1].
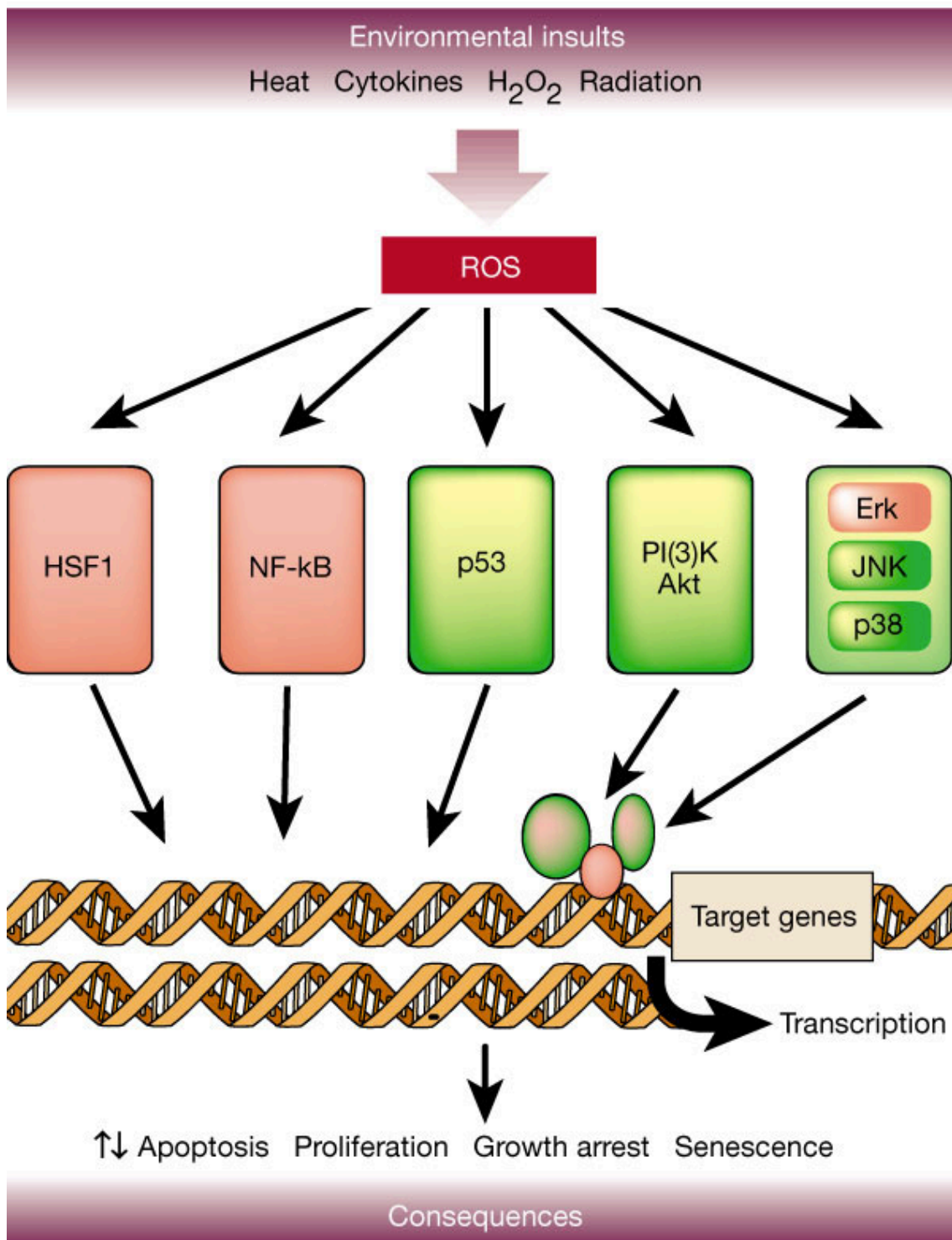
Fig. 2.1.1-2 Signalling pathways activated by the formation of oxidants. Figure has been reproduced from [1].

2.1.2 Lipid peroxidation

Lipid peroxidation is a process of deterioration of unsaturated fatty acids that is induced by oxygen in the presence of initiators such as free radicals or metal ions. Lipid peroxidation results in oxidation of plasmatic lipoproteins, that can cause the formation of atherosclerotic plaques [7], and moreover can damage biological membranes causing fluidity and permeability alteration of the membrane.

Lipid peroxidation takes place in three different steps: initiation, propagation and termination. During the first step, a hydrogen atom is lost by the allylic methylene group conjugated with a double bond in the unsaturated fatty acid chain (LH), as a consequence of the action of an hydroxyl radical (ROO*), and a radical is formed (L*) on the corresponding carbon atom. During the propagation step, radicals quickly react with molecular oxygen, forming peroxy radicals (LOO*), which in turn subtract a hydrogen atom from another molecule of unsaturated fatty acid to form a hydroperoxide (LOOH) and another radical. The propagation reactions leads to the formation of a kinetic chain in which for each radical ROO • generated are consumed more molecules of LH and, for each molecule of LH which reacts one molecule of oxygen is lost. In the termination phase, the free radicals produced during the process react with each other and give rise to inactive non-radical products [8].

If an antioxidant is added to the system (IH), during the propagation phase of lipid peroxidation, this reacts with the peroxy radicals by interrupting the radical chain. An antioxidant, according to its characteristics, is able to block one or more radical chains donating hydrogen atoms, with the consequent formation of free radicals (I •) relatively stable.

Lipid peroxidation products have been extensively studied as modulators of DNA synthesis as well as of cell proliferation. In particular, a growing

11

number of experimental data concerning the involvement of hydroperoxy-
and hydroxy-derivatives of polyunsaturated fatty acids in the control of cell
proliferation and other cellular responses have been published.
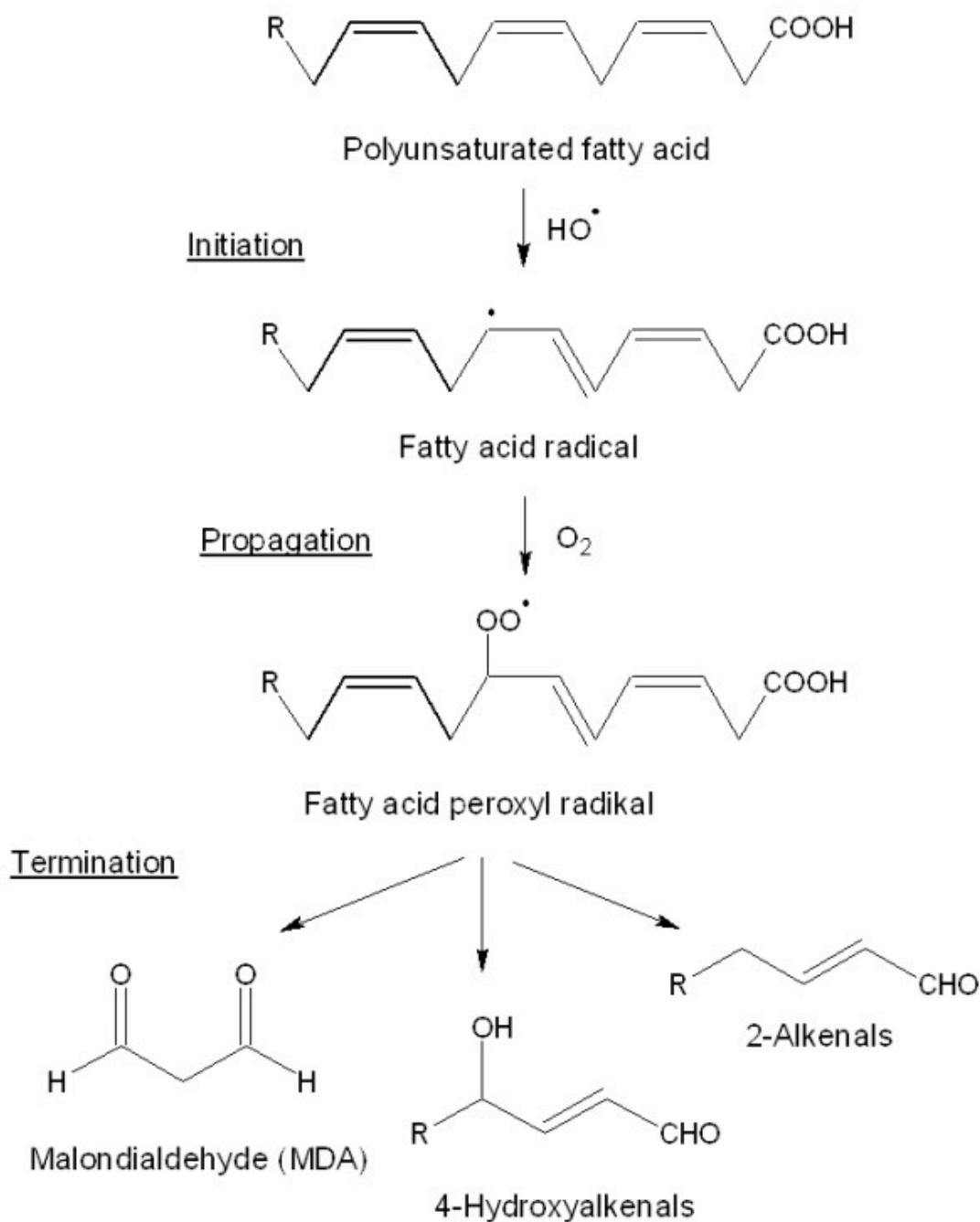
Fig.1.1.2 Steps in lipid peroxidation process. Figure has been reproduced from [122].

2.1.3 Oxidative stress in cancer cells and adult stem cells.

An altered balance in ROS homeostasis has been found in many types of cancer cells, often together with altered levels of antioxidant enzymes. [9] Low levels of ROS are generally associated with promotion of cell proliferation and differentiation [10], intermediate levels of ROS result in transient or permanent cell cycle arrest [11] whereas an excessive increase in ROS production can cause oxidative damages, as that observed in many solid tumors that show increased levels of damage products such as oxidized DNA bases [12].

For these reasons the modulation of ROS levels is important for the maintenance of a normal cell growth and can be used to either stimulate an abnormal cancer cell growth or to kill tumor cells.

ROS can be produced by growth factors and cytokines in order to exert their biological effects in cancer, or by inflammatory cells in order to lead to oxidative stress-induced cell death [13,14,15,16].

At sub-lethal concentrations ROS can act as primary messengers and can regulate the cell cycle progression. Previous studies show that ROS cause cell cycle arrest together with an upregulation of p53 expression in different types of tumors [17,18].

Apparently the experimental evidence on the role of ROS in cancer progress is contradictory, resulting in cell proliferation and growth arrest, but it has to be considered that cell response can differ due to the molecular background, the concentration of individual ROS species and the antioxidant concentration [19].
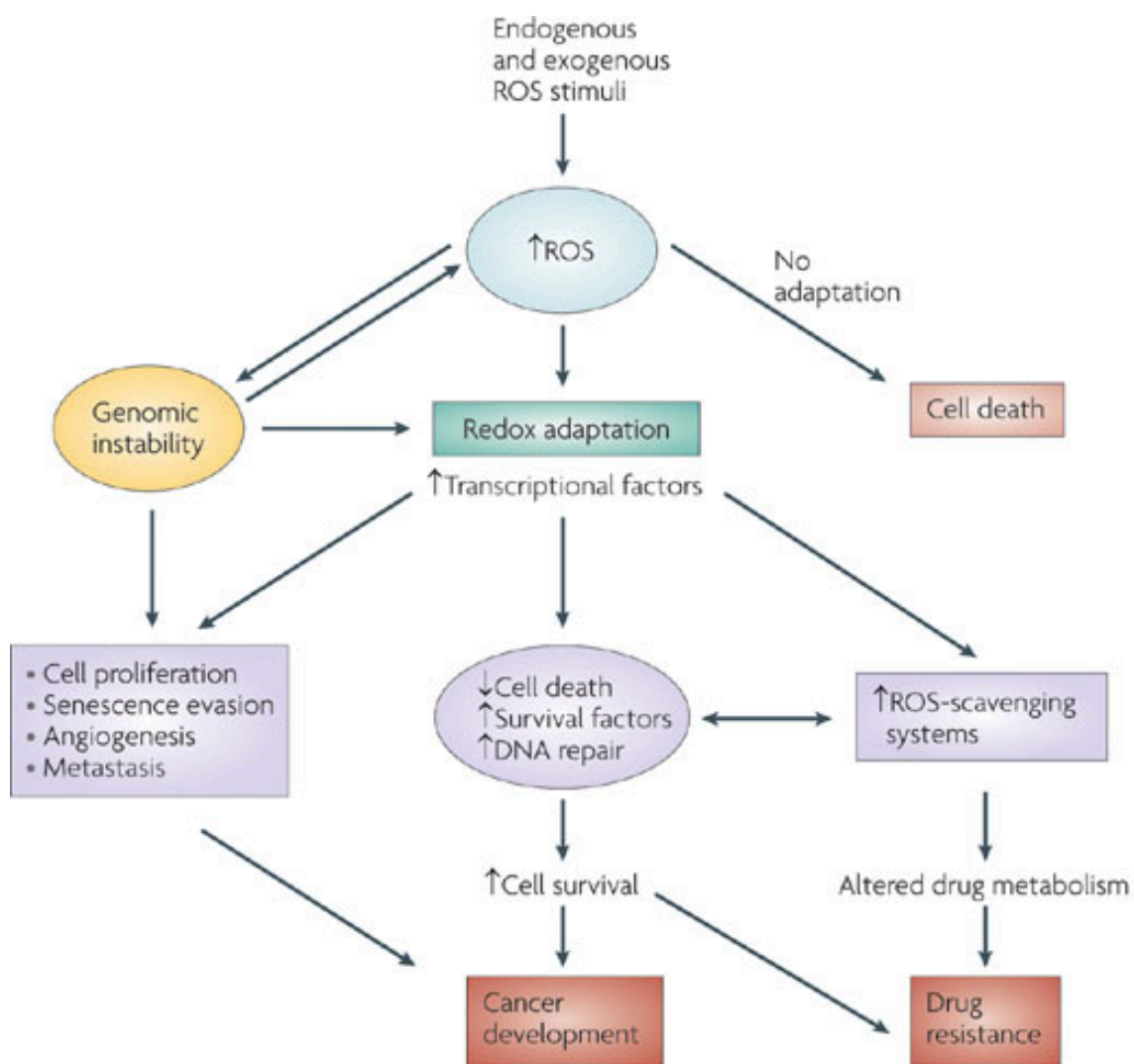
Fig. 2.1.3. Adaptation to oxidative stress in cancer development and drug resistance. Figure has been reproduced from [123].

The manipulation of energetic metabolism can have a strong impact in the regulation of stem cells state [20].

In this context ROS can be considered signaling molecules that can take part in the crosstalk between metabolism and stem cell fate [4].

In embryonic stem cells (ESCs) an increase in ROS levels results in a transient arrest of the cell cycle in G2/M phase while a continuous exposure to ROS causes apoptosis [21].

ESCs energetic metabolism is for the most part based on glycolysis and the penthose phosphate pathway that quickly provide ATP and precursors for nucleotide biosynthesis [22,23].

If a forced activation of oxidative phosphorylation is caused from the outside, this results in loss of stem cells properties and increased differentiation or apoptosis [4,24].

In adult stem cells, as hematopoietic stem cells (HSCs), low levels of ROS have been found, according with the metabolic state of these cells that is based on aerobic glycolysis. [25]

The dependence on glycolysis of adult stem cells can be due to their usual location in hypoxic niches and the low energy requirements they need to maintain their quiescent state. [26]

On the contrary, it has been shown that an increase in ROS, which are mostly produced from mitochondrial respiration, results in the loss of stem cells maintenance and quiescence. [27]

2.2 9-hydroxystearic acid

9-hydroxystearic acid (9-HSA) belongs to the class of the endogenous lipid peroxidation products, and has been identified in epithelial cells, normal human embryonic intestine cells, and human colon adenocarcinoma. [28,29,30,31]

The content of lipid peroxidation short and long chain derivatives as well as the antioxidant defenses was found to be decreased in tumor as compared to normal tissue, and their amount is inversely correlated with tumor growth in cancer cells.

Therefore the hypothesis is that since they are greatly diminished in tumors, they become unable to exert their normal controlling function on cell division.

9-HSA administration, at micromolar concentration, to a human colon cancer cell line (HT29) results in a strong inhibition of cell proliferation and in a change in the cellular phenotype towards a more benign one, together with an induction of $p21^{WAF1}$ expression, in a p53 independent manner.

9-HSA nuclear localization has been detected at the maximal level six hours after administration. The analysis of histone acetylation at this time shows an increase of histone H4 hyperacetilation, with modification on Lys-5 and Lys-12. The nuclear localization and the other observed effects, suggest a correlation with the biological activities of the HDAC inhibitor.

Subsequent studies clarified that 9-HSA effects are related to the inhibition of histone deacetylase 1 (HDAC1) activity through a direct fatty acid/enzyme interaction, which has been demonstrated by using an in silico docking procedure [32]. Both the two enantiomeric forms of 9-HSA interact with the catalytic site of Hdac1, thereby blocking substrate access, but the interaction of the (R) enantiomeric form is more stable with interaction energy of − 8.45 kcal/mol compared to − 1.97 kcal/mol of the (S) enantiomeric form. [33]

The two enantiomeric forms of 9-HSA also showed different inhibition properties on Hdac1 enzymatic activity and a different grade of inhibition of cell growth, with a more pronunciated effect of the (R) enantiomer.
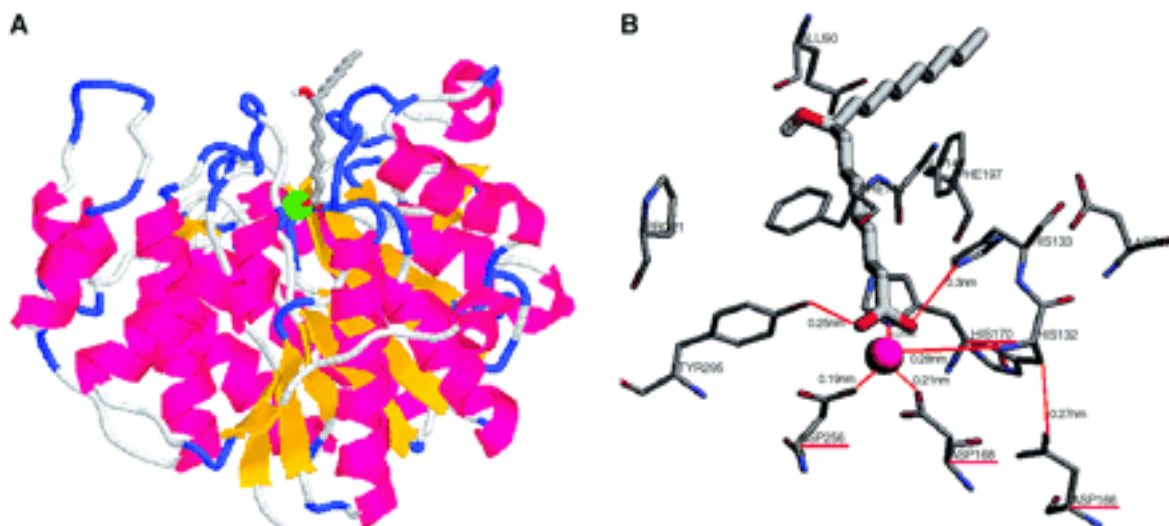
Fig. 2.2. Docking of 9-HSA to zinc-dependent human HDAC1. Figure has been reproduced from [33].

The activity of 9-HSA has been evaluated on protein expression of two fundamental cell cycle regulators, p21 and cyclinD1. P21 belongs to the Cip/Kip class of cyclin dependent kinases inhibitors (CKI), acting by the inhibition of cyclin CDK2/A, cyclin CDK1/B, cyclin CDK2/E, and cyclin CDK4/D.

The cyclin dependent kinases are a family of proteins that regulate the progression of the cells through the different phases of the cell cycle, and are composed of a catalytic and a regulatory subunit. Their activity is regulated by the inhibition by the CKIs and by cyclic phosphorylation and dephosphorylation of the catalytic subunit, which result in the subsequent degradation of cyclin subunits.

The treatment with (R)-9-HSA results in increased levels of p21 with respect to the control, and in decreased levels of cyclinD1; this effect was only observed with the (R) enantiomeric form. At a transcriptional level, the expression of cyclinD1 is not significantly influenced either by R-9 or S-9, while p21WAF1 transcription is significantly upregulated by R-9.

17

Finally the treatment with (R)-9-HSA causes the dissociation of the cyclinD1/HDAC1 nuclear complex, as observed by confocal microscopy analysis. [34]

2.3 Histone deacetylases family and their function

Histone deacetylases can be divided in four classes.

The class I consists of HDAC 1, 2, 3, and 8, and shows high homology with the yeast enzyme Rpd3. These enzymes are ubiquitously expressed, but are mostly present in the nucleus. Their structure consists of a conserved deacetylase domain with short amino and carboxy-terminal extensions. HDAC1 and HDAC2 have been found together as part of repressive complexes such as sin3, NuRD and CoREST, while HDAC3 has been found in different complexes, as N-CoR-SMRT [35].

The class II consists of IIa and IIb.

- Class IIa includes HDAC4, 5, 7 and 9. Differently from others HDACs, class IIa HDACs are expressed in restricted tissues, as muscles, heart or brain. The enzymes of this class present binding site, for the interaction with proteins and transcription factors such as MEF2, localized on large N-terminal extensions.

- Class IIb includes HDAC6 and HDAC10. The first is mainly localized in the cytoplasm, has two deacetylase domains and a C-terminal zinc finger, and can directly deacetylate cytoskeletal proteins and transmembrane proteins. HDAC10 on the contrary has not been well characterized [36].

- class IV includes just HDAC11. This enzyme has a high structural homology with class I and II, in particular regarding the deacetylase domain. HDAC11 is localized in brain, muscle, heart, but its role is still not well clarified.
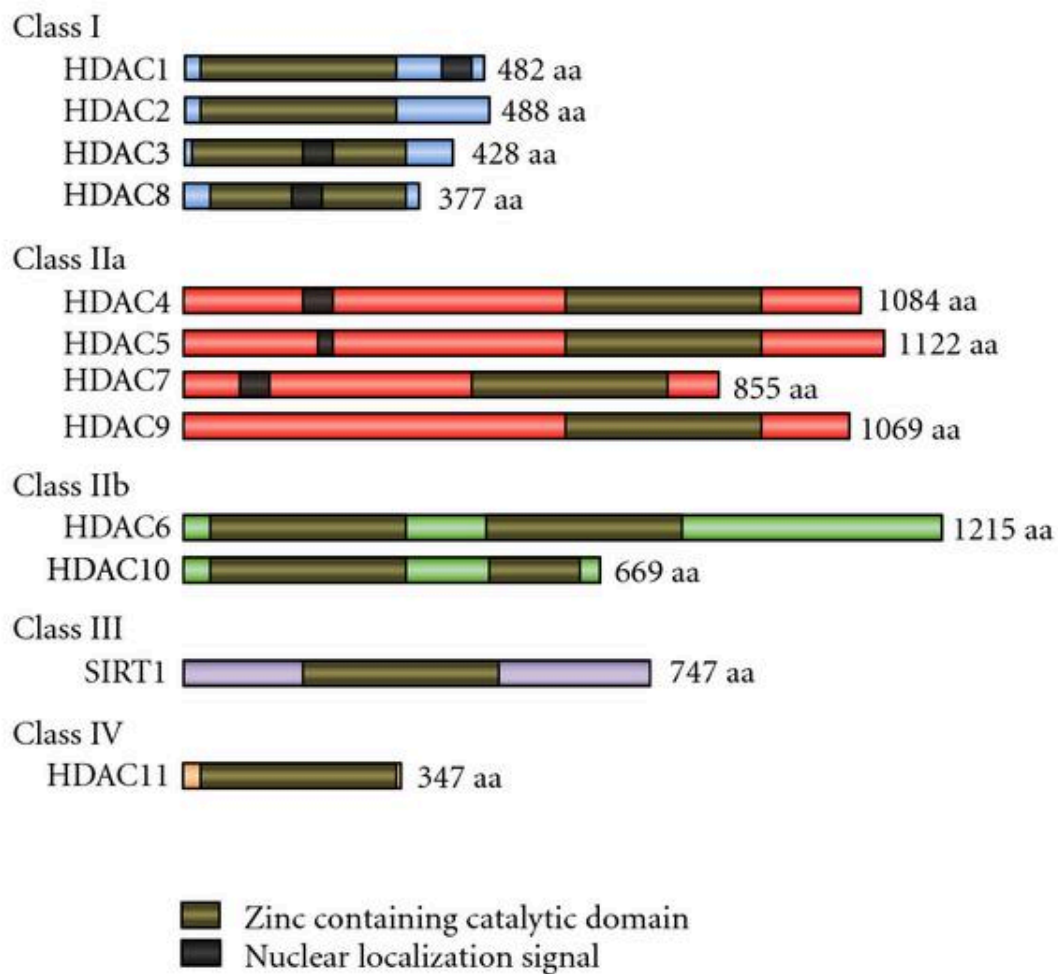
Fig.2.3 Schematic representation of histone deacetylase families. Figure has been reproduced from: http://www.hindawi.com/journals/bmri/2011/475641/fig1/.

HDACs structure consists of an active site at the bottom of the channel, which contains a zinc atom, and a rim that delimits the channel and that represent a pocket for the substrate.

HDACs act by removing acetyl groups from histone lysine tails, thus increasing the positive charge of histone and facilitating high-affinity

binding with DNA, that result in a condensed chromatin structure, and an inhibition of transcription.

To exert their activity on gene transcription, HDACs are recruited to target sequences through the association with transcriptional activators and repressors, or the incorporation in transcriptional complexes. Although histone deacetylation is generally associated to gene silencing, new evidences suggest that HDACs can activate certain genes as already observed in yeast, where the deletion of HDAC1 and 2 homologue, Rpd3, results in in repression of transcription.
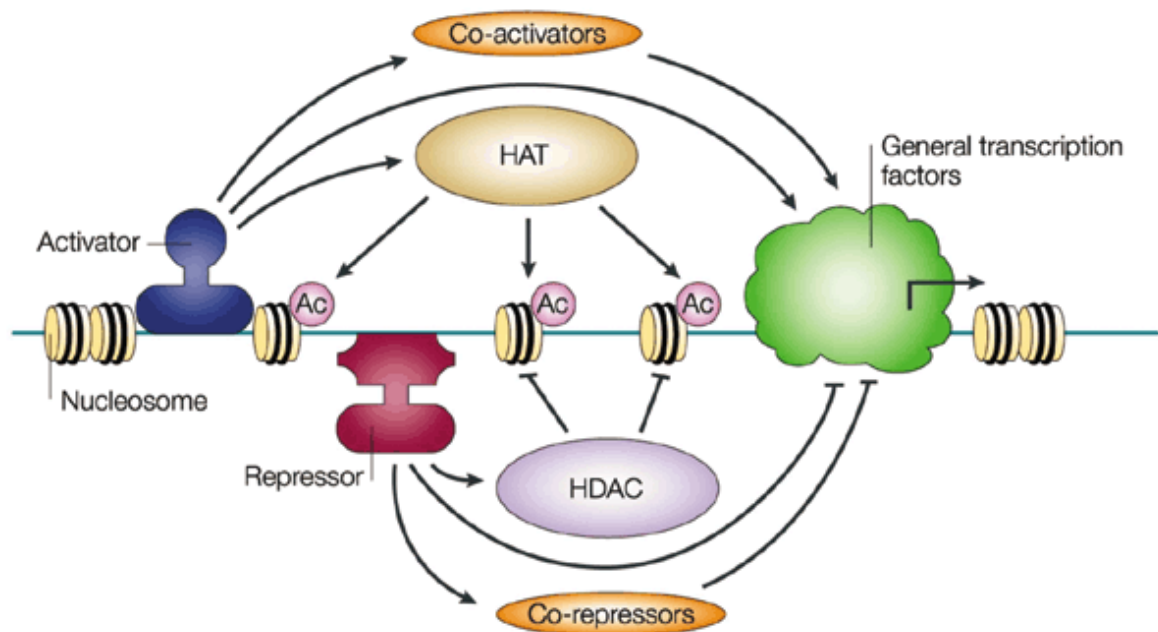
Fig. 2.3-2 The role of histone deacetylase (HDAC) and histone acetyl transferases (HAT) in the regulation of gene transcription. Figure has been reproduced from [124].

Besides affecting gene transcription, HDACs have been also found to interact with different non-histone proteins such as transcription factors and co-regulators, through post-translational modification. [37]

HDACs play important regulation roles in cancer and development.

Focusing on the role in cancer, previous studies showed an aberrant expression of individual HDACs in different tumors, for example of HDAC1 in colon, prostate and breast tumor [38,39,40]. These studies suggest that altered expressions or mutations of gene encoding the enzymes HAT and HDAC could result in an abnormal transcription of genes involved in differentiation and apoptotic processes and could induce proliferation of undifferentiated cells and give rise to tumors.

An example is the regulation of the expression of the cyclin-dependent kinase inhibitor p21WAF1. P21 is inactivated by hypoacetylation of the promoter, and the treatment with HDAC inhibitor leads to an increase in both the acetylation of the promoter and gene expression, together with the inhibition of tumor-cell growth [40].

Also the deacetylation of non-histone proteins has a role in the HDACs regulation of processes in cancer. For example, HDAC1 can deacetylate the tumor suppressor p53, while p53 acetylation is required to promote protein stability and activation [41].

During normal development HDAC1 is required for a proper growth in mice, where its silencing results in proliferation defects and general growth retardation. In zebrafish the deletion of HDAC1 results in skeletal and neuronal defects. In this model this seems to be correlated with the regulation of Wnt signaling pathway [42].

2.3.1 HDAC inhibitors

The chemical components of this class of molecules derive from both natural and synthetic sources. They are able to inhibit HDACs of class I, II and IV, and can be divided in chemical classes as hydroxamic acid derivatives, carboxylates, benzamides, and cyclic peptides.

All HDAC inhibitors contain (I) a metal-binding domain (ZnC), which is able to chelate Zn^{2+} in the active site of the enzyme; (II) a linker domain, which occupies the enzymatic channel, preventing the binding of the substrate; (III) a surface domain which takes contact with the rim.

The two most known HDAC inhibitors (HDACi) are trichostatin A (TSA) and suberoylanilide hydroxamic acid (SAHA), that act by inhibiting the enzymatic activity of all isoforms except class IIa HDACs.

Regarding the epigenetic mechanism of action of HDACi, has to be considered that the inhibition of deacetyation is not always correlated to an upregulation of gene expression, since acetylation is not the only post-translational modifications that occurs, the ratio of upregulated to downregulated genes being approximately 1:1.

Moreover has to be considered that chromatin is not the only target of HDACi action. Other targets can be transcription factors and proteins and this can result in indirect transcriptional effects, or can lead to alterations in DNA repair processes with increased accumulation of DNA damage in the more sensitive cells [43,44].

HDAC pharmacologic inhibitors are used in the therapy of a broad range of diseases: they induce growth arrest, differentiation or apoptosis.

The mechanisms responsible for the effect of HDAC inhibitors on cancer cells have not yet been completely understood: they comprehend changes in gene transcription, production of reactive oxygen species, induction of cell-cycle arrest [44].

HDACs inhibitors are used in the therapy of different types of cancer. Cancer cells indeed exhibit a high level expression of HDAC enzymes and a consequent hypoacetylation of histones, as observed in lymphomas and colon adenocarcinoma. Moreover previous data suggest that transformed cells are more sensitive to HDACi-induced apoptosis compared to normal cells.

As consequence of these findings several HDAC inhibitors are now used in cancer therapies, e.g. trichostatin A and vorinostat [45].

Besides their role in cancer therapy, HDACi have also other therapeutic applications in nonmalignant diseases, as modulators of inflammatory and immune response. Some of these molecules are in preclinical studies for the therapy of neurodegenerative diseases, Huntington-like syndrome, and other are able to modulate stem cell survival in vitro [46].

2.4 9-HSA in vivo characterization: strategy

In order to characterize the mechanism of action of 9-HSA in vivo, was chose the zebrafish model.

Zebrafish has been introduced as a model for developmental genetics by George Streisinger at the University of Oregon in the early 1980s [47].

Several are the advantages of zebrafish over mammalin models, like its ex utero development, its rapid development and its optical transparency, but all these characteristics will be describe in deep in paragraph 2.4.1.

Besides the general features that make this model suitable in several research fields, a further advantage that renders zebrafish suitable for our study is the high identity of sequence between zebrafish and human HDAC1 (Fig. 2.4).

Furthermore the role of histone deacetylation in zebrafish development has been deeply investigated. Studies on HDAC1 mutants, morphants and

inhibitors all showed increased in global histone acetylation and severe phenotypes, which are in several cases more severe in *hdac1* morphants, suggesting that both maternally and zygotically provided Hdac1 contributes to embryonic development [48, 49, 50, 51, 52, 53, 54].

The combination of these features makes it the most suitable model for the characterization of the mechanism of action of 9-HSA in vivo, in order to shed some light on the possible involvement of the molecule in the control of cell proliferation and differentiation during normal development.

MALSSQGTKKKVCYYYDGDVGNYYYGQGHPMKP

HRIRMTHNLLLNYGLYRKMEIYRPHKANAEEMT

KYHSDDYIKFLRSIRPDNMSEYSKQMQRFNVGE

DCPVFDGLFEFCQLSTGGSVAGAVKLNKQQTDI

AINWAGGLH**HAKKSEASGFCYVNDIVLAILELL**

KYHQRVLYIDIDIHHGDGVEEAFYTTDRVMTVS

FHKYGEYFPGTGDLRDIGAGKGKYYAVNYPLRD

GIDDESYEAIFKPIMSKVMEMYQPSAVVLQCGA

DSLSGDRLGCFNLTIKGHAKCVEYMKSFNLPLL

MLGGGGYTIKNVARCWTFETAVALDSTIPNELP

YNDYFEYFGPDFKLHISPFNMTNQNTNDYLEKI

KQRLFENLRMLPHAPGVQMQAIPEDAVQEDSGD

EEDDPDKRISIRAHDKRIACDEEFSDSEDEGQG

GRRNAANYKKPKRVKTEEEKDGEEKKDVKEEEK

ASEEKMDTKGPKEELKTV
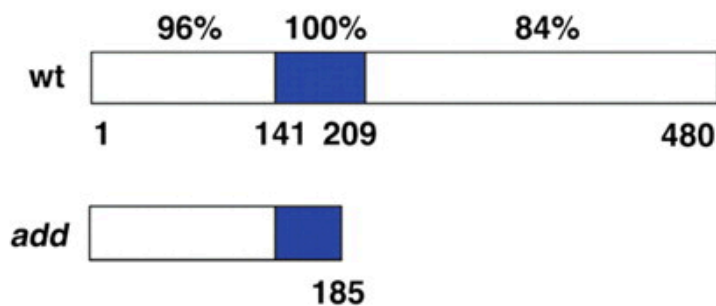
Fig. 2.4 Amino acid sequence of HDAC1 and its predicted structure of wild type and add mutant. Nonsense mutation occurs at 185 E (underline) within the Hdac catalytic region (bold letters in sequence, blue in schematic drawing below). Below is reported the percentage of identical amino acids in zebrafish and human HDAC1 in each domain. Figure has been reproduced from [73].

2.4.1 Zebrafish as model organism

Zebrafish (*Danio rerio*) is a tropical fish, native of the Himalayan region, belonging to the family of Cyprinidae [55].

The name comes from the pigmented and horizontal blue stripes on the side of the body that extend to the end of the caudal fin.

The zebrafish can grow to 6.4 cm in length, and male and female can be easily distinguished from their body shape, which is slender for the male as compared to that of the female that exhibits a larger belly [56].

Fig.2.4.1 Two specimens of zebrafish: on the left a male, on the right a female. Figure has been reproduced from: https://visalakshiramani.wordpress.com/articles/water-kingdom/ideal-for-research/.

Zebrafish has emerged as an important vertebrate model organism for scientific and medical research for several positive features.

In the scientific research zebrafish is often used in developmental biology studies thanks to its high fecundity, its rapid external development and the transparency of its eggs.

Every single mating couple can produce hundreds of fertilized eggs and the fertilization can be also modulated controlling the light-dark cycle.

The embryonic development of zebrafish is very rapid, with the formation of almost all major organs in the first 24 hours after fertilization, a complete organism is obtained within five days after fertilization [57].

Moreover thanks to the transparency of the eggs, all the different steps of early embryogenesis can be easily visualized and analyzed by microscope [58].

Another advantage is represent by the genome characteristics of zebrafish.

Its genome is diploid, composed of 25 paired chromosomes whose genome consists of about 1.5 x 10 billion base-pairs, compared with mammalian genome sizes of about 3 x 10 billion base-pairs.

Zebrafish genome has been fully sequenced and large numbers of mutants have been isolated, many of which show phenotypes that reflect the one observed in human diseases, and therefore provide a powerful approach for gaining insight to the corresponding pathophysiology [59].

For these reasons in the last years zebrafish has become a suitable model also in medical research.

An example of its application in medical research is cancer research, which use zebrafish as model to understand the formation, growth, and spread of malignant tumors.

Zebrafish can spontaneously develop almost any type of tumor [60], and the biology of its cancer is very similar to that of humans.

From a genomic analysis a high level of conservation between zebrafish and humans, comprehending several cell-cycle genes, tumor suppressors, and oncogenes, and many cancer related mutations have been found in these two organisms [61]. These characteristics make it a useful model for

the study of cancerogenesis and for the pharmacological screening of new anti-cancer drugs [62,63, 64].

The suitability of zebrafish as a model for a large-scale screening of molecules, originates from the possibility to analyze the range of chemical effects in a complete organism that shows a similarity of response to chemicals as mammals [65].
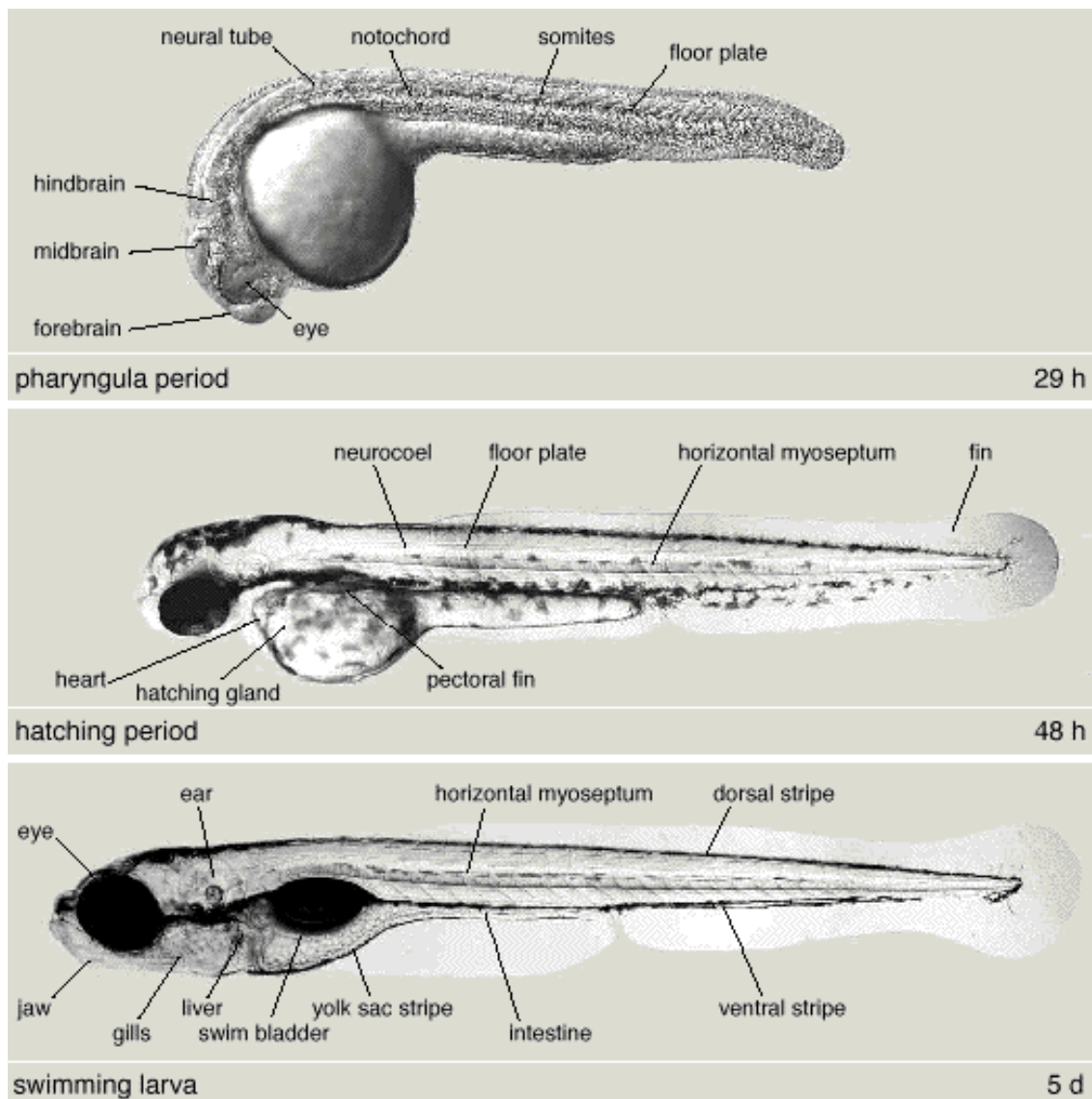
Fig. 2.4.1-2. Zebrafish development from 29 hours post fertilization to 5 days post fertilization. Figure has been reproduced from http://people.hsc.edu/faculty-staff/edevlin/edsweb01/new_page_9.htm.

2.4.2 Zebrafish embryonic development

The embryonic development of zebrafish is short, a complete adult organism is already formed 72 hours post fertilization, growing at the temperature of 28.5°C.

- The fertilized eggs are in the <u>zygote period</u> until the first cleavage occurs, almost 40 minutes after fertilization. The zygote is about 0.7 mm diameter at the moment of fertilization. After the first cleavage the cells divide with interval of about 15 minutes.

- During the <u>cleavage period</u> that lasts from 40 minute to 2 hours after fertilization, six cell divisions occur leading to a final step of 64-cell stage.

- From 2 to 5 hours post fertilization, the embryo is in the <u>blastula period.</u>
  During this period the epiboly begins to form the yolk layer and the epiboly.
  Embryo at 128-cell stage finally arise the 30% epiboly stage, with the formation of blastoderm.

- From 5 to 10 hours post fertilization the embryo is in the <u>gastrula period </u>that last from the 50% epiboly stage to the bud stage. During this stage the epiboly formation continues and embryonic axis and primary germ layers start to be produced.

- From 10 to 24 hours post fertilization the <u>segmentation period</u> take place.
  The embryo develops from 1 somite stage to 26 somite stage. The embryo elongates, the precursors of primary organs appear, the tail bud becomes more prominent and the first movements are visible. The

yolk, that is still the only embryo component that provides the nutrients, is more clearly defined.

- From 24 to 48 hours post fertilization the embryo is in the <u>pharyngula period</u>, and it develops from prim-5 stage to high-pec stage.

  The morphogenesis of the bilaterally paired pectoral fins starts, pigment cells, the pigmented retinal epithelium and the neural crest-derived melanophores start to differentiate. The circulatory system and the heart begin to function, and the yolk starts to become thin and its shape is more conical. During this period marked behavioral development are visible, as the response to tactile stimuli and the rhythmic bouts of swimming.

- From 48 to 72 hours post fertilization in the <u>hatching period</u>, the embryo develops from long-pec stage to protruding-mouth stage. During this stage the morphogenesis of the primary organs reaches completeness. The first cartilages start to develop, the yolk almost disappears. The larva starts to swim and to move its jaws, pectoral fins and eyes. From a behavioral point of view larvae are now capable of escaping, catching of prey and feeding [66].
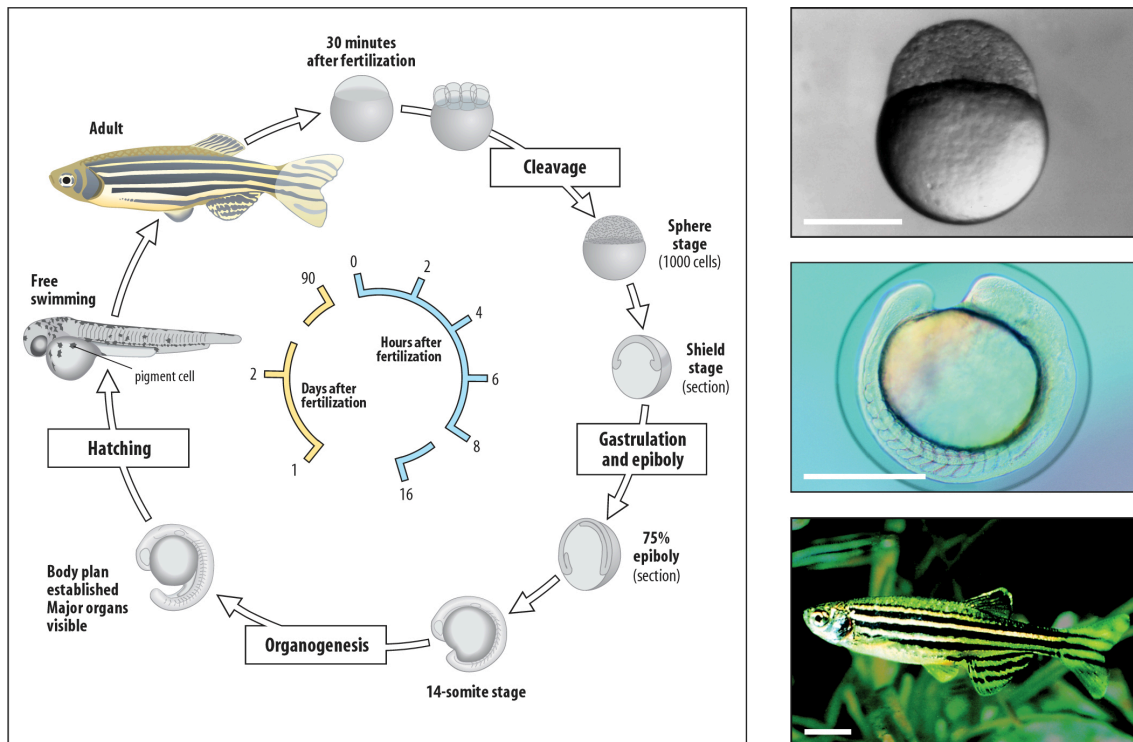
Fig. 2.4.2. Zebrafish life cycle**.** Figure has been reproduced from http://www.mun.ca/biology/desmid/brian/BIOL3530/DEVO_03/devo_03.html

2.4.3 Zebrafish neurogenesis

Neurogenesis is the process by which differentiated post-mitotic neurons rise from a pool of undifferentiated neural progenitors.

In zebrafish as in other vertebrates, the early stages of neurogenesis are regulated by the action of transmembrane-spanning proteins as Notch and Delta.

These two proteins are cleaved intracellularly and promote the transcription of genes encoding transcriptional repressors of the hairy/enhancer of split [E(spl)] family inside the cell.

The E(spl) proteins repress genes required for the 26adoption of a neuronal fate, as the bHLH genes [67].

In zebrafish two genes of the bHLH family, *ascl1b* and *ngn,* are required for specification of epiphyseal neurons, for the formation of Rohon-Beard sensory neurons and for the specification of dorsal root sensory ganglia [68].

Moreover two zebrafish orthologous of mouse *Hes1* and *Hes5*, two *E(spl)* proteins, are expressed in the developing CNS. *Her6*, which is the orthologue of *Hes1*, seems to inhibit the expression of proneural genes as ngn1 during early neurogenesis. While *Her4* similarly to its orthologue *Hes5*, is required in later stages of neurogenesis to repress ngn1 in the neural plate [69,70].

During retinal neurogenesis in zebrafish, the postmitotic progeny is initially generated in the ventronasal retina and then neuronal production spreads to the entire neural retina [71].

The driving force that leads to the neuronal production comes from the interaction between the optic stalk and the neural retina, and is then regulated by the relay of the Hedgehog short-range signaling [72,73].

In addition to the Hedgehog signaling, another short-range signaling pathway that affects the proliferation of retinoblasts in zebrafish retina, is the Hh signaling pathways. Hh induces cell-cycle exit of retinoblasts, and its function can be modulated indirectly by Wnt signaling through the activation of cAMP-dependent protein kinase (PKA), a direct inhibitor of Hh signaling [74, 75].

2.4.4 *Zebrafish retina development and anatomy*

The first sign of retina development is visible in zebrafish embryo at 6 somite stage, with the formation of the optic lobe. Subsequently at 11-12 somite stages the pigmented epithelium and the neural retina become visible, and at the 14 somite stage the lens start to be formed. In the early stages of retinal development, the optic cup consists of two layers: one that

will form the retina, the pseudostratified neuroepithelium, and the other of pigmented epithelial cells. The first neurons that are formed in the retina are the ganglion cells, around 29-34 hpf, but at 36 hpf there is still no lamination. Finally at 60 hpf almost all the different neuronal subtpypes are distinguishable, and are organized in three nuclear layers separated by to plexiform layers [76].

The three nuclear layers are: (I) ganglion cell layer (gcl), (II) the inner nuclear layer (inl), (III) the photoreceptor cell layer (pcl). These three layers are separated by the inner plexiform layer (ipl) and the outer plexiform layer (opl). The pcl of the zebrafish retina contains five photoreceptor types: rods, short single cones, long single cones, and long and short members of the double cone pair. Six major types of neuron form Zebrafish retina: photoreceptors, horizontal cells, bipolar cells, amacrine cells, interplexiform cells and ganglion cells [77].

Photoreceptors are completely developed by 48 hpf. They express six visual pigments, the opsin genes, and constitute biological sensor for intense sunlight and illumination of the night. When lights activate opsins, a chain reaction start that involves changes in photoreceptor membrane potential that are then passed to the interneurons of the inner retina [76,78].

Horizontal cells constitute inhibitory neurons. They receive input from the photoreceptors and transfer it to bipolar cells. When activated in response to light stimuli, they can antagonize the bipolar cells receptive fields and are thus required in detecting light contrasts.

Bipolar cells receive spatial, color and luminance information from photoreceptors in the outer retina and carry them to amacrine and ganglion cells in the inner retina. They are connected to photoreceptors through the formation of two types of synapses in the OPL, ribbon synapses and flat contact. Based on their response to white light bipolar cells that can be

classified in ON or OFF cells; the first one depolarize in response to light spots, the second ones hyperpolarize [79].

Amacrine cells have an inhibitory function in the zebrafish retina. They modulate the transmission of visual information from photoreceptors via bipolar cells and ganglion cells. They take contact with bipolar and ganglion cell dendrites in the IPL. In the IPL the processes of cells that hyperpolarize with increased light intensity are confined to the outer half of the IPL, whereas processes of cells that depolarize are in the inner half [80, 81].

Interplexiform cells are dopaminergic cells that constitute a signaling pathway which connect the inner to the outer plexiform layers. In the inner plexiform layer they receive all the input and then in the outer nuclear layer they make contacts onto horizontal cells [82].

Ganglion cells are the neurons that connect the eye to the brain. In the retina retinal ganglion cells (RGCs) are connected with bipolar and amacrine cells in the IPL through synapses in order to receive excitatory and inhibitory inputs. RGCs axons through the optic nerve arrive to the brain, where they transfer visual information to the higher centers [83].

retinal ganglion cells

amacrine cells

bipolar cells

horizontal cells

photoreceptors
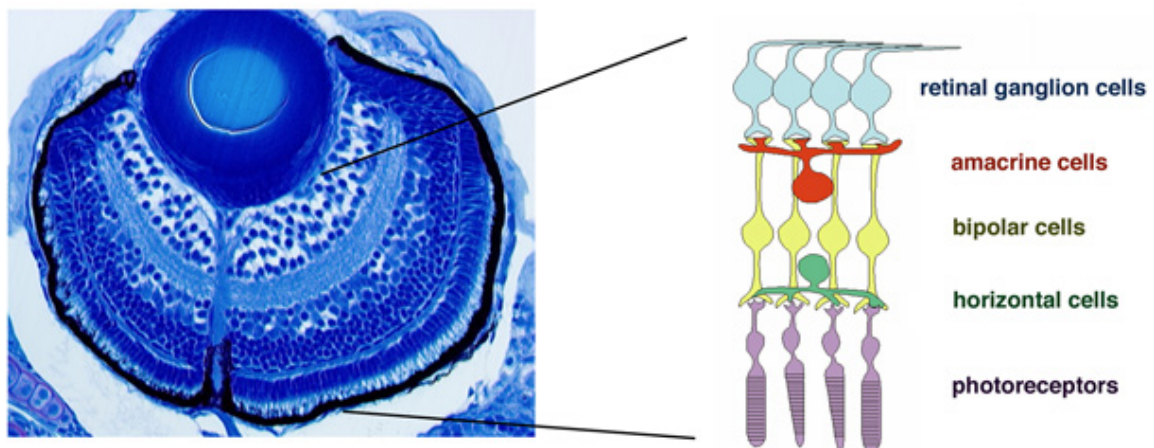
Fig.2.4.4. Zebrafish retina anatomy at 3 days post fertilization, with all the six major classes of retinal neuron. Figure has been reproduced from https://groups.oist.jp/dnu/fy2011-annual-report.

2.4.5 HDAC1 and zebrafish development

HDAC1 role in zebrafish development has been investigated through the use of mutants and morphants for HDAC1 and enzymatic inhibitors. In all the cases was observed an increase in histone acetylation [50].

Many HDAC1 mutant alleles have been identified in screens for embryonic essential genes [84], hematopoietic stem cells [85], development of the liver, pancreas [50], retina [53] and neural crest [86, 49]. Many phenotypes have been correlated with HDAC1 mutation raising the possibility that alterations in chromatin structure as a result of persistent histone acetylation could direct cell fate decisions.

HDAC1 morphants phenocopy most mutant alleles, although in several cases morphants have a more severe phenotype [52, 48, 53, 54, 49]. This demonstrates that both maternally and zygotically provided Hdac1 contributes to embryonic development. The phenotypes of *hdac1* mutants and morphants reflect the first developmental events that require Hdac1 activity. On the other hand, the use of HDAC1 inhibitor provides the capability of blocking HDAC1 activity at any stage of development and reveal stage-specific functions. For instance, adding the HDACi valproic acid (VPA) to early embryos at 6 hpf results in a small liver phenotype (Fig. 2A) but adding it later at 72 hpf does not [51].

2.4.6 Role of HDAC1 in zebrafish neurodevelopment

HDAC1 is required in zebrafish for the proper development of the retina.

35

Previous studies showed that the absence of HDAC1 results in an abnormal differentiation. In HDAC1 mutant at 96 hours post fertilization (hpf), indeed, the retina is smaller and lacks the typical lamination. The optic stalk, which is required until 36 hpf to maintain the connection between the ancient retina and the brain, instead of degenerate in the HDAC1 mutant is enlarged, and lacks differentiation markers. In the retina HDAC1 controls differentiation of the different cellular subtypes. The silencing of HDAC1 results in the deficiency of retinal ganglion cells (RGCs), amacrine and bipolar cells, double cone and rod photoreceptors as well as Mueller glia.

Together with the inhibition of differentiation, the lack of HDAC1 results also in an aberrant proliferation in the retina still at 72 hpf. At this time point HDAC1 mutants show BrdU positive cells throughout the retina, as proof of the failure of precursors cell to exit from the cell cycle. The effect on the cell cycle can be a consequence of the aberrant expression of cyclinD1 and cyclinE2 in HDAC1 mutant zebrafish. These two cyclins are normally expressed in the proliferating precursors, but are downregulated in differentiated cells, while in HDAC1 mutants are still markedly expressed at 48 hpf [53].

Yamaguchi et all [54] showed that these effects due to the lack of HDAC1 in zebrafish retina, can be explained with the requirement of HDAC1 for the switch from proliferation to differentiation of retinal cells. In their work they found that in HDAC1 mutant the two signaling pathways mediated by Wnt and Notch are activated. In zebrafish retina Wnt signaling has been found to promote proliferation while Notch to inhibit differentiation, therefore in normal conditions HDAC1 promotes the exit from the cell-cycle and the neurogenesis.

The link between HDAC1 activity and the inhibition of Wnt and Notch pathways is confirmed by the analysis of transcription of genes that are

effectors or downstream targets of these two signaling pathways, in HDAC1 mutant retina. In the absence of HDAC1 the expression of *cyclinD1* and *cmyc* is upregulated and also the one of *her4* and *her6,* two zebrafish ortholog of Hes1, the Hairy/enhancer-of-split-related. Hes1 is a neurogenic inhibitor whose activation is required for the inhibition of the expression of proneural genes by Notch.

In zebrafish hindbrain HDAC1 is required to maintain the responsiveness of neuronal precursors cells to hedgehog signaling.

In the absence of HDAC1 the hindbrain is segmented and disorganized, the anterior rhombomeres do not present the typical mediolateral expansion, as the midbrain that fails the characteristic ventricular expansion. Forebrain, midbrain and hindbrain are all formed but smaller. The reduction of cell proliferation rate in HDAC1 mutant is reversible and interests just a particular step of neurogenesis, around 25 hpf.

The evidences suggest that HDAC1 role in zebrafish hindbrain is also correlated to the inhibition of Notch signaling pathway. In HDAC1 mutant embryos the transcription of the proneural genes *ascl1b* and *ngn1* is almost absent, and this could be and indirect consequence of the loss of HDAC1 repression of Notch-activated target genes, as *Her6* whose expression is upregulated in the dorsal diencephalon and the hindbrain rhombomeres 5 and 6, all regions undergoing neuronal specification. The increase in the expression of these Notch target genes, can be responsible also for the impairment of the response to the hedgehog signaling of neuronal precursors in the hindbrain. The expression of *ngn1* gene is positively regulated by the hedgehog signaling, and a possible explanation of HDAC1 inhibition of the response to this signaling pathway can be the inhibition of the expression of this proneural gene [52].
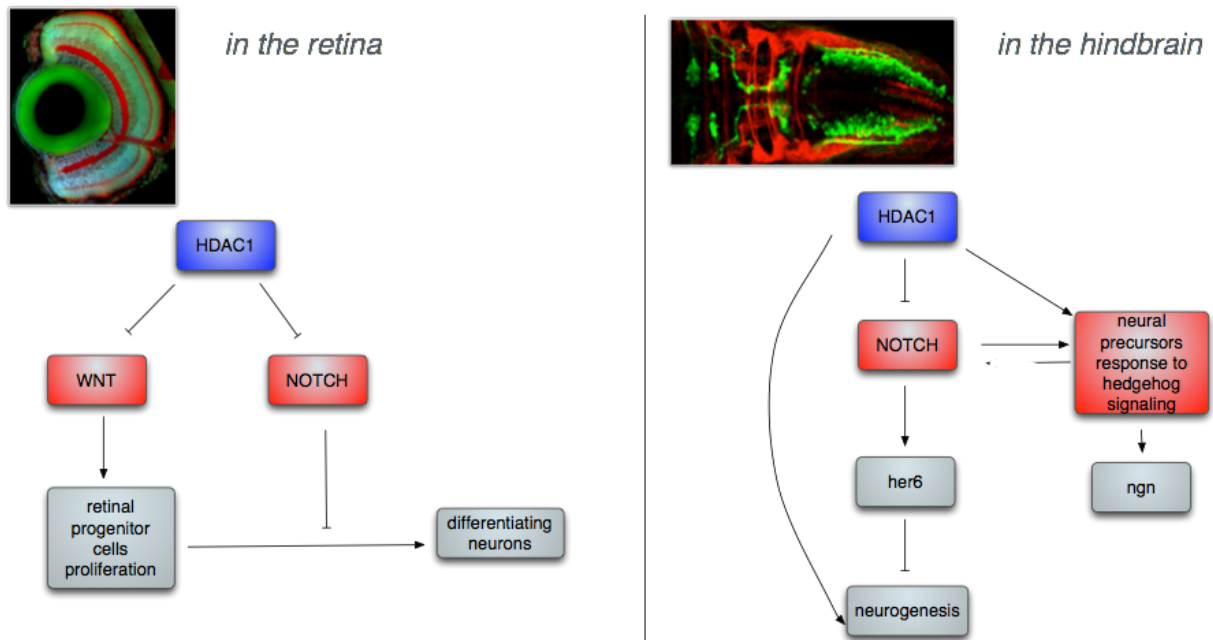
Fig. 2.4.6. Schematic representation of HDAC1 requirement in zebrafish retina and hindbrain development.

2.4.7 Stem cells niches in zebrafish retina

The evidence that in zebrafish, retinal neurogenesis continues postembryonically in a region of the retina called the ciliary marginal zone (CMZ) gave rise to the hypothesis of the presence of a stem cell niche in this region [87].

Moreover in the adult teleost fish retina another source of progenitors has been discovered in central retina. These progenitors are localized in the outer nuclear layer (ONL) where they generate rod photoreceptors.

The precursors found in the ONL are originally produced in the inner nuclear layer (INL) from more slowly proliferating precursors, and then move to the ONL along the radial fiber of the Muller glial cells [88].

38

Both these two sources of retinal stem cells are responsible for the regeneration of retinal cellular subtypes in the injured retina.

In the CMZ *Raymond at all* [89], showed that the most primitive and multipotent retinal stem cells are located in the most peripheral region of the CMZ adjacent to the ciliary epithelium, while more restricted retinal progenitors are localized more centrally, closer to the differentiated retina. In this two distinct regions of CMZ, previous studies suggest the presence of a different activity of Notch-Delta signaling pathway that plays an important role in cell fate decision [90].

In the most peripheral region of the CMZ moderate signals of Notch-Delta pathways are visible, while in the central region the signals are even lower.
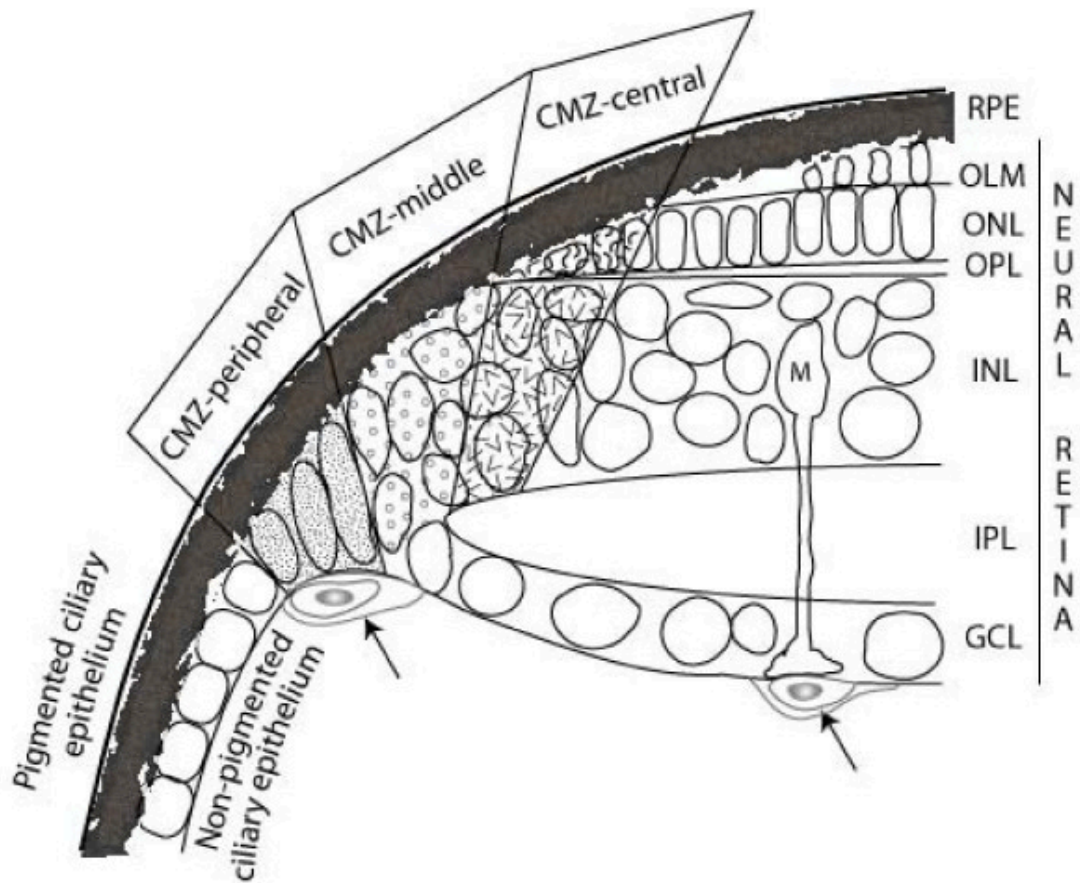
Fig. 2.4.4. Schematic drawing of histological landmarks that define four areas in the CMZ: peripheral, middle, central-inner and central-outer. Figure has been reproduced from [89].

3 Aim of the research

An altered transcriptional regulation is one of the major events that lead to the oncogenic transformation of normal cells. An altered balance between the action of histone acetyl transferases and histone deacetylases (HDACs) has been observed in different types of cancer. Thus new molecules acting as HDACs inhibitors started to be considered potential anticancer drugs.

9-hydroxistearic acid (9-HSA) is an endogenus lipid peroxidation product, which acts as a histone deacetylase inhibitor. Its administration in colon cancer cells (HT29), at micromolar concentration, results in a significant inhibition of cell proliferation along with differentiation toward a more benign phenotype.

The final aim of this thesis work is to investigate the action of (R)-9-HSA in vivo during normal development and cell differentiation, in order to understand if an endogenous lipid peroxidation product can regulate the molecular pathways involved in the control of proliferation and differentiation in normal conditions.

The animal model used for this study is zebrafish, because of the high similarity between its HDAC1 enzyme and the human one and the well characterized role of HDAC1 in zebrafish neural development.

To reach the final aim of the project, the initial aims were:

1. To verify if 9-HSA is endogenously produced in zebrafish embryos, as already observed in human cell lines.

2. To assess the activity of (R)-9-HSA in the new experimental model and verify the homology of the target of action of (R)-9-HSA with the one observed in human cell lines.

3. To understand if the phenotype resulting from the treatment with (R)-9-HSA could reproduce the one observed in zebrafish mutant for HDAC1.

4. To investigate the possible effect of oxygen reactive species (ROS) on the regulation of stem cell fate during zebrafish retina development.

Immunostaining, in situ hybridization techniques, lipid extraction and analysis, TUNEL assays, proliferation assays and in vivo imaging analysis were performed in order to evaluate the biological effects induced by (R)-9-HSA on zebrafish embryos, particularly on zebrafish retina.

4   Material

4.1 Zebrafish methodology

4.1.1 Zebrafish mantainance

Zebrafish were breeding and raising following standard protocols, and according to French and European Union animal welfare guidelines.

They were maintained in a zebrafish housing system by Tecniplast (Tecniplast Deutschland GmbH), using conditioned water, in tanks of 3.5L. Water temperature was maintained at 26-28°C and air temperature at 27-29°C. In this system 10-20% of the water in each fish tank is exchanged per day as zebrafish waste contains ammonium compounds, which are highly toxic. In addition, biological filters were used to detoxify the water. The biological filters provide a large surface area to grow denitrifying aerobic bacteria like Nitrosomonas and Nitrobactor, which degrade ammonium compounds to nitrite.

In the fish room also the lighting conditions were regulated in order to reproduce the circadian rhythm, with 14 hours of light and 10 hours of dark.

Zebrafish were feeding differently depending on their age, but always 2-3 times per day. The babies were fed with Paramecium, one-cell organisms that can be found in freshwater environments. The adults were fed with brine shrimps also called Artemia. Artemia are very small aquatic crustaceans native to inland saline environments that, during their life cycle, can produce a resting cyst that after being cleaned and desiccated is canned for shipment and feeding.

4.1.2 Breeding

Zebrafish embryos are obtained easily by crossing adult fish.

Females and males can be distinguished by body-shape and colour; egg-producing females have a big belly and their colour is blue-grey, males are slender and their colour is more pink-like.

For the production of the embryos used in this study, one male and two females were put together in a crossing tank the day before their crossing, but they were maintained separated until the day after by a transparent divider. In the crossing tanks, adult zebrafish were all maintained separated from the new produced eggs by the presence of an inlaid septum, in order to preserve the eggs that could be eaten from the adult zebrafish.

Using this condition they start to mate as soon as there is light on the next morning and they are again put together; this is important because microinjections require synchronized and/or early embryos.

4.1.3 Raising of larvae

The eggs produced were collected using a strainer, and washed with system water. Then eggs were transferred to Petri dishes rinsing the strainer with eggs water (NaCl 5.03 mM, KCl 0,17 mM, $CaCl_2$ $2H_2O$ 0.33 mM, $MgSO_4$ $7H_2O$ 0.33 mM, Methylene blue 0,1 % (w/v), ddH_2O) and kept in incubator (~28.5 °C). Every day the dishes water was changed and the eggs were observed under a stereomicroscope to distinguish the fertilized eggs from the ones unfertilized, and to eliminate the last ones.

Larvae were maintained in the incubator till the time required to perform the experiments, except the ones used to give birth to new generation.

In this case larvae were kept in dishes till day 5 and then were transferred to a main fish tank.

4.1.4 Genotyping of embryos

For this study three lines of zebrafish embryos were used, AB and TL wild-type and a strain mutant for the protein HDAC1.

The HDAC1 -/- mutant line is add[rw399] and was a kind gift from Prof. Ichiro Masai lab (University of Tokyo).

Starting from the mutant male donated by Prof Masai I created a new generation of add[rw399]mutant zebrafish, by crossing it with a wild-type female.

The progeny was then genotyped, with the fin clip procedure.

For every fish a small piece of the tail fin was cutted and stored in 100% methanol at -20°C for 1 hour or eventually overnight.

Afterwards, samples were thawed and dried 10 minutes at 72°C. The digestion was then effectuated by adding proteinase K (1/10 in TE buffer) and incubating at 55°C overnight. The following day, samples were heated at 95°C for 10 minutes and TE buffer was added to each sample. The analysis of the genotype was then effectuated by a PCR reaction, on 1 μl of diluted DNA.

The PCR reaction mix was constituted as follows:

- 10x buffer

- dNTP 10mM

- primer mix 25μM

- Taq DNA polymerase

- H2O

Thermocycler program for genotyping PCR			
Step	Temperature in °C	Time	
Preheating	94	2 minutes	35x
Template Melting	94	30 seconds	
Annealing	63	30 seconds	
Extension	72	1minute	
End	4	forever	

At the end of the PCR reaction all the samples were incubated overnight at 55°C for digestion, in the following reaction mix:

- 10x NE buffer 3
- 100 mg/ml BSA
- ApoI restriction enzyme

The following day, digestion products were run on a 2% agarose gel.

The agarose gel was prepared by suspending agarose powder in TBE-buffer at a percentage of 2%. The suspension then heated in a microwave till the solution was completely clear. The gel then was left on the bench to cool down (hand warm, ≤60°C), before 2 μl ethidium bromide (500 μg/ml) per 50 ml gel were added.

The ethidium bromide was distributed homogenously by carefully shaking the flask. The run was effectuated at a voltage of around 150 volt for 30 minutes.

The expected band was around 100 bp.

4.1.5 Microinjections

The injection needles were obtained starting from borosilicate glass capillaries using a needle puller (P-97 Flaming/Brown Micropipette Puller). Microinjection of early zebrafish embryos was performed under a stereomicroscope (Leica MZ FLIII) using a micromanipulator and a nitrogen gas injector.

The embryos were microinjected when they were still non-dechorionated embryos, between zygote and 4 cells stage. Injection was carried out through the chorion into the yolk, 10-15 minutes after fertilization. Prior the injection, embryos were immobilized on eggs water/1% agarose dishes with furrows to hold them in place. The agarose-dishes are made by

diluting 1% agarose in eggs water, heating this solution and suddenly put it in the Petri dish where it will form a gel.

The diameter of the injected drop of injection solution was around one tenth of the diameter of the embryo. The injection solutions were filled into the needles using microloader tips, and their final amount was controlled using a valve controlled by a pedal.
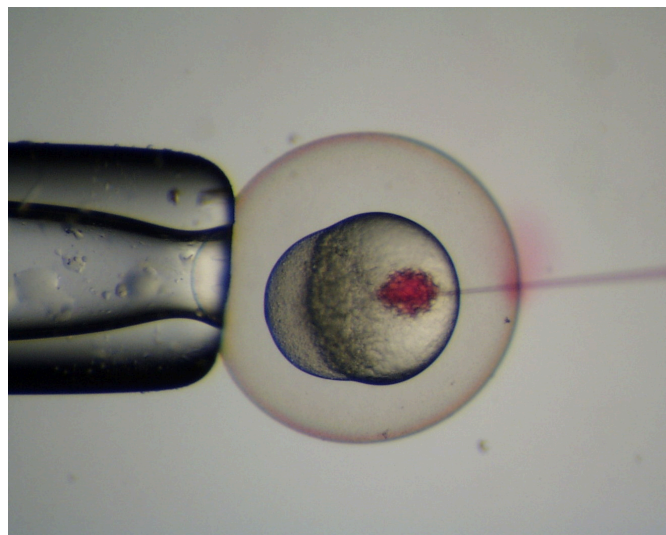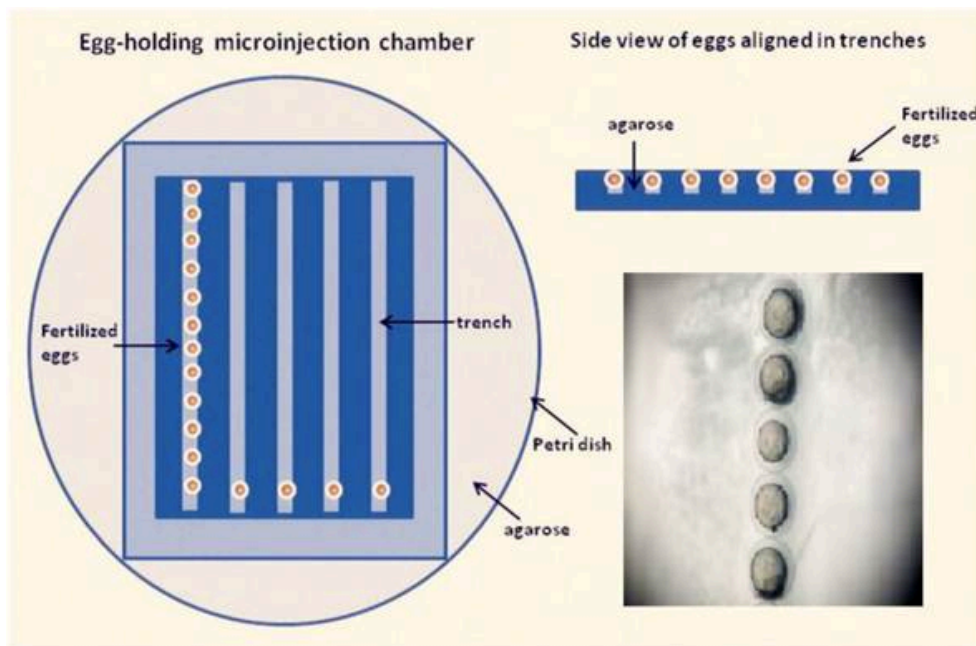
Fig. 4.1.5. In the first images the microinjection chamber, in the one below the injection in the yolk of the embryo. The red is due to the phenol red present in the injection

solution. Figures have been reproduced from [84] and
http://theconversation.com/animals-in-research-zebrafish-13804.

4.1.6 Microinjection solutions

9-hydroxystearic acid was prepared from powder and solubilizing it in
dimethylsulfoxide (DMSO, Sigma Aldrich), to obtain a solution with a
final concentration of 33mM. DMSO was used pure.

To both the solutions was added the 0.1% of phenol red solution, in
order to control the amount of solution injected. The solution was
prepared starting from the powder (Sigma Aldrich) and diluting it in the
injection solutions.

4.1.7 Dechorionation of embryos

Zebrafish embryos can be dechorionated either in a mechanical or
enzymatic way.

The manual dechorionation can be done with forceps, and is usually
performed from late somitogenesis, while for the early stages the
enzymatic dechorionation is safer.

For the enzymatic way, embryos were put in agarose gel coated dishes,
because once dechorionated they are fragile, could stick to the plastic
and be damaged. The agarose-dishes were prepared as already described
in paragraph 4.1.5.

Embryos were put in agarose-dishes and then pronase (10mg/ml in eggs
water) was added. The reaction was let going till the first embryos could
be seen without chorion. Then the embryos were transfer into a glass
beaker with medium, and were washed three times to remove all traces
of pronase before being transferred to a Petri dish.

4.2 Total lipid-extraction

A total lipid extract has been obtained from embryos from day 0 to day 5.For each time point two hundred wild-type embryos were used.

Embryos were dechorionated with pronase and fixed at -20°C in lipid extraction mixture ($CHCl_3$:MeOH 2:1 –BHT 0,01%).

At the moment of the extraction they were thawed and transferred to a dounce homogenizer and then dounced several times.

To complete the homogenization they were sonicated 3 times (10 sec, 60-62% power), and were stored, in lipid extraction mixture, at 4°C overnight.

The day after the whole lipid extract was filtered at 4°C using a delipidised filter, and was dried under nitrogen flow. The pellet was then resuspended in $CHCl_3$ and stored at -20°C overnight.

Once samples were thawed they were eluted on a Bond Elut column (Agilent) in order to separate the different classes of lipids.

Three different fraction were eluted, with three different eluent:

- neutral lipids, with $CHCl_3$/2-propanol (2:1)
- fatty acids, with 2% acetic acid in diethyl ether
- phospholipids, with 1% methylene chloride in hexane

(R)-9-HSA should be in the II phase, which is the one that has been analyzed in mass spectrometry.

4.2.1 ESI-MS

Electrospray ionization mass spectrometry (ESI-MS) provides a sensitive tool for studying, at femto-mole quantities in micro-litre sample volumes, non-volatile and thermally labile bio-molecules.

Mass spectrometry is an analytical technique that allows toobtain information on structure and molecular mass of analyte molecules after

their conversion to ions. The molecules are introduced into the ionization source of the mass spectrometer, to reduce them to positive or negative charges. The ions then travel through the mass analyzer and arrive at different parts of the detector according to their mass/charge (m/z) ratio. The signals collected by the detector are recorded by a computer system. Data are finally represented in a graph that shows the relative abundance of the ions generated according to their m/z ratio [91].

In this work LC-MS analyses were performed on a PU-1558 liquid chromatograph (Jasco, Tokyo, Japan) interfaced with a LCQ Duo (ThermoFinnigan, San Jose, CA) mass spectrometer equipped with an electrospray ionization (ESI) source (4.5 eV) and operated with an Ion Trap analyzer. HPLC separation was carried out on a Waters XTerra™ MS C18, 3.5 μm (3.0 × 150 mm inner diameter) column using a mobile phase consisting of methanol-0.05% acetic acid in water (80:20, v/v) at a flow rate of 0.2 ml/min and an injection volume of 20 μl.

LC-MS analyses were conducted operating in both full scan and single ion monitoring (SIM) modes (negative polarity). The mass spectra were recorded over the *m/z* range 50–450 (3 microscans/s), providing the total ion current (TIC) chromatograms. SIM chromatograms were also obtained at *m/z* 300 $[M - H]^-$, the base peak of the deuterated 9-HSA. Capillary temperature was 220°C. A calibration graph was obtained for the quantitative assay of deuterated 9-HSA-d. A standard solution of the hydroxy acid was prepared by dissolving the powder in methanol to obtain a final concentration of 43.2 mM [33].

4.3 Histone acetylation analysis

For the analysis of the histone acetylation pattern was chose an immunohistochemical approach. Although immunohistochemistry is not a quantitative technique, like western blot, it can yield qualitative data on histone acetylation. Moreover it was important to define the effect of 9-HSA in a tissue specific manner, in particular in the retina, and for this reason immunohistochemistry was the most suitable techniques, differently from western blot which can be performed on a whole embryo protein lisate.

4.3.1 Hyperacetilated Histone H4 Immunostaining

Zebrafish embryos were fixed at 24 and 48 hours post injection and prepared as will be described in paragraph 4.4.1.

Zebrafish retina sections were incubated with a primary antibody anti-hyperacetylated histone H4 (Penta) (06-946, Millipore), 1:500 in PBST; and then with an Alexa546 fluorophore-conjugated secondary antibody diluted 1:500 (Invitrogen Molecular Probes) together with DAPI nuclear marker (Sigma) 1:500 diluted in PBST.

4.4 Proliferation analysis

4.4.1 Phosphorylated Histone H3 antibody immunohistochemistry

Histone H3 is one of the protein constituents of chromatin, during mitosis this particular histone is phosphorylated at a specific serine residue.

Immunohistochemistry of this marker of cell division enables the identification of actively dividing cells to identify differences in proliferation in specific cell groups. In this work it was look at pH3 localization in zebrafish hindbrain and retina, in order to analyze the differences in proliferation between DMSO treated embryos, 9-HSA tretaed embryos and HDAC1 mutant embryos wild type siblings.

The analysis of phospho-histone H3 incorporation has been carried out on whole-mount zebrafish embryos 24 hours post injection (hpi) with DMSO or (R)-9-HSA, and on retina sections of zebrafish embryos 48 and 72 hpi.

For the whole-mount analysis of phospho-histone H3, embryos 24 hours post injection (hpi) with DMSO or (R)-9-HSA were dechorionated and fixed overnight in 4% (w/v) paraformaldehyde PFA in PBS [NaCl (Sigma) 8 g/L, Na_2HPO_4 (Sigma) 1,15 g/L, KCl (Sigma) 0,2 g/L, KH_2PO_4 (Sigma) 0,2 g/L] at 4°C. The day after PFA was removed and embryos were stored overnight at -20°C in Methanol 100%.

The next day embryos were rehydrated through a graded series (75%, 50% and 25%) of methanol in PBS, washed twice in PBS and incubated in 10% v/v goat serum in PBS for 1 hour. Embryos were then incubated with anti-phosphorylated histone H3 antiserum overnight at 4°C.

The day after they were washed briefly in 10% goat serum in PBS, then washed four times, each for one hour in PBS, and incubated one hour in 10% goat serum in PBSBT (PBS supplemented with 0.1% (w/v) BSA and 0.05% (v/v) Tween 20), before incubation with anti-rabbit IgG conjugated to horseradish peroxidase overnight at 4°C.

After a brief wash in 10% serum in PBSBT and four washes each for 1 hour in PBSBT, embryos were equilibrated in 0.3 mg/ml Diamino Bezadine (DAB) in PBS for 10 minutes, and then H_2O_2 was added to 0.03% v/v final.

Color reaction was allowed to develop for 15-30 minutes before being stopped by several rinses with water, then in PBS. Embryos were cleared in 90% glycerol in PBS.

For the analysis of phospho-histone H3 positive cells in the retina, zebrafish embryos were fixed overnight in 4% PFA in PBS at -20°C, in groups of 20 embryos of matched developmental stage.

After fixation and overnight in methanol, the embryos were embedded in 30% sucrose in phosphate-buffered saline (PBS) at 4°C overnight.

The day after the sucrose was replaced by a solution 150 mM Tris-HCl (pH 9.0), and embryos were heating in this solution at 70°C for 15 minutes.

Embryos were cooled down and the Tris buffer solution was replaced by 30 % sucrose for one more overnight. Then embryos were transferred to a plastic mold and horizontally oriented in Tissue-Tek O.C.T. Compound (Sakura Finetech), the formation of the cryoblock started immediately by putting the mold at -80°C for 10 minutes.

The cryosamples were then transferred to the cryotome (ThermoScientific) at -20°C.

Cryosections with a thickness of 12 um were obtained and were collected on Superfrost Plus slides (Fisher Scientific), and air dried at room temperature for three hours. Once dried, cryosections were washed with PBS-Tween solution for 5 minutes three times, and were then blocked in 10% normal goat serum (Jackson ImmunoResearch Laboratories) in PBST [0.1% Tween-20 (v/v; Sigma) in PBS (pH 7.4] for 1 hour at room temperature. The slides were incubated overnight with the primary antibody anti phospho-histone H3(ser10) (06-570, Millipore) 1:500 in PBST, in a humidified chamber at 4°C.

The following day, sections were washed three times in PBS-Tween and then incubated for 2 h in a blocking solution containing Alexa488

fluorophore-conjugated secondary antibody diluted 1:500 (Invitrogen Molecular Probes) and DAPI nuclear marker 1:500 (Sigma), washed three times in PBST, and mounted in Fluoromount (Sigma). Slides were air-dried in the dark from 4 h to overnight. Images were then acquired using a Zeiss LSM 710 confocal microscope (Zeiss).

4.4.2 PCNA assay

Proliferating cell nuclear antigen is a 36 kD nuclear protein associated with the cell cycle. Proliferating cell nuclear antigen (PCNA) is an evolutionarily well-conserved protein found in all eukaryotic species [92]. PCNA act as a processivity factor of DNA polymerase δ, which is required for DNA synthesis during replication [93, 94, 95]. However, besides DNA replication, PCNA activity is associated with other vital cellular processes such as chromatin remodelling, DNA repair, sister-chromatid cohesion and cell cycle control [96].

For the analysis of proliferating cells nuclear antigen (PCNA) expression and localization zebrafish embryos at 48 and 72 hpi were used. Samples were prepared as already described in paragraph 4.4.1, with the only exception of the fixation overnight, that for this experiment was carried out in 4% PFA in Ethanol.

Zebrafish retina sections were incubated overnight with anti-PCNA antibody clone PC10 (AB477413, Sigma Aldrich) 1:500 diluted in blocking solution (10% normal goat serum in PBST) at 4°C in a humidified chamber. The signal was detected using an Alexa546 fluorophore-conjugated secondary antibody diluted 1:500 (Invitrogen Molecular Probes) together with DAPI nuclear marker (Sigma) 1:500 in blocking solution.

4.4.3 Brdu incorporation

Bromo-deoxyuridine (BrdU) is a halogenated thymidine analogue that is incorporated into newly synthesised DNA during DNA replication in vitro and in vivo [97]. Within the cells, these analogues are phosphorylated and incorporated into DNA via the nucleotide salvage pathway [98, 99, 100].

Embryos 48 hpi were dechorionated and immobilized in agarose after having been anesthetized with 1mM Tricaine. Then they were injected into the yolk with 50 mM BrdU (Sigma) solution. The injection solution was composed by: BrdU final concentration 50 mM, Phenol Red final concentration 0.5%, and ddH$_2$O.

12 hours after BrdU injection, the embryos were washed and fixed 20 minutes at room temperature with 4% paraformaldehyde (PFA) in PBS. Then as for phopsho-histone H3 staining, embryos were embedded overnight in sucrose.

The day after embryo were transferred to a plastic mold and horizontally oriented in Tissue-Tek O.C.T to prepare the blocks for the cryosections. The cryosections obtained by the cryotome, with a thickness of 12 um, were let to dry for two hours at room temperature and then were rehydrated with PBTD (PBS supplemented with 0.1% Tween20 and 1% DMSO). The slides were treated with 2N HCl for 20 minutes at 37°C to denature the DNA double helix, and the reaction was stopped with 5 washes in PBS. After a blocking of 2 hours in 5% normal goat serum in PBTD, the sections were incubated with unconjugated anti-bromodeoxyuridine (PRB1-U, Phoenix) 1:1000 in block solution overnight at 4°C.

The next day slides were washed with PBTD and then incubated with Alexa546 fluorophore-conjugated secondary antibody diluted 1:500 (Invitrogen Molecular Probes) in blocking solution 1.5 hours at room

temperature. Finally slides were marked with the nuclear marker DAPI 1:500 in blocking solution for 5 minutes at room temperature.

4.5 Apoptosis detection

A hallmark of apoptosis is extensive genomic DNA fragmentation that generates a multiples DNA double-strand breaks (DSBs) with accessible 3'-hydroxyl (3'-OH) groups. **T**erminal deoxynucleotidyl transferase d**U**TP **N**ick **E**nd **L**abeling **(TUNEL)** assay is used to identify apoptotic cells by the terminal deoxynucleotidyl transferase (TdT)-mediated addition of labeled (X) deoxyuridine triphosphate nucleotides (X-dUTPs) to the 3'-OH end of DNA strand breaks that are subsequently visualized depending on the introduced label, thus serving as parameter for the percentage of apoptotic cells within the analyzed cell population [101].

Apoptosis was detected in whole zebrafish embryos at 48hpi by TUNEL assay, using Apoptag Peroxidase In Situ Apoptosis Detection Kit (Millipore).

The embryos were fixed in 4% PFA in PBS for 2 hours at room temperature and then stored in methanol at -20°C.

The day after they were:

- rehydrated through a dilution series of methanol (MeOH) in PBST (PBS supplemented with 0.1% Tween)
- digested with Proteinase K (10 μg/ml) for 30 minutes at room temperature.
- fixed in 4% PFA for 15 minutes
- washed several times in PBST
- incubated in ethanol/100% acetic acid 2:1 at -20°C for 15 minutes
- washed in PBST several times

- equilibrated for 15 minutes at room temperature in 75 µl equilibration buffer
- transferred to 15 µl terminal transferase enzyme solution mixed with reaction buffer 1:2, 0.3 % TritonX-100
- incubated on ice for 1 hour
- incubated at 37°C for 1 hour
- washed in stop solution for 5 minutes at room temperature
- incubated 45 minutes at 37°C
- washed several times in PBT
- incubated several hours in blocking solution (10% goat serum in PBT) at room temperature
- incubated with α-DIG Fab fragments conjugated to alkaline phosphatase (Roche).

The second day of the experiment, embryos were washed in PBT for a total time of 3 hours, then equilibrated in staining buffer (100 mM Tris pH 9.5, 100 mM NaCl, 50 mM $MgCl_2$, 0.1% Tween) two times for 10 minutes.

Finally embryos were stained in staining buffer with NTB and BCIP, and washed in PBT.

After the staining, the embryos were embedded in gelatin/albumin with 4% glutaraldehyde, and 20 µm sections of the retina were cut using a VT1000 S vibratin blade microtome (Leica). The sections were analyzed on a Leica Upright Widefield epifluorescence microscope.

4.6 Transcription analysis

Gene transcription analysis was carried out using two techniques: in situ hybridisation (ISH) and quantitative reverse transcription polimerase chain reaction (qRT-PCR).

In situ hybridization is a powerful and versatile tool for the localization of specific mRNAs in cells or tissues, ISH doesn't provide quantitative information but qualitative information about the location of mRNA within the tissue samples.

Conversely qRT-PCR is a sensitive quantitative technique used for absolute quantitation, but doesn't provide data about the spatial gene expression patterns.

4.6.1 In-situ hybridization

1. Fixation

Embryos were fixed, at 48 hours after injection, in 4% PFA in PBS, overnight at 4°C. The next day the PFA/PBS was replaced by 100% methanol and embryos were stored overnight at -20°.

2. Rehydration and hybridization with digoxigenin-labelled antisense probe
The embryos were rehydrated with washes of 5 minutes, through a dilution series of MeOH in PBST at room temperature. Then they were washed two times for 5 minutes in PBST, and afterwards were digested with proteinase K 10 μg/ml at room temperature. Again embryos were quickly rinsed in PBST, refixed in paraformaldehyde 4% in PBS for 20 minutes at room temperature and washed 5 times in PBST for 5 minutes. Embryos were then prehybridized in HY4 buffer for 1 hour at 70°C, and successively hybridized with the antisense dioxygenine labeled RNA probes diluted in HY4 buffer overnight at 70°C.

3. Immunodetection of hybridised probe

The day after, embryos were washed: (I) two times in 50% formamide/50% 2xSSC, 0,1%tween-20 for 30 minutes at 70°C; (II) once in 2xSSC, 0,1% tween-20 for 15 minutes at 70°C; (III) twice in 0,2xSSC, 0,1% tween-20 for 30 minutes at 70°C; (IV) in PBS-Tween for 20 minutes, twice at room temperature.

Embryos were then incubated in blocking buffer (5% goat serum in PBST) 8 hours at room temperature, and incubated overnight at 4°C with the anti-DIG antibody (Roche) 1:2000 in blocking buffer.

4. Alkaline phosphatase (AP) staining with BCIP/NBT chromogenic substrate

The day after embryos were washed 6 times in PBST for 20 minutes at room temperature, and twice in staining buffer (100mM Tris pH 9.5; 100mM NaCl; 50mM MgCl2 and 0,1% tween) for 5 minutes at room temperature. Finally the probe was detected by colored reaction using NBT/BCIP (Roche) at least 1 hour at room temperature, which was stopped by washes in PBST. Finally the embryos were refixed in 4% PFA in PBS for 1 hour at room temperature and stored at 4°C.

5. Preparation of the dioxygenine (DIG) labeled RNA probes

Full-length cDNA sequence were cloned into PCR 4-TOPO vector (Invitrogen), which has T3 and T7 RNA polymerase sites flanking the insert. Sequence analysis confirmed the orientation of gene insertion and thus the priming site necessary for generating sense and antisense probes.

To obtain the antisense dioxygenine (DIG) labeled RNA probes, plasmids were digested overnight with the indicated restriction enzyme at 37°C.

Digested DNA were purified with the kit NUCLEOSPIN GEL EXTRACTION PCR CLEAN UP (Roche) and then were transcribed by mixing them with: 10x DIG-RNA labelling mix (Roche); 10x transcription buffer (Roche); T7 RNA polymerase; RNAesy and ddH2O. The reaction was incubated 2 hours at 37°C, and then samples were incubated with DNAs (Ambion) for 15 minutes at 37°C. Probes were purified with the kit NUCLEOSPIN RNA II (Machinery Nagel), and checked by running them on a 2% agarose gel, and then stored at -20°C.

6. Vibratome sections and confocal microscopy

After staining, whole-mount embryos were washed twice in PBST.

Then embryos were embedded in gelatin/albumin with 4% of Glutaraldehyde and sectioned (20 µm) on a VT1000 S vibrating blade microtome (Leica). The sections were analyzed on a Leica Upright Widefield epifluorescence microscope and the images were processed using ImageJ, Adobe Photoshop and Adobe Illustrator software.

4.6.2 Real time reverse transcription quantitative polymerase chain reaction

Total RNA was prepared using the TRIzol Reagent (Invitrogen).

The preparations were done following the manufacturer's instructions for RNA-preparations from tissue-samples. For the comparative gene expression experiments at 2 total RNA was extract from 90 embryos per sample. Dechorionated embryos were pooled together and TRIzol was added. The pooled embryos in TRIzol were then snap frozen in liquid nitrogen and transferred directly to the - 80°C freezer until total RNA extraction.

Pooled embryos were transferred from -80°C freezer directly on to ice and as the TRIzol reagent melted the tissue was aspirated through a 1 ml syringe to fully homogenise the tissue for RNA extraction. 0.2 mL of chloroform were added per 1 mL of TRIzol® Reagent used for homogenization. The tube was shaked vigorously by hand for 15 seconds, incubated for 2–3 minutes at room temperature and then centrifuged at 12,000 × g for 15 minutes at 4°C. The upper aqueous phase was removed of the sample by angling the tube at 45° and pipetting the solution out. Avoid drawing any of the interphase or organic layer into the pipette when removing the aqueous phase. For the RNA isolation, 0.5 mL of 100% isopropanol were added to the aqueous phase per 1 mL of TRIzol® Reagent used for homogenization. The samples were incubated at room temperature for 10 minutes and centrifuged at 12,000 × g for 10 minutes at 4°C. The pellet was then washed with 1 mL of 75% ethanol per 1 mL of TRIzol® Reagent used in the initial homogenization. It was then briefly vortexed and centrifuged at 7500 × g for 5 minutes at 4°C. Finally the pellet was resuspended in RNAse H2O and quantified by spectrophotometry.

cDNA was generated with SuperScript II reverse transcriptase (Invitrogen) and then quantified by Nanodrop spectrophotometer and let run on a gel to check for the effective synthesis.

For real time PCR amplification, a 20 μL reaction contained 1.3 μL of RT product, 10 μL SYBR green Supermix (Bio-Rad) in the presence of 300 nM of specific primers. Amplification was performed in a StepOnePlus Real-Time PCR system and the following primers were used to validate the data from *in situ*.

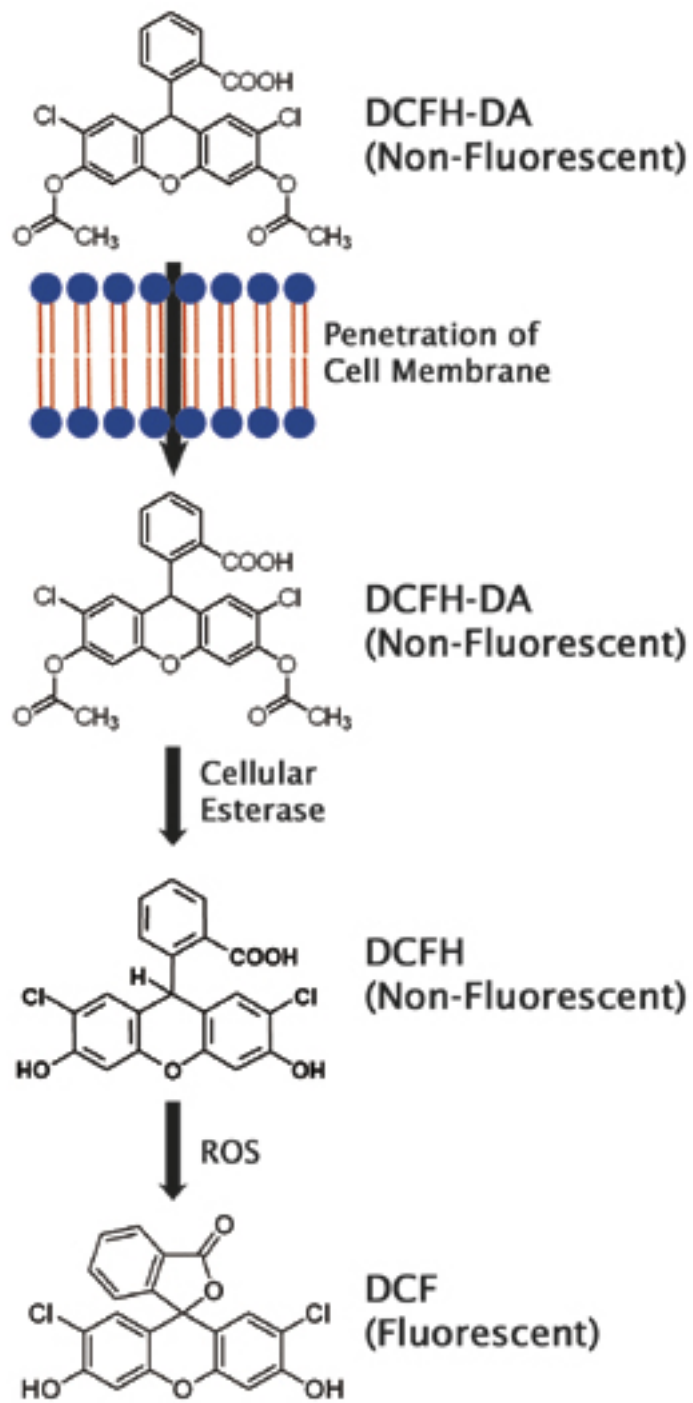| Gene	GenBank Accession Number	Primer Seq 5' – 3'	Tm in °C	Product lenght (bp)
Ngn1 fw	NM_131041.1	ATCTGGGCAACTTTCGGAGAC	59,4	102
Ngn1 rev		GCATCTGCCATGCAGCTTAG	59,4	
Her6 fw	NM_131079.1	AATGACCGCTGCCCTAAACA	57,3	102
Her6 rev		TCACATGTGGACAGGAACCG	59,4	
c-myc fw	NM_001040051.1	GCGCATTACAGAGCATCCGA	60.88	133
c-myc rev		CCAAGGCATTGTTGGGCTTC	60.04	
p27b fw	NM-212792.2	GCTCCTGTCTCGACTCATCG	61,4	116
p27b rev		TGTGGGTGTCGGACTCAATG	59,4	
cyclinD1 fw	NM_131025.4	TCCCTCCATGATTGCAGCAG	59,4	80
cyclinD1 rev		ATGAGAGGCAACTGTCGGTG	59,4	
Islet1 fw	NM_130962.1	AATGGCAGCAGAGCCCATTT	57,3	147
Islet1 rev		GGTCGAGGGTTGGCATTGTA	59,4	

4.7　Reactive oxygen species detection

The generation of reactive oxygen species (ROS) was investigated either in a direct and an indirect manner.

ROS were directly detected using an indicator for reactive oxygen species that is H_2DCFDA, and indirectly analyzing the formation of an endogenous lipid peroxidation product like 4-HNE.

4.7.1　H_2DCFDA assay

H_2DCFDA was used to detect the presence and the localization of reactive oxygen species (ROS) in zebrafish retina. H_2DCFDA is a derivate of fluorescein that diffuses into cell cytoplasm where it is deacetylate by esterases, and further oxidized by many different ROS species (hydrogen peroxide, hydroxyl radicals and eroxynitrite)　forming a deacetylated oxidized product, DCF [102].

Fig.4.7.1   Figure   has   been   reproduced   from http://www.komabiotech.co.kr/www/product/productdesc.phtml?seq=515.

A solution of 10mM H$_2$DCFDA was prepared diluting the powder in DMSO.

Zebrafish embryos at 48 and 72 hours post fertilization (hpf) were incubated with H$_2$DCFDA (50 µM) for 2 hours, in fish water in the dark at 28°C. At the end of the incubation time, embryos were anesthetized with Tricaine before to be mounted in agarose and analyzed on a Zeiss LSM710 confocal microscope (Zeiss).

Fluorescence was excited with a 488 nm laser and detected from 500 to 550 nm. The images were analyzed using ImageJ, Adobe Photoshop and Adobe Illustrator software.

4.7.2 4-hydroxynonenal immunostaining

The 4-hydroxy-2-alkenals are the most prominent lipid peroxidation products and are implicated as key mediators of oxidative stress [103].

4-hydroxynonenal (4-HNE) is a α,β-unsaturated aldehyde, highly reactive thanks to the conjugation of the double bond with the aldehyde function.

4-HNE is formed from the oxidation and degradation of ω-6 PUFAs (linoleic and arachidonic acid) [104]. The exact mechanism of formation for 4-HNE is debated, but it is thought that β-cleavage of the hydroperoxide [9S- or 13S-hydroperoxy-9Z, 11E-octadecadieneoic acid (9S-HPODE, 13S-HPODE)] creates an intermediate precursor, 4-hydroperoxy-2E-nonenal (4-HPNE), which is reduced to 4- HNE [105].

The immunostaining was performed as already described in the paragraph 1.2.1, with little modification.

For the washes of slides was used a solution of PBS supplemented with 1% DMSO and 0.1% Triton, and the blocking was carried out in a solution of PBS supplemented with 1% BSA, 1% DMSO and 0.1% Triton.

Retina sections of wildtype embryos at 48 and 72 hpi were incubated with a primary antibody anti 4-hydroxynonenal (ADI) 1:100 in PBS/1% DMSO/

65

0,1% Triton, and then with a secondary antibody Alexa488 fluorophore-conjugated secondary antibody diluted 1:500 (Invitrogen Molecular Probes) together with DAPI nuclear marker (Sigma) 1:500 in PBS/1% DMSO/ 0,1% Triton.

5 Results

5.1 9-HSA is endogenously produced in zebrafish embryos.

9-HSA belongs to a class of lipid peroxidation products that have been found to be endogenously produced in human cancer cell lines [28, 29]. To elucidate if 9-HSA could be endogenously produced also in vivo, in zebrafish, a total lipid extraction was performed on whole embryos at 5 dpf. In order to have a control sample, the extraction was performed at the same time on a human colon cancer cell line (HT29), in which the endogenous production of 9-HSA has already been detected. The embryos were let grow until 5 dpf and then the lipid extraction was performed using the Folch method. The quantification of the endogenous amount of 9-HSA has been calculated considering the ratio of the signal of the internal standard (IS) and the one of 9-HSA. The signal of 9-HSA has been correlated with the amount of the added IS (50ng/ml) and is approximately 63 ng/ml. In the figure 1 is reported: in the panel below the chromatogram of the signal intensity obtained in matrix. In this chromatogram is visible a non-optimal purification, with several detectable signals. The parallel injection of 9-HSA in the calibration line confirmed the linearity of the response (R^2> 0,99). The analysis demonstrates that 9-HSA is endogenously produced in zebrafish embryos at 5 dpf, as already observed in human cell lines.

These data let us speculate the possible involvement of 9-HSA in the endogenous regulation of cellular signaling pathways, as already proposed in human cell lines.
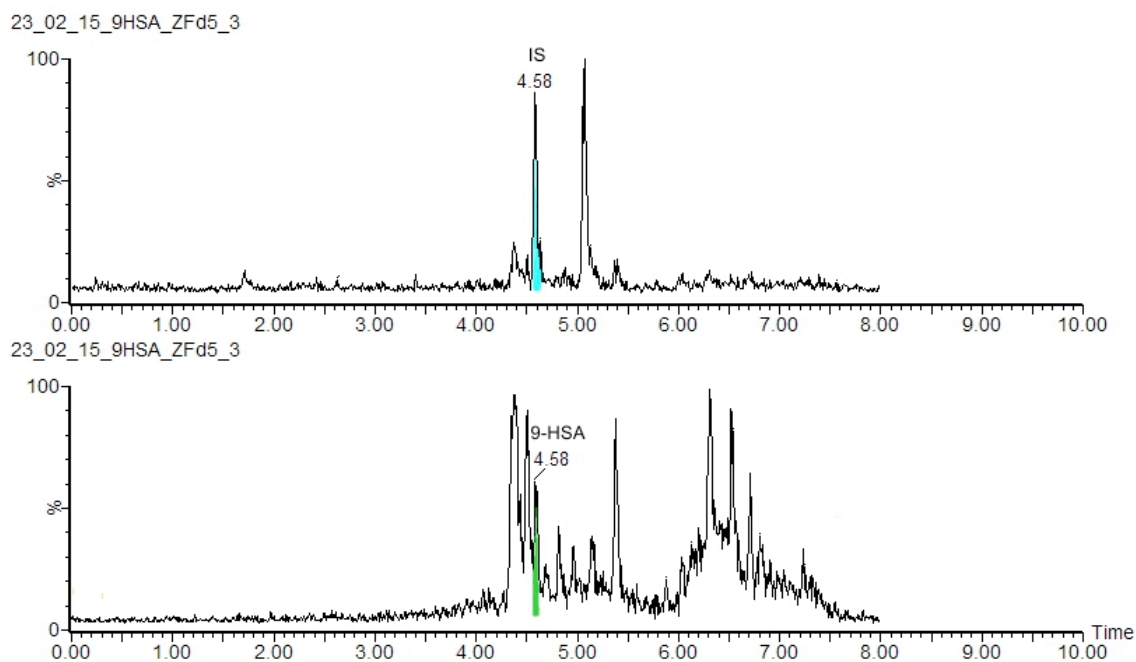
Fig. 1. Chromatogram relative to zebrafish embryos at 5 dpf. In the upper panel is highlighted the peak relative to the IS. In the panel below the peak relative to the endogenous 9-HSA.

5.2 Zebrafish HDAC1 activity is inhibited by (R)-9-HSA

To assess that (R)-9-HSA acts in zebrafish as an HDAC1 inhibitor, as already observed in human cancer cell lines, the level of histone acetylation was analyzed in embryos treated with the molecule at different time point, and was then compared with the acetylation levels observed in wild type embryos and *add^{rw399}* mutant embryos at the same time point.

Immunostaining analysis, using an anti-acetylated histone H4 antibody, showed higher acetylation levels in (R)-9-HSA treated embryos that were comparable with that of *add^{rw399}* mutants. The effect on HDAC1 activity was observed at 48 and 72 hours post injection and fertilization (Fig. 2).
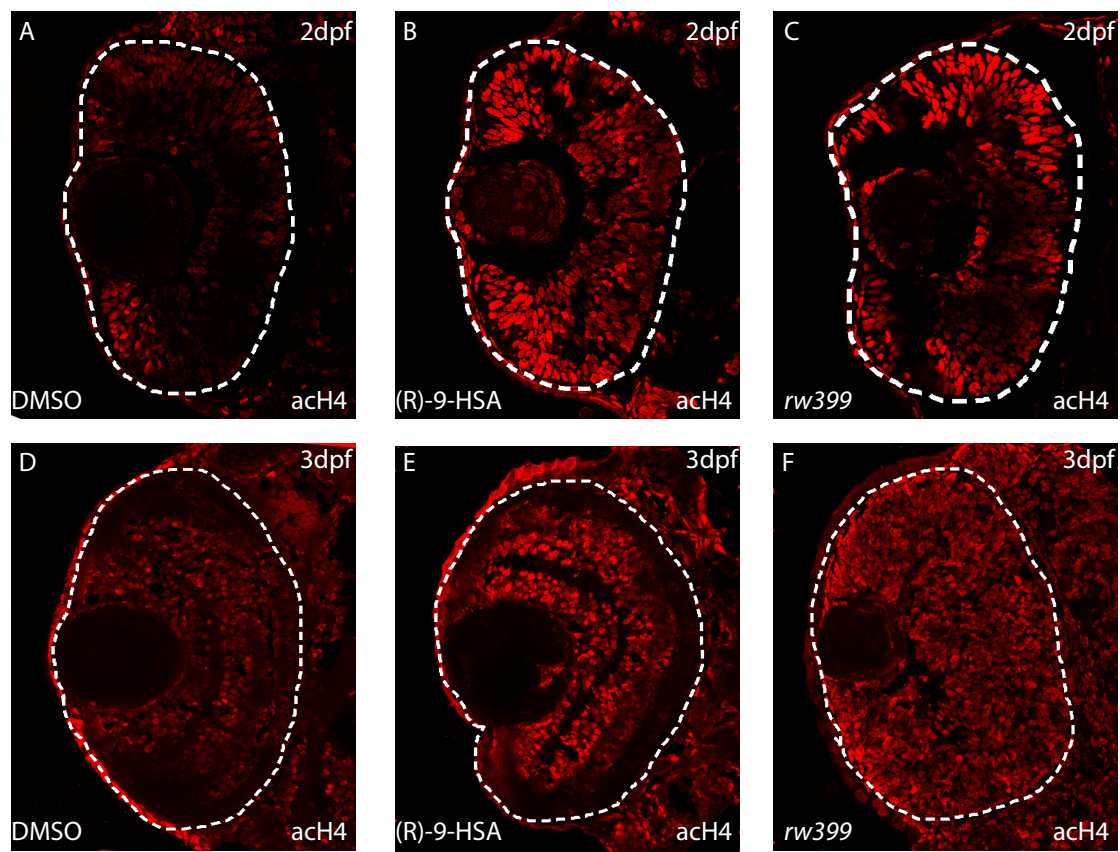
Fig.2 (R)-9-HSA inhibits the enzymatic activity of HDAC1. (A,B,C) cryosections of zebrafish retina 48 hpf/hpi, labeled with an antibody anti-hyperacetylated histone H4 (red). (A) cryosection of DMSO treated retina, (B) cryosection of (R)-9-HSA treated retina, (C) cryosection of *r399* mutant retina. (D, E, F) cryosections of zebrafish retina 72 hpf/hpi, labeled with an antibody anti-hyperacetylated histone H4 (red). (D) cryosection of DMSO treated retina, (E) cryosection of (R)-9-HSA treated retina, (F) cryosection of *r399* mutant retina. Sections were counterstained with DAPI.

Immunostaining experiments were repeated at least three times on groups of 20 embryos for each samples. Data shown are representative examples of each experiment.

5.3 (R)-9-HSA regulates cell proliferation in a tissue dependent manner

To elucidate if the inhibition of the enzymatic activity of HDAC1 observed after the treatment with (R)-9-HSA was inducing abnormalities in the signaling pathways normally under control of HDAC1, we decided to focus our analysis on two tissues of zebrafish embryo where the requirement of HDAC1 is well documented, and its function is opposite.

HDAC1 is required both in zebrafish hindbrain and retina to regulate Notch and Wnt pathways.

It has already been reported [52,54] that, in add^{rw399} mutant embryos, the retina appears multifolded without its proper lamination, and showed a severe reduction of cellular subtypes as retinal ganglion cells and photoreceptors.

Masai et all [73] demonstrated that the overgrowth of add^rw399 retina was a consequence of the continue proliferation of retinal progenitors cells, that in the absence of HDAC1 are not capable of exit from the cell cycle and differentiate in the different retinal subtypes.

It was examined if the (R)-9-HSA inhibition of HDAC1 activity could reproduce the effects on cell proliferation and differentiation already observed in add^{rw399}.

Histone H3 is phosphorylated on serine 10 during chromosome condensation in mitosis, and for this reason is considered a marker of the late G2/M phase of the cell cycle.

A phospho-histone H3 assay was performed to quantify the percentage of cells block in this phase of the cell cycle.

The experiment was performed on zebrafish hindbrain at 24 hours post injection (24hpi).

It has been reported that HDAC1 activity is required in the hindbrain for a proper formation of neuronal subtypes and glia, and its loss of function affects cell proliferation at 24 hpf [52].

The count of phospho-histone H3 positive cells revealed a reduction of the proliferation after the treatment with the molecule compared to the control (Fig.3).
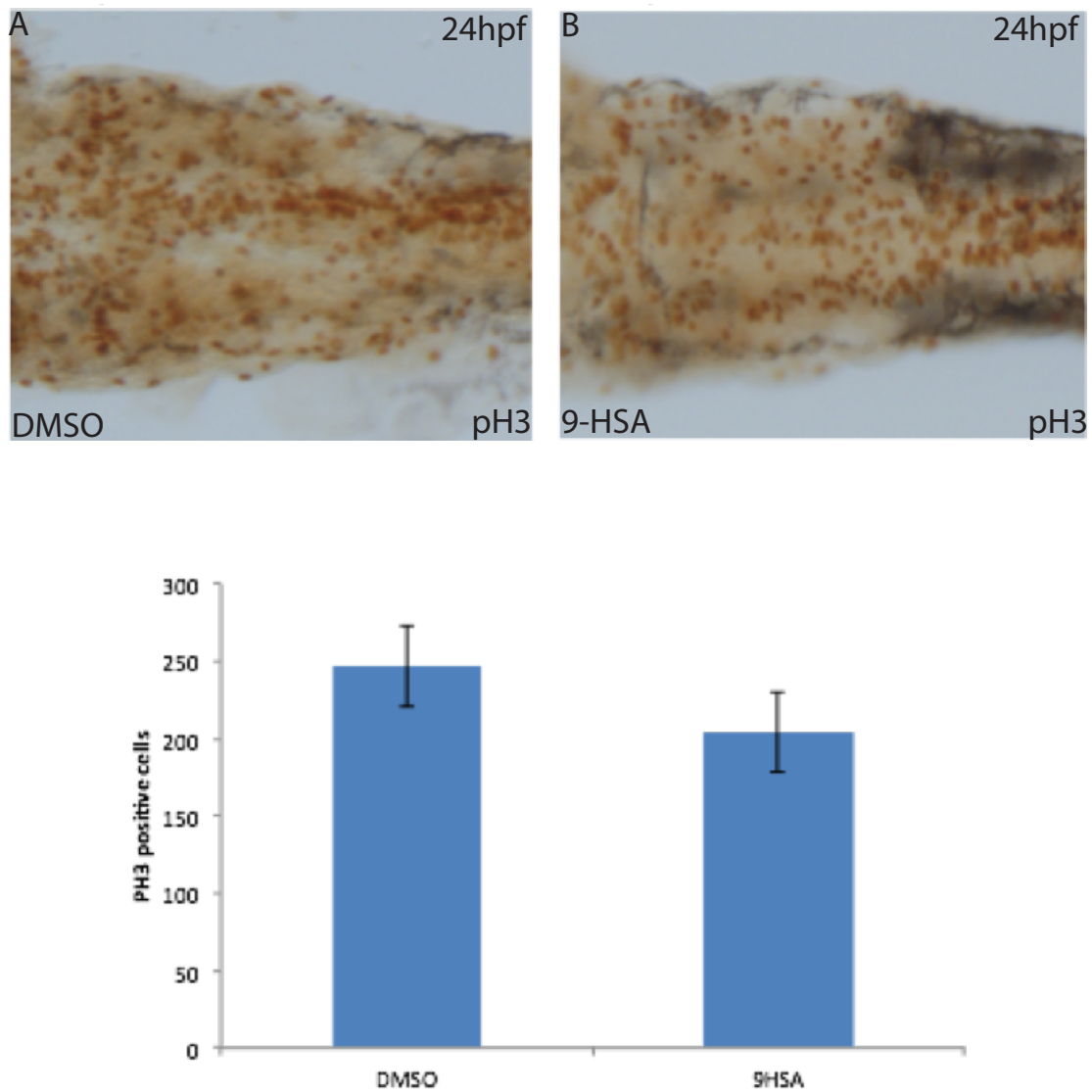

Fig. 3 (R)-9-HSA effect on cell proliferation in zebrafish hindbrain 24 hpi. (A, B) dorsal views of hinbrains from (A) DMSO treated embryos, (B) (R)-9-HSA treated embryos, immunostained for the mitosis marker phospho-H3. In the panel below the quantification after the staining, with the count of the positive cells for phospho-H3 in

DMSO and (R)-9-HSA treated embryos. Experiments were all repeated at least three times on groups of 20 embryos for each sample.

Data shown are representative examples of each experiment. Data are presented as mean ± Standard deviation (SD). p = 0,005

To evaluate phospho histone H3 incorporation in cells in the retina, an immunostaining, with the antibody anti phospho-histone H3, on retina cryosections from embryos at 48 and 72 hpf/hpi was performed. The labeling of the retina with anti-phosporilated histone H3 antibody revealed that at 48 hpi the percentage of cells in the M phase of the cell cycle was higher in the (R)-9-HSA treated embryos and add^{rw399} mutant embryos compared to the wild-type (Fig.4).
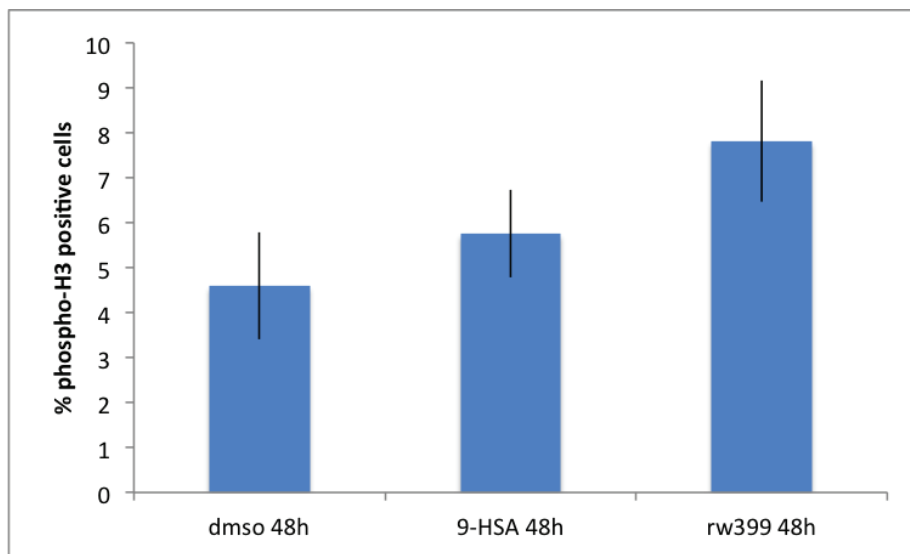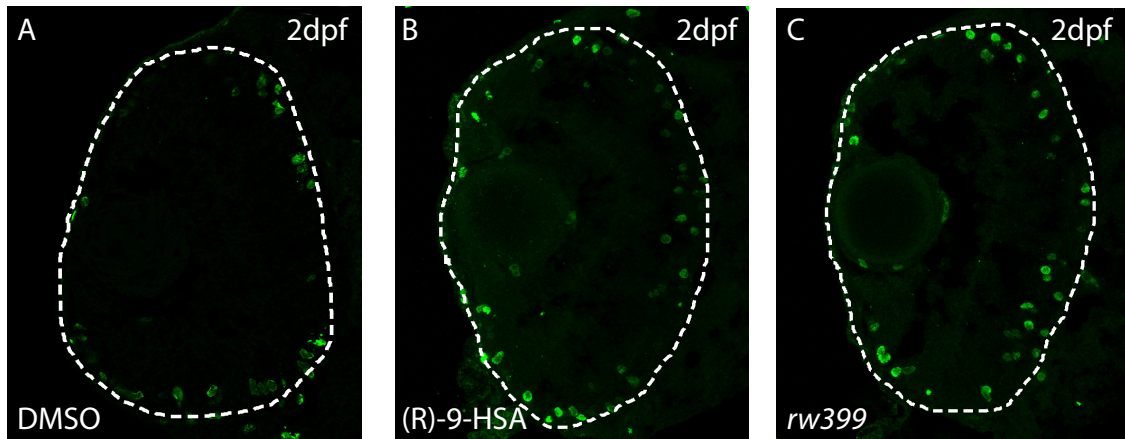
	pH3histone (%)	standard deviation
dmso 48h	4,6	1,2
9-HSA 48h	5,76	0,98
rw399 48h	7,82	1,35

Fig.4 (A,B,C) labeling with anti –phospho-histone H3 antibody (green) of cryosections at 48 hpi of retina from (A) DMSO treated embryos, (B) (R)-9-HSA treated embryos, (C) *rw399* mutant embryos. In the histogram below the percentages of the number of mitotic cells labeled with anti-phopshorylated histone H3 antibody to total number of cells marked with DAP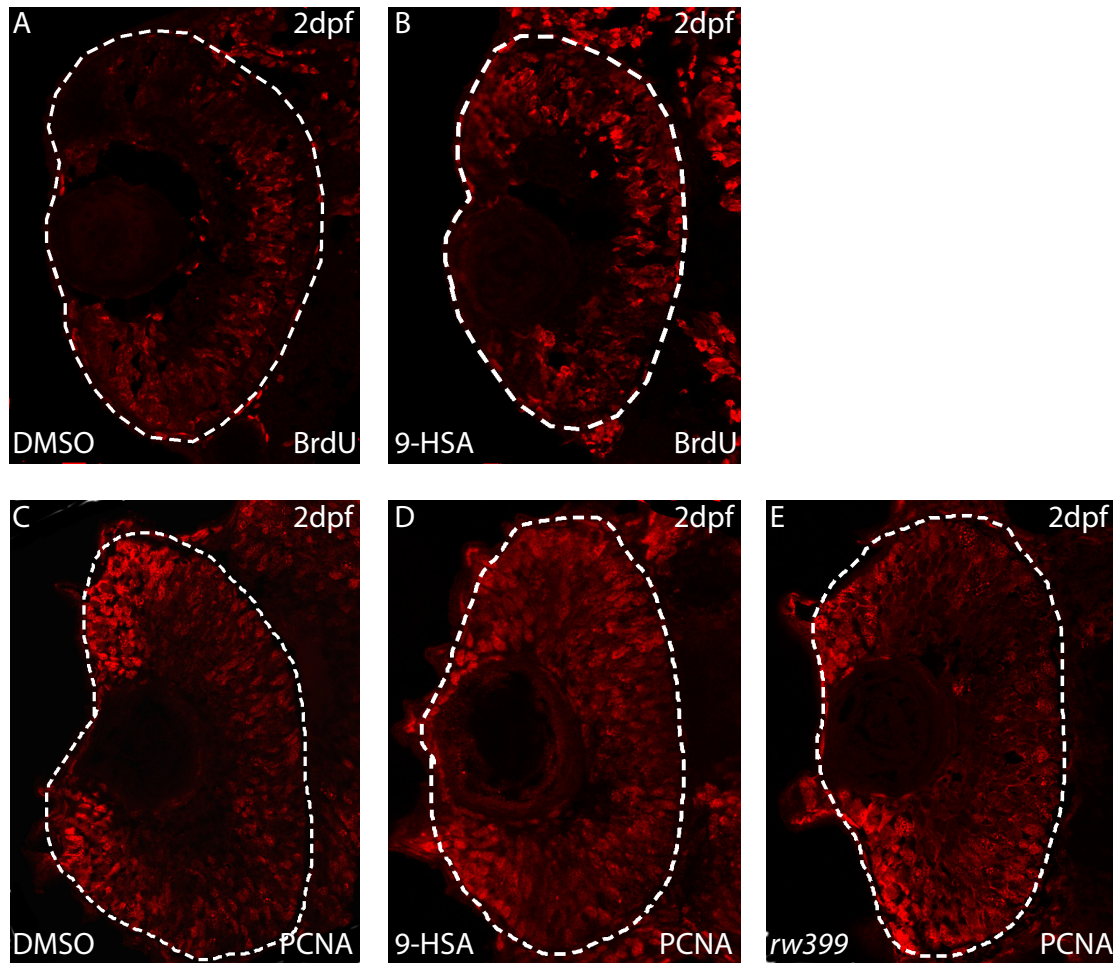I. Data are presented as mean ± Standard deviation (SD). Immunostaining experiments were repeated at least three times on groups of 20 embryos for each sample. Data shown are representative examples of each experiment.

To analyze the amount of cells in the S phase of the cell cycle, an immunostaining for the bromodeoxyuridine (BrdU) on retina cryosections at 48 hpi was performed.

BrdU is an analogue of thymidine and can thus be incorporated into newly synthesized DNA double strand of replicating cells.

The labeling of dividing cells with BrdU revealed that at 48 hpi, in the retina of (R)-9-HSA treated embryos and wild-type embryos, the pattern of expression of mitotic cells was the same as the one resulting from the proliferating cell nuclear antigen (PCNA) staining at the same time point, with most part of the mitotic cells localized in the ciliar marginal zone (CMZ) and the outer nuclear layer (ONL) (Fig.5).

Fig.5 BrdU labeling of 48 hpi retina cryosections of (A) DMSO treated embryos, (B) (R)-9-HSA treated embryos. (C, D, E) PCNA staining of 48 hpf/hpi retina cryosections of (C) DMSO treated embryos, (D) (R)-9-HSA treated embryos, (E) *rw399* mutant embryos.

Immunostaining experiments were repeated at least three times on groups of 20 embryos for each sample. Data shown are representative examples of each experiment.

A TUNEL assay was used to analyze the possible apoptotic effect of (R)-9-HSA in the retina at 48 hpi, but no increase of TUNEL positive cells was visible compared to the control (Fig.6).
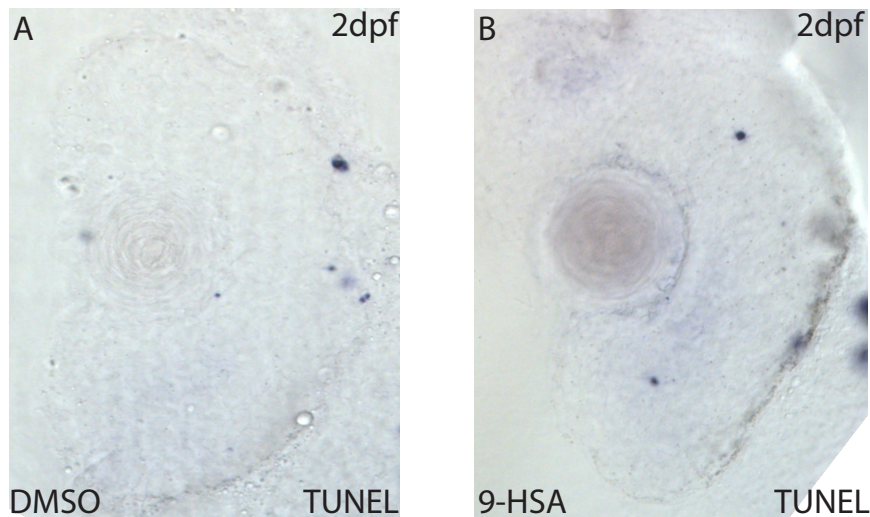
Fig.6 TUNEL assay on 48 hpi retina sections of (A) DMSO treated embryos and (B) (R)-9-HSA embryos. Apoptotic cells are stained in violet.
The most representative figures were choose from a total number of analyzed samples that is: DMSO n=8, 9-HSA n=6. (n = number of embryos)

The effect on cell proliferation in the retina was analyzed also at 72 hpi, using the same markers already investigated at 48 hpi.

In retinas at 72 hpi the difference between the percentage of cells undergoing M phase in (R)-9-HSA treated embryos and DMSO treated embryos was even more pronounced, and all the positive cells were localized in the CMZ and ONL.

In DMSO treated retina at 72hpi, the cells positive for PCNA were very few and all localized in the CMZ, whereas in the (R)-9-HSA treated

embryos, the amount of PCNA positive cells was increased and they were localized for the majority all along the CMZ, and in the ONL (Fig.7).
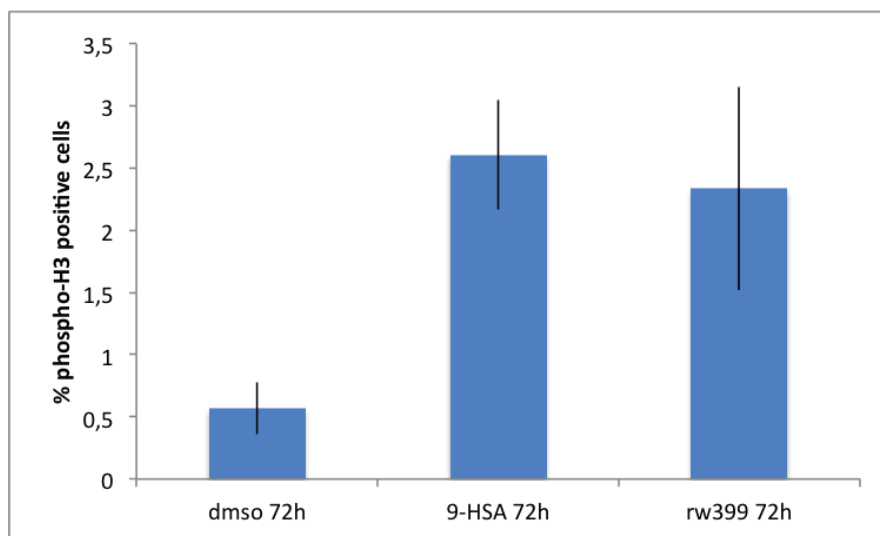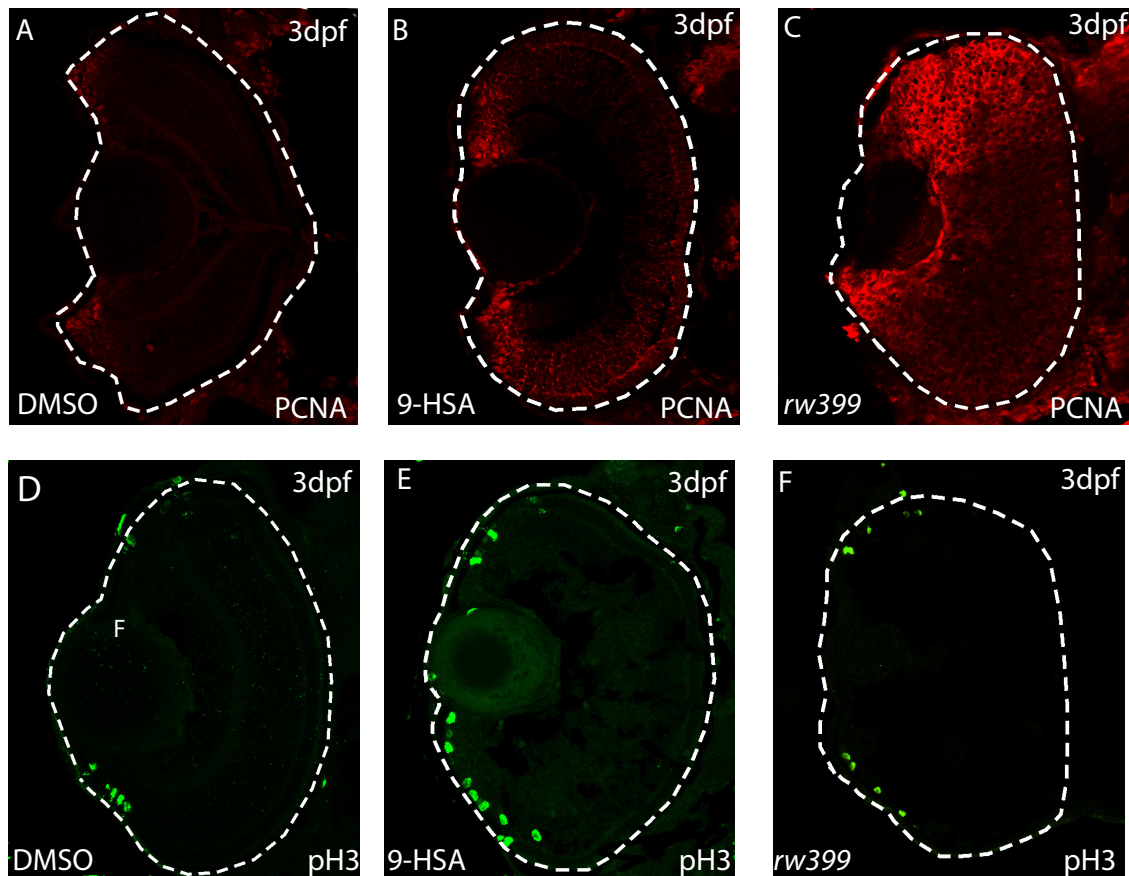
	pH3histone (%)	standard deviation
dmso 72h	0,56	0,2
9-HSA 72h	2,605	0,43
rw399 72h	2,33	0,81

Fig.7 (A, B, C) PCNA staining (red) of 72 hpf/hpi retina cryosections of (A) DMSO treated embryos, (B) (R)-9-HSA treated embryos, (C) add^{rw399} mutant embryos. (D, E, F) phospho-histone H3 staining (green) of 72 hpf/hpi retina cryosections of (C) DMSO treated embryos, (D) (R)-9-HSA treated embryos, (E) add^{rw399} mutant embryos. The signal of both PCNA and phospho-H3 is localized within the CMZ.

In the graph the percentages of the phospho-histone H3 positive cells to total number of cells in add^{rw399} and DMSO and (R)-9-HSA treated retinas are reported. Data are presented as mean ± Standard deviation (SD).

Immunostaining experiments were all repeated at least three times on groups of 20 embryos for each samples. Data shown are representative examples of each experiment.

5.4 (R)-9-HSA inhibits cell differentiation in zebrafish retina

To clarify if the effect of (R)-9-HSA on cell proliferation in the retina was correlated with an impairment of cells differentiation as well, the expression of different retinal subtypes at 48 and 72 hpi was analyzed.

Zn5 is a marker of retinal ganglion cells, the labeling of 48 hpi DMSO treated retina, (R)-9-HSA treated retina and add^{rw399} mutant retina with zn5 antibody showed that there was no differentiation of retinal ganglion cells in the (R)-9-HSA treated retina and in the add^{rw399} mutant retina (Fig.8).
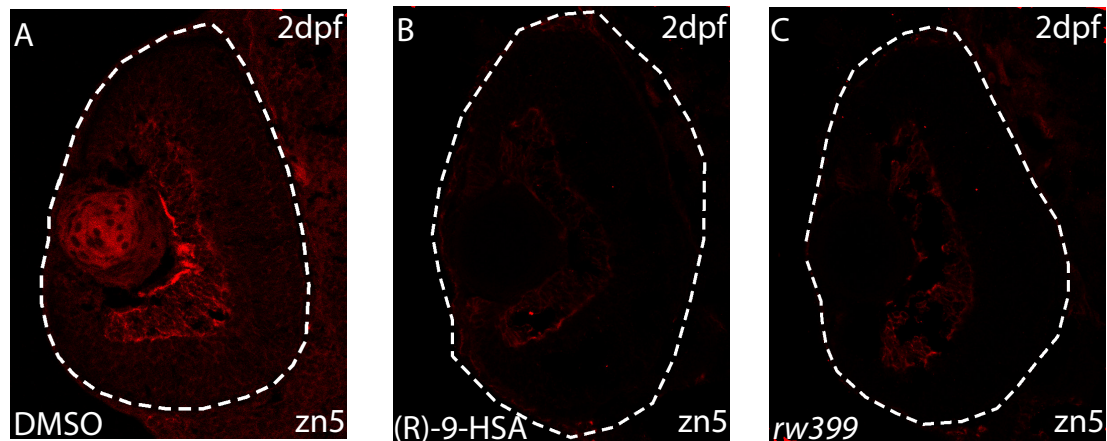
Fig.8 Labeling of retinas from (A) DMSO treated embryos, (B) (R)-9-HSA treated embryos, (C) *add*^{rw399} mutant embryos at 48 hpf/hpi with the zn5 antibody, which stains retinal ganglion cells (red).

Immunostaining experiments were all repeated three times on groups of 20 embryos for each samples. Data shown are representative examples of each experiment.

At 72 hpi the majority of the different retinal subtypes are normally already formed and detectable.

Parvalbumin (PVA) is a marker of amacrine cells. The analysis of its expression at 72 hpi revealed the complete absence of these cellular subtypes in *add*^{rw399} mutant and (R)-9-HSA treated retina. (Fig.9)

The specification of photoreceptors was investigated using an anti zpr1 antibody. The number of differentiated photoreceptors was strongly reduced in (R)-9-HSA treated retina, while they were completely absent in *add*^{rw399} mutant (Fig.9).

Finally was analyzed the presence of Muller cells using an antibody for glutamine synthetase. As already observed for the other retinal subtypes, Muller cells were not formed in *add*^{rw399} mutant and (R)-9-HSA treated retina, while they were well visible in the control (Fig.9).
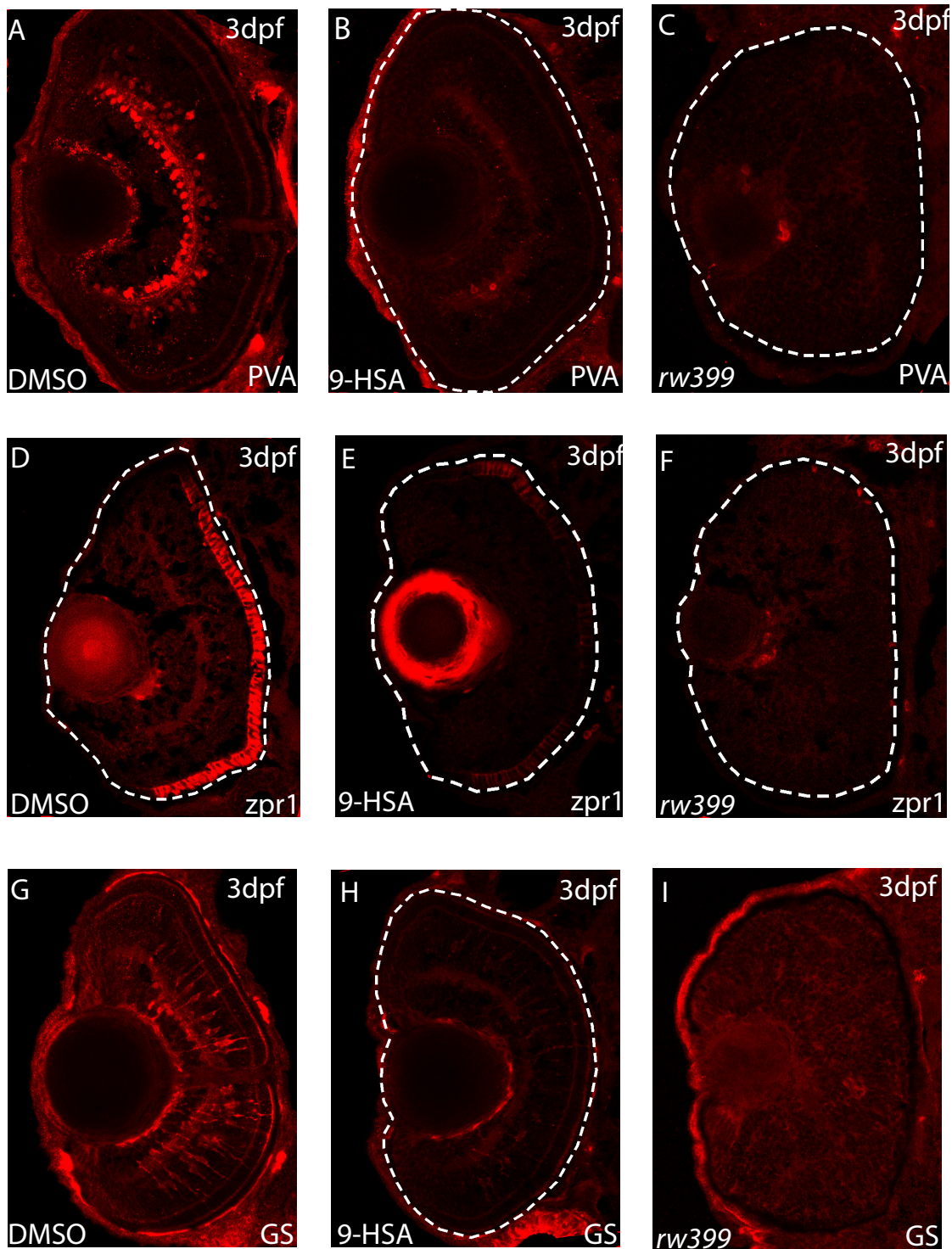
Fig.9 (A, B, C) Labeling of retinas from (A) DMSO treated embryos, (B) (R)-9-HSA treated embryos, (C) *add^rw399* mutant embryos at 72 hpi with the PVA antibody, which stains amacrine cells (red). (L, M, N) Labeling of retinas from (L) DMSO treated

embryos, (M) (R)-9-HSA treated embryos, (N) *add^{rw399}* mutant embryos at 72 hpi with the zpr1 antibody, which stains double cone photoreceptors (red). Labeling of retinas from (G) DMSO treated embryos, (H) (R)-9-HSA treated embryos, (I) *add^{rw399}* mutant embryos at 72 hpi with the anti-glutamine synthetase antibody, which stains Muller glial cells (red).

Immunostaining experiments were all repeated three times on groups of 20 embryos for each samples. Data shown are representative examples of each experiment.


5.5 (R)-9-HSA interfers with gene transcription both in the retina and the hindbrain

To elucidate which are the events upstream the effects on cell proliferation that we observed in the retina and the hindbrain, we examined the expression of genes involved in the regulation of cell cycle and differentiation. In order to validate the in situ hybridization results with quantitative data, a qRT-PCR analysis was set up.

Ngn1 is a proneural gene [106], it is a target of Notch-dependent transcriptional repression, driven by the zebrafish Notch target gene her6 [107, 69, 52].

At 48 hpi ngn1 transcription was reduced in the (R)-9-HSA and in the *add^{rw399}* hindbrain, whereas her6 transcription was increased in the diencephalon of (R)-9-HSA treated embryos and *add^{rw399}* mutant compared to the DMSO treated embryos. The qRT-PCR analysis confirmed the data for ngn1 expression in *add^{rw399}* mutant but not in the 9-HSA treated, whereas for her6 expression a slide induction of the gene is visible in 9-HSA treated and *add^{rw399}* mutant.
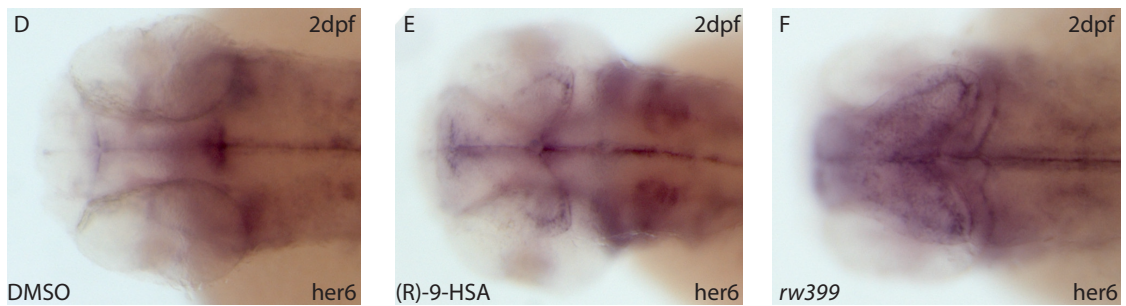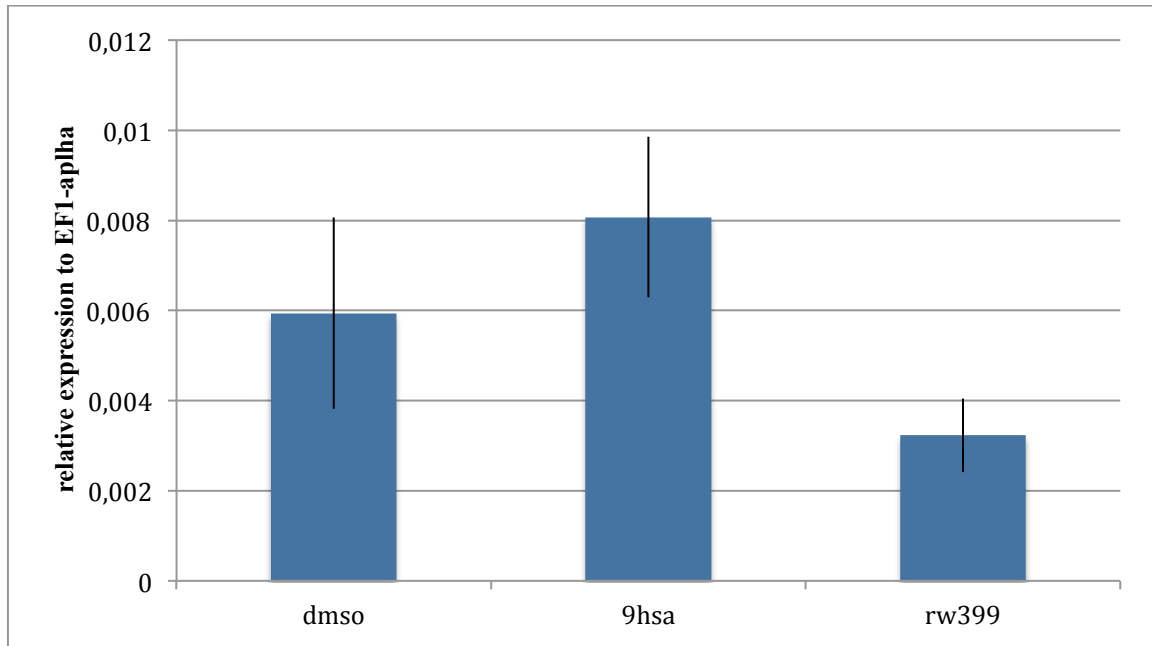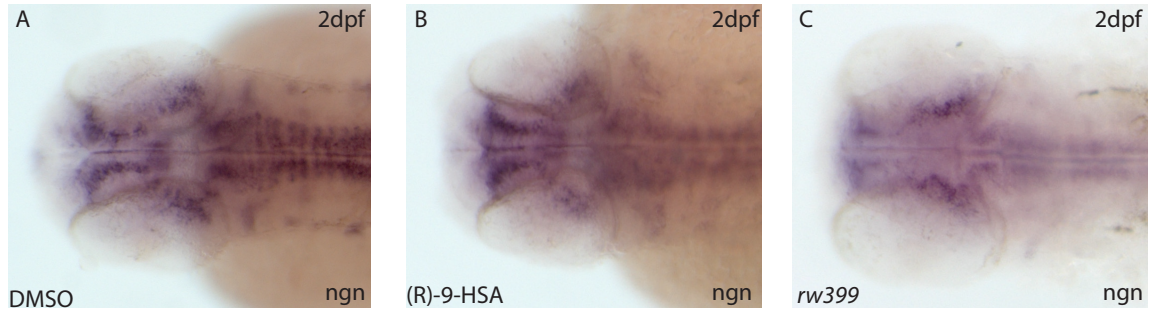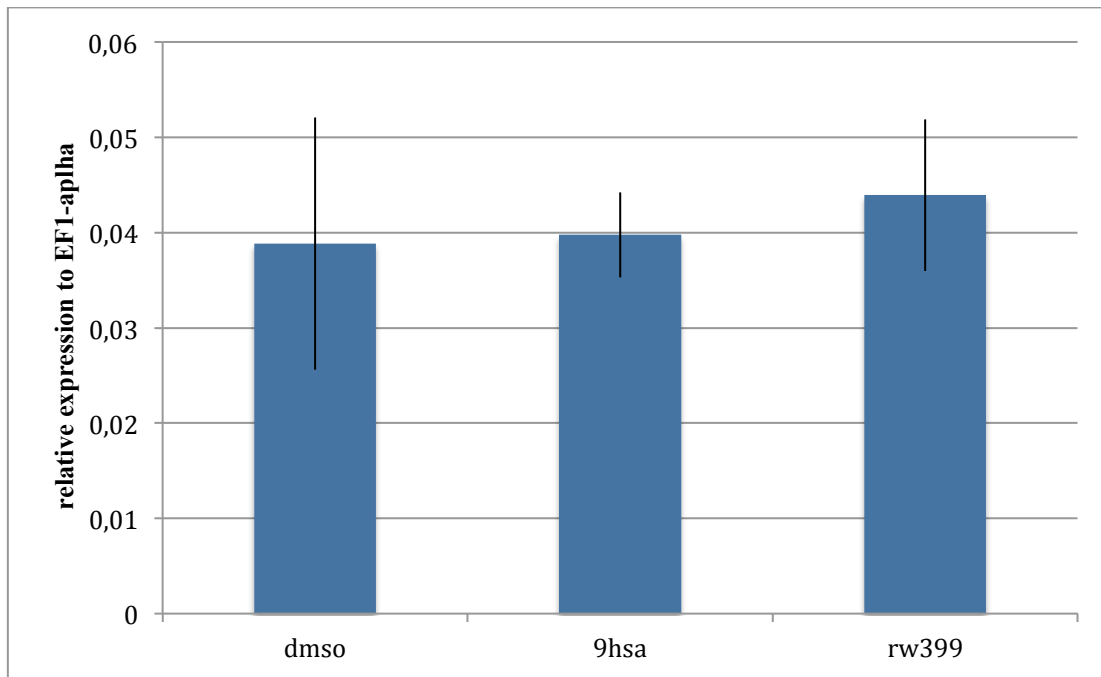
Fig.10 (A, B, C) in situ hybridization analysis of the expression of the proneural gene ngn1 in the hindbrain and the dorsal diencephalon of (A) DMSO treated embryos, (B) (R)-9-HSA treated embryos and (C) add^{rw399} mutant embryos, 48 hpf and 48 hpi

(D, E, F) analysis of the expression of the Notch target gene her6 in the hindbrain and the dorsal diencephalon of (D) DMSO treated embryos, (E) (R)-9-HSA treated embryos and (F) add^{rw399} mutant embryos, 48 hpf and 48 hpi. In all panels, views are dorsal and anterior is towards the left.

All the experiments were repeated three times on groups of 20 embryos for each sample. Data shown are representative examples of each experiment.

In the graphs are reported the data from qRT-CR respectively for ngn1 and her6. qRT-PCR were repeated three times using independent RNA isolation. Data are presented as mean ± Standard deviation (SD), and are normalized to the expression of the housekeeping gene EF1-alpha. p value < 0,05

The analysis was then focused on the effect on the transcription of the proto-oncogene c-myc.

C-myc is involved, in zebrafish, in the regulation of cell proliferation and differentiation [73]. Its expression was highly affected in the retina of the embryo at 48 hpi. At this time point c-myc expression in DMSO treated retina was confined in the most peripheral region of the CMZ, while in (R)-9-HSA treated retina at 48 hpi its expression persisted in the CMZ but also spread to the central retina and in the *add^{rw399}* mutant its transcript was detectable in almost all the retina suggesting a severe upregulation of its transcription in the absence of HDAC1. The qRT-PCR analysis confirmed the data obtained from the *in situ* analysis, showing a slide induction of the gene in 9-HSA treated and *add^{rw399}* mutant respect to the control (Fig.11).
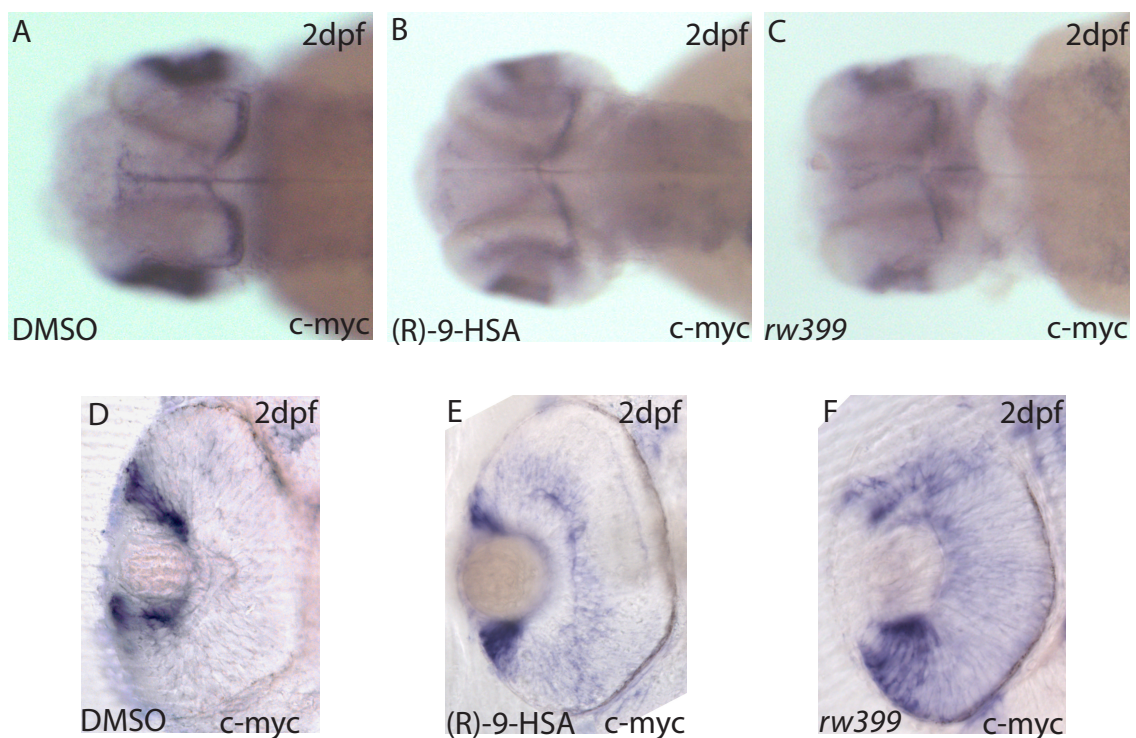
Fig.11 (A, B, C) in situ hybridization analysis of the expression of the proneural gene c-myc in the hindbrain and the dorsal diencephalon of (A) DMSO treated embryos, (B) (R)-9-HSA treated embryos and (C) add^{rw399} mutant embryos, 48 hpf and 48 hpi. (D, E, F) expression of c-myc in retina sections from (D) DMSO treated embryos, (E) (R)-9-HSA treated embryos and (F) add^{rw399} mutant embryos, 48 hpf and 48 hpi.
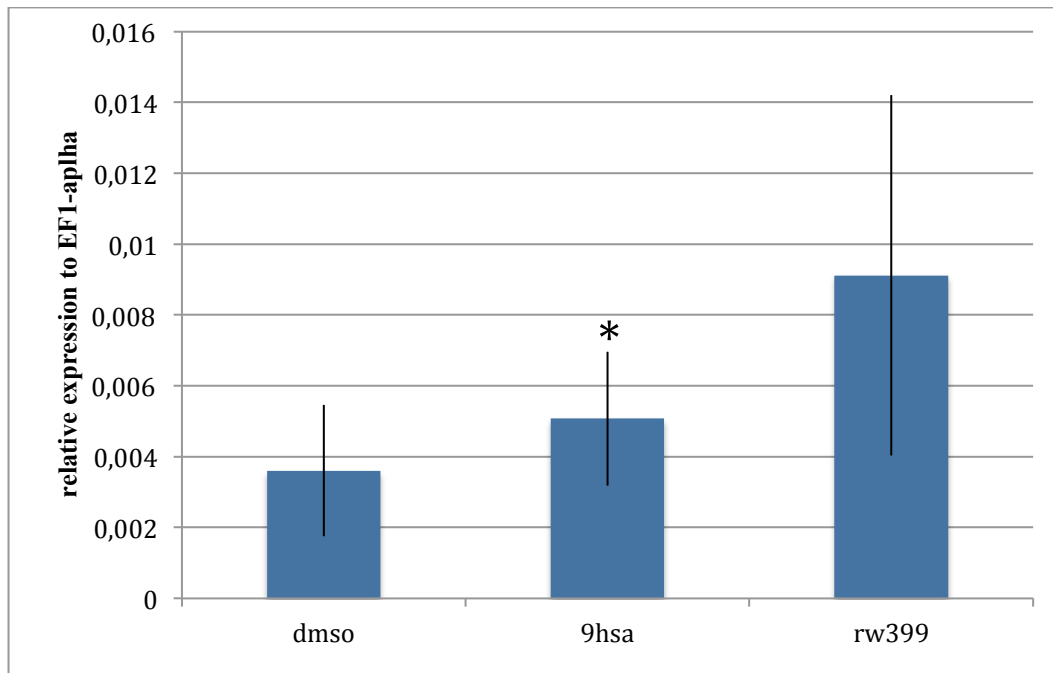
All the experiments were repeated three times on groups of 20 embryos for each samples. Data shown are representative examples of each experiment.

In the graph are reported the data from qRT-CR for c-myc. qRT-PCR were repeated three times using independent RNA isolation. Data are presented as mean ± Standard deviation (SD), and are normalized to the expression of the housekeeping gene EF1-alpha. * p value < 0,05

(R)-9-HSA effect on the transcription of two important regulators of the cell cycle: cyclinD1 and p27, which act downstream of HDAC1 [73], in the retina was then analyzed.

At 48hpi, p27 transcription was downregulated in (R)-9-HSA treated retina and more severely in add^{rw399} mutant retina, where its signal was no more detectable. CyclinD1 expression was on the contrary upregulated both in (R)-9-HSA treated and add^{rw399} mutant retina, with the transcript detectable in the entire retina, while in the DMSO treated retina it was localized just in the CMZ (Fig.12).

The qRT-PCR analysis confirmed the data for p27 expression in add^{rw399} mutant but not in the 9-HSA treated, whereas for cyclinD1 expression a slide induction of the gene is visible in 9-HSA treated but a reduction in its expression is observed in add^{rw399} mutant.

G 2dpf
DMSO cyclind1

H 2dpf
(R)-9-HSA cyclind1

I 2dpf
rw399 cyclind1

L 2dpf
DMSO cyclind1

M 2dpf
(R)-9-HSA cyclind1

N 2dpf
rw399 cyclind1
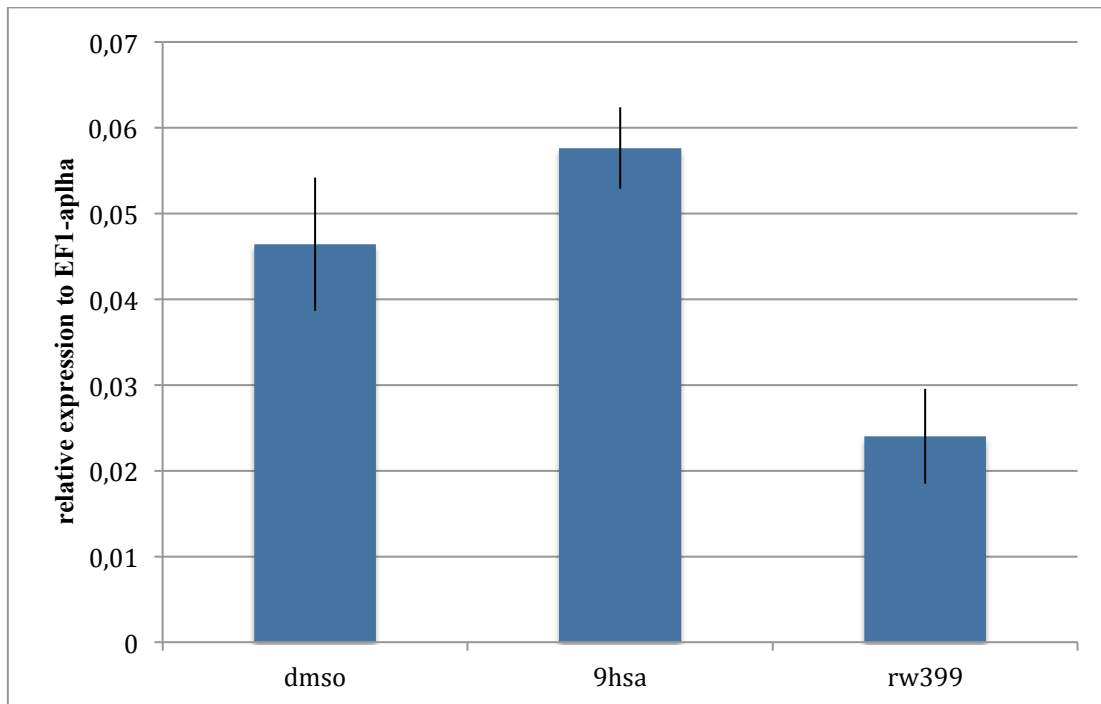
Fig.12 In situ hybridization analysis of two fundamental regulators of the cell cycle: p27 and cyclinD1. (A, B, C) expression of p27 in the hindbrain and the dorsal diencephalon of (A) DMSO treated embryos, (B) (R)-9-HSA treated embryos and (C) *add^{rw399}* mutant embryos, 48 hpf and 48 hpi. (D, E, F) expression of p27 in retina sections from (D) DMSO treated embryos, (E) (R)-9-HSA treated embryos and (F) rw399 mutant embryos, 48 hpf and 48 hpi.

(G, H, I) in situ hybridization analysis of the expression of cyclinD1 in the hindbrain and the dorsal diencephalon of (G) DMSO treated embryos, (H) (R)-9-HSA treated embryos and (I) rw399 mutant embryos, 48 hpf and 48 hpi. (L, M, N) expression of cyclinD1 in retina sections from (L) DMSO treated embryos, (M) (R)-9-HSA treated embryos and (N) rw399 mutant embryos, 48 hpf and 48 hpi.
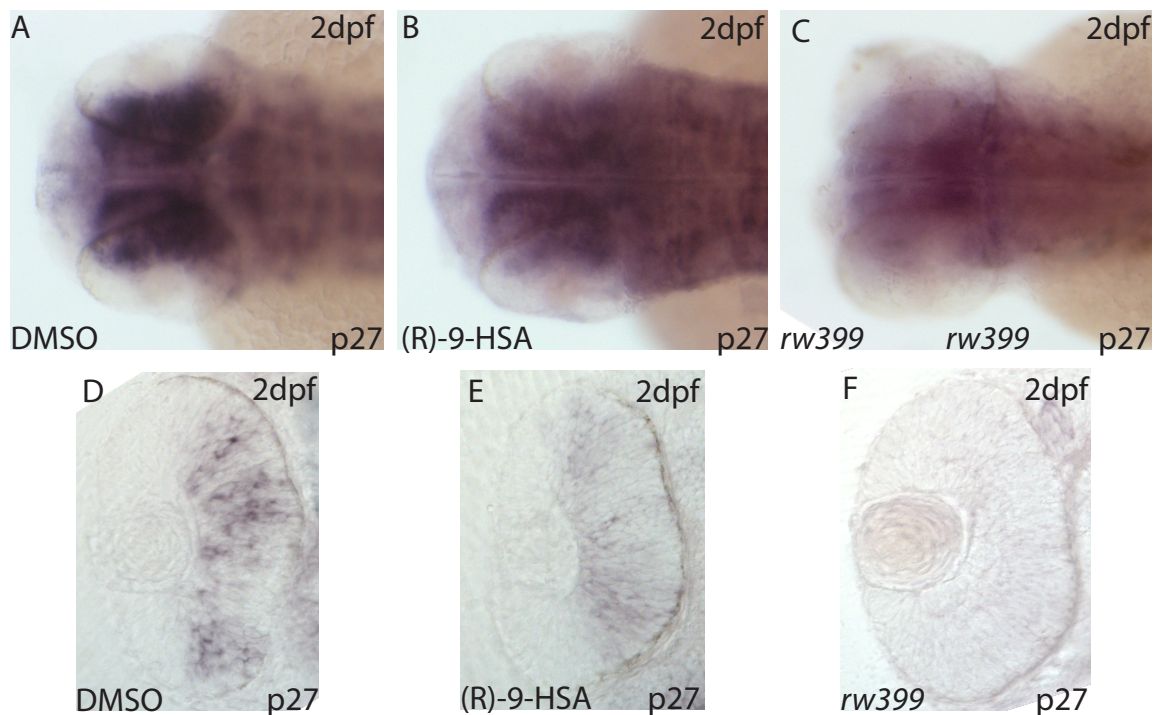
All the experiments were repeated three times on groups of 20 embryos for each samples. Data shown are representative examples of each experiment.

In the graphs are reported the data from qRT-CR respectively for p27 and cyclinD1. qRT-PCR were repeated three times using independent RNA isolation. Data are presented as mean ± Standard deviation (SD), and are normalized to the expression of the housekeeping gene EF1-alpha. p value < 0,05
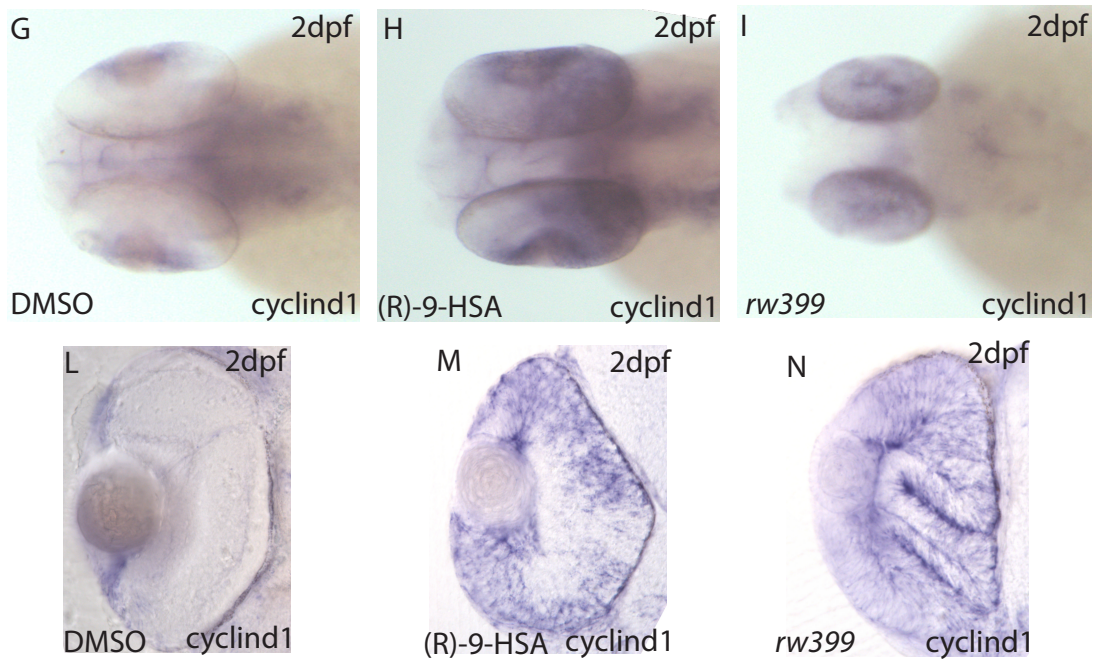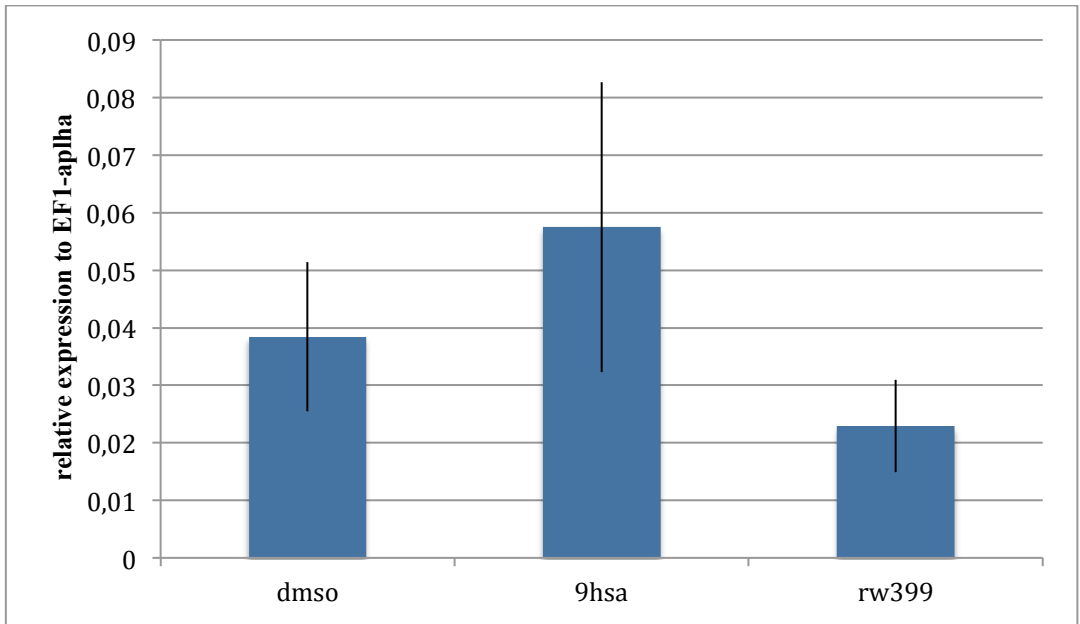
Finally the expression of Islet1 was examined, a differentiation marker that in wild type embryos is generally localized in ganglion and amacrine cells already at 36 hpf [108].

At 48 hpf Islet1 expression was reduced in (R)-9-HSA treated retina and add^{rw399} mutant retina. After the treatment with (R)-9-HSA, Islet1 was still detectable just in a delimited region of the central retina and its expression was also reduced in the hindbrain region (Fig.13). The qRT-PCR analysis confirmed the data for Islet1 expression in add^{rw399} mutant but not in the 9-HSA treated, where an induction of the gene is detectable compared to the control.
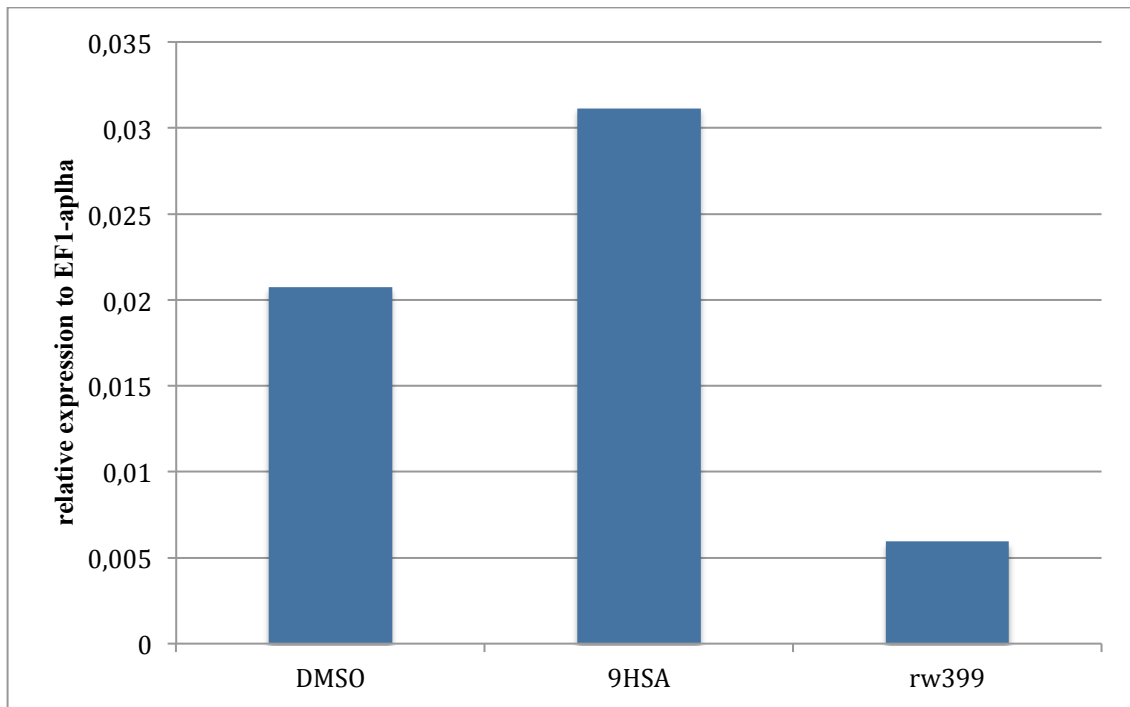
Fig.13 (A, B, C) in situ hybridization analysis of the expression of the differentiation marker Islet1 in the hindbrain and the dorsal diencephalon of (A) DMSO treated embryos, (B) (R)-9-HSA treated embryos and (C) add^{rw399} mutant embryos, 48 hpf and 48 hpi. (D, E, F) expression of Islet1 in retina sections from (D) DMSO treated embryos, (E) (R)-9-HSA treated embryos and (F) add^{rw399} mutant embryos, 48 hpf and 48 hpi.
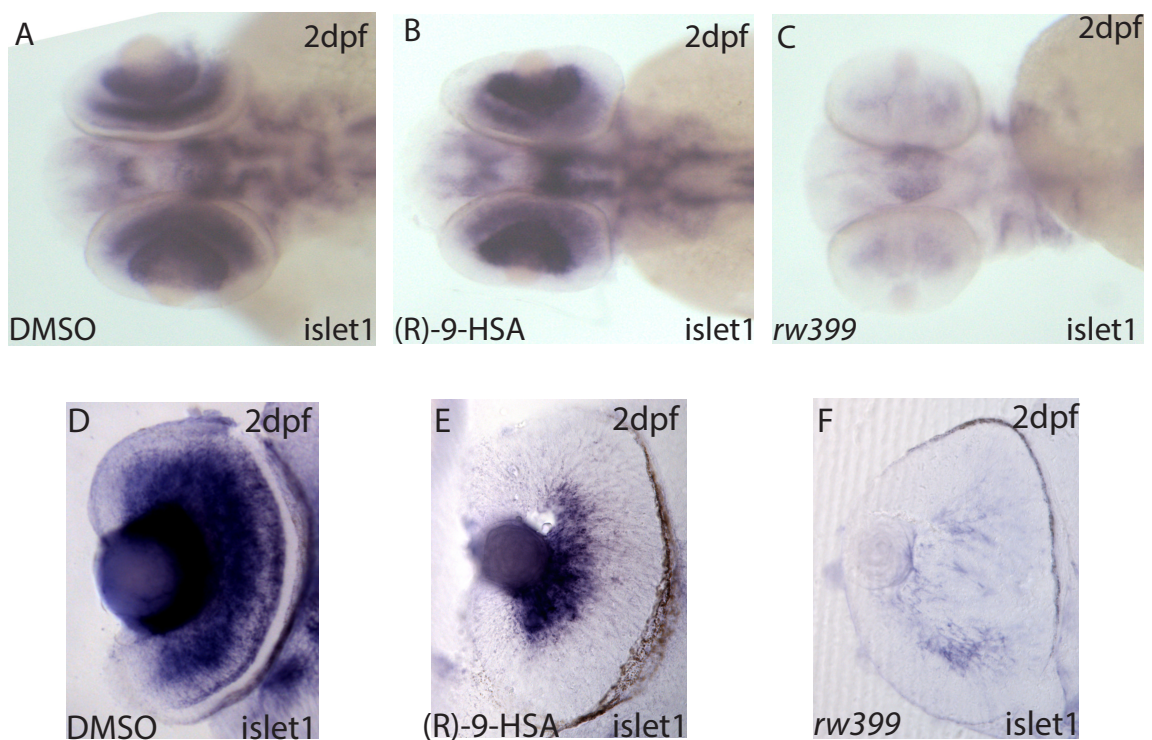
All the experiments were repeated three times on groups of 20 embryos for each sample. Data shown are representative examples of each experiment.

In the graph are reported the data from qRT-CR respectively for Islet. In this case qRT-PCR was performed just once in triplicate. Data are presented as mean, and are normalized to the expression of the housekeeping gene EF1-alpha.

5.6 Ros are produced at highest level in retina ciliary marginal zone.

Previous studies confirmed the presence of two kinds of specialized niches of retinal stem cells, one in the CMZ and one around some Muller glia in the differentiated retina [89].

Due to the observation that the hyperproliferation induced by (R)-9-HSA treatment in the retina, was localized in the CMZ (Fig.3 and Fig.4) the oxidative state of the CMZ in the wild-type retina was analyzed, in order to understand if the effect of the molecule was correlated with an imbalance in the redox state of retinal stem cells.

The endogenous production of ROS in the retina of wild-type zebrafish embryos was analyzed at 72 hpf using the radical sensor H_2DCFDA. The analysis showed that the presence of ROS is localized in the CMZ.

Subsequently, since (R)-9-HSA is an endogenous lipid peroxidation by-product, was examined the expression of one of the major lipid peroxidation products in zebrafish retina, the 4-Hydroxynonenal (HNE).

The labeling of 72 hpf wild-type retina with the anti 4-Hydroxynonenal antibody revealed the presence of this product in the CMZ, confirming the data observed with the radical sensor H_2DCFDA.
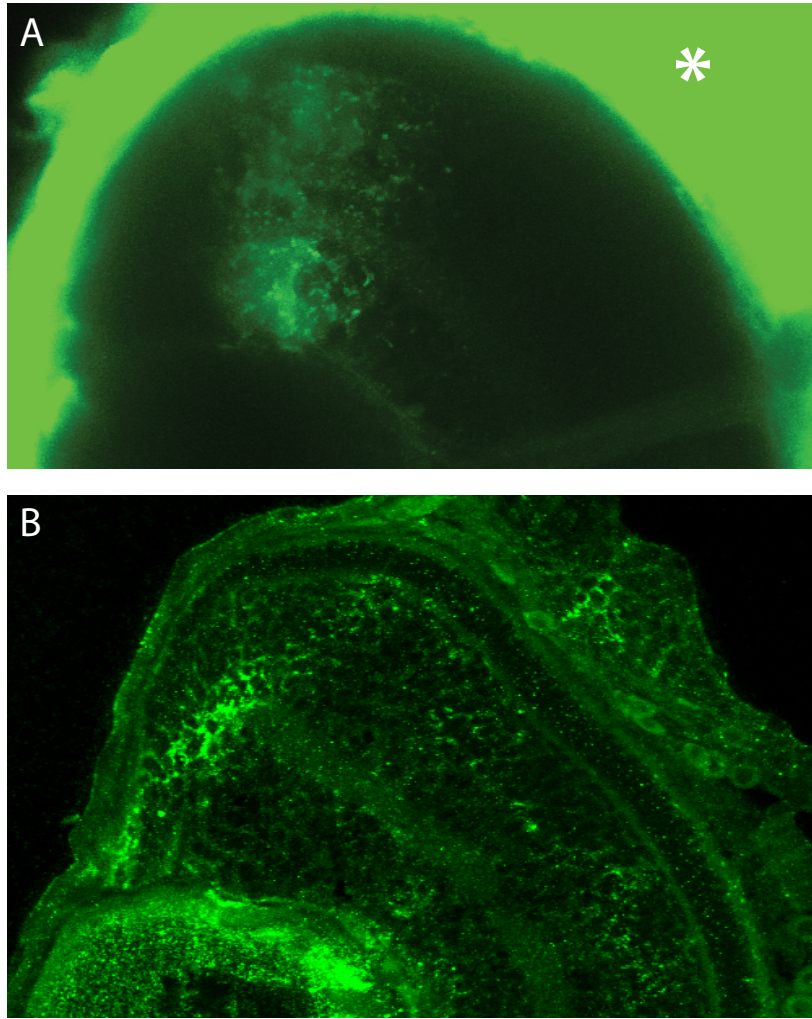
Fig.14 (A) In vivo ROS detection in the retina of wild-type embryos 72 hpf using the fluorescent probe (H2DCFDA). (B) labeling of the retina of wild-type embryos 72 hpf with anti-HNE antibody. In both the images views are the upper half of lateral views of the retina.

* autofluorescence due to the presence of high levels of ROS on the skin of the lived fishes. ROS and HNE are abundant in the CMZ of the retina.

All the experiments were repeated three times on groups of 20 embryos for each sample. Data shown are representative examples of each experiment.

For 4-HNE immunostaining cells were counterstained with DAPI.

6 Conclusions

The final aim of this project was to analyze the effects of (R)-9-HSA administration on the regulation of cellular processes as proliferation and differentiation during normal development.

9-hydroxistearic acid (9-HSA) is an endogenous lipid peroxidation by-product that acts as an HDAC1 inhibitor. Since its concentration decreases in tumors compared to normal tissue it has been tested on human tumor cell lines.

Its administration in colon cancer cells (HT29), at micromolar concentration, results in a significant inhibition of proliferation along with cell differentiation toward a more benign phenotype. In order to get this final point, these preliminary questions were addressed:

- At first, was investigated if 9-HSA was endogenously produced in zebrafish, as already observed in human cell lines.

The analysis of the total lipid extracts from zebrafish embryos 5 dpf reveals that 9-HSA is endogenously present at the concentration of 63 ng/ml.

The same analysis performed on total lipid extracts from zebrafish at early stages of development, day 0, reveals very low level of the acid, too low to be quantified in ESI-MS.

These data suggest a possible correlation between 9-HSA endogenous amount and zebrafish differentiation stages.

It should be interesting to investigate which are the pathways responsible for HDAC1 production, and when it starts to be produced.

 - It had to be verified the homology of the target of action of (R)-9-HSA with the one observed in human cell lines.

(R)-9-HSA acts in human cancer cell lines inhibiting HDAC1 enzymatic activity [28-33]. In order to verify this hypothesis all the experiments were performed together on (R)-9-HSA treated embryos and of add^{rw399} mutants.

The comparison between the phenotype resulting from the treatment with (R)-9-HSA and the one of add^{rw399} mutants suggest that the molecule maintains the characteristics of HDAC1 inhibitor also in vivo, in zebrafish. The effects of the molecule modeled the one of HDAC1 deletion, and maintain the specificity of action in a tissue dependent manner.

To verify the effect of the enzymatic activity of HDAC1 were analyzed the histone acetylation levels of histone H4 that are known from the literature to be increased after the treatment with 9-HSA in human tumor cell lines. The levels of histone acetylation were analyzed in embryos treated with the molecule at different time point with an immunostaining assay on zebrafish retina cryosections using an antibody for the hyperacetylated histone H4. Immunostaining analysis showed higher acetylation levels in (R)-9-HSA treated embryos compared to the control that were comparable with that of *add^{rw399}* mutants. This effect on HDAC1 activity was observed at 48 and 72 hours post injection and fertilization.

This analysis provides an important data on which is the mechanism of action of 9-HSA in zebrafish but should be confirmed with a quantitative analysis, using western blot technique. A limitation of western blot could be however the impossibility to evaluate the histone acetylation pattern in a tissue specific manner because the protein extract is obtained from the total embryo.

- After observing the inhibitory effect of (R)-9-HSA on HDAC1 enzymatic activity, it was investigated if the treatment with the molecule could reproduce the effect of HDAC1 deletion on cell proliferation and differentiation in zebrafish hindbrain and retina. In zebrafish retina and hindbrain, the phenotype that resulted from the treatment with (R)-9-HSA was similar to that already observed in zebrafish mutant for HDAC1 (add^{rw399} mutants).

The experiments reported in this thesis demonstrate that (R)-9-HSA inhibits proliferation in zebrafish hindbrain at 24 hpi (Fig.2), according with the role of HDAC1 in this tissue, where it is required for the neurogenesis in response to the hedgehog signaling.

The analysis of the effect on the retina, shows on the contrary a hyperproliferation after treatment with the molecule.

At 48 hpi a hyperproliferation is distinguishable in (R)-9-HSA treated retina and in add^{rw399} mutant retina, but the effect is not remarkable (Fig.3-4). The analysis of BrdU incorporation was used to examine the rate of proliferation that correlates with the number of BrdU-labeled cells. BrdU was incorporated within 12 hours at 48 hpi. The analysis of positive cells for BrdU shows that there is not a significantly increased in BrdU incorporation in (R)-9-HSA treated embryos compared to the control (Fig.4), suggesting that the percentage of cells undergoing the S phase within 12 hours is not significantly different from that in DMSO treated embryos. The analysis of cells in the S phase of the cell cycle in the retina was confirmed with a PCNA staining at the same time point, at 48 hpi. The amount of positive cells for PCNA in either (R)-9-HSA treated retina and add^{rw399} mutant retina was similar to the one observed in DMSO treated retina, with a slight hyperproliferation that is anyway not remarkable compared to the control, as at this time point the retina is normally highly proliferative.

At the same time point after treatment the possible pro-apoptotic effect of (R)-9-HSA, has been analyzed by TUNEL assay. By the analysis of the positive cells in retina sections it is possible to affirm that at 48 hpi the molecule doesn't cause apoptotic death (Fig.5).

The effect of (R)-9-HSA on cell proliferation in the retina is more evident at 72 hpi. The analysis of phospho histone H3 and PCNA expression at this

time point revealed that the ratio of the number of dividing cells to total number of cells in (R)-9-HSA treated retina and add^{rw399} mutant retina is significantly different from that in DMSO treated retina, suggesting that the percentage of cells undergoing the M phase is altered in the absence of HDAC1. Moreover the immunostaining shows that the hyperoproliferation induced by (R)-9-HSA is only localized in the CMZ and in the ONL of the zebrafish retina (Fig.6).

It is known from the literature that HDAC1 deletion results in the retina either in the failure of cells progenitors form cell cycle and in an inhibition of their differentiation. For this reason together with the analysis of the effects on cell proliferation it has been evaluated the effect of the (R)-9-HSA on cellular differentiation of retinal subtypes.

Zn5 is a marker of retinal ganglion cells, the labeling of 48 hpi DMSO treated retina, (R)-9-HSA treated retina and *add^{rw399}* mutant retina with zn5 antibody showed that there was no differentiation of retinal ganglion cells in the (R)-9-HSA treated retina and in the *add^{rw399}* mutant retina (Fig.8).

At 72 hpi the majority of the different retinal subtypes are normally already formed and detectable.

Parvalbumin (PVA) is a marker of amacrine cells. The analysis of its expression at 72 hpi revealed the complete absence of these cellular subtypes in *add^{rw399}* mutant and (R)-9-HSA treated retina. (Fig.9)

The specification of photoreceptors was investigated using an anti zpr1 antibody. The number of differentiated photoreceptors was strongly reduced in (R)-9-HSA treated retina, while they were completely absent in *add^{rw399}* mutant retina (Fig.9).

Finally was analyzed the presence of Muller cells using an antibody for glutamine synthetase. As already observed for the other retinal subtypes, Muller cells were not formed in *add^{rw399}* mutant retina and (R)-9-HSA

treated retina, while they were well visible in the control (Fig.9). These data suggest that the most of retinal cells in the (R)-9-HSA treated embryos and add^{rw399} mutant embryos fail to differentiate into neurons and glial cells.

To elucidate which are the events upstream the effects on cell proliferation and differentiation observed in the retina and the hindbrain, it <u>has been examined the effect of (R)-9-HSA on the expression of genes involved in the regulation of cell cycle and differentiation and in Wnt and Notch signaling pathways.</u>

The transcription analysis was performed using in situ hybridization technique and qRT-PCR, in order to have both qualitative and quantitative data.

The in situ hybridization assay showed a reduction in the expression of the pro-neural gene *ngn1* in the hindbrain after the treatment with (R)-9-HSA for 48 hours. Probably the downregulation of *ngn1* transcription is a consequence of the upregulation, in the same tissue, of the Notch target gene *her6* that acts directly repressing proneural genes expression (Fig.9) [109, 110, 107].

C-myc is a proto-oncogene involved, in zebrafish, in the regulation of cell proliferation and differentiation [72, 111].

In wild type retina, c-*myc* [112] was expressed in the most peripheral region of the CMZ where retinal stem cells are located. We found that its expression is highly affected in the retina of embryos (R)-9-HSA 48 hpi, where it persists in the CMZ but also spreads to the central retina and in the add^{rw399} mutant its transcript was detectable in almost all the retina suggesting a severe upregulation in the absence of HDAC1.

To elucidate the effect of (R)-9-HSA on cell proliferation it was examined the expression of two cell-cycle regulators: *cyclin D1* (*ccnd1*) [113] and *p27b* [73].

In various cell types the progression of the cell cycle is regulated by different combinations of cyclins and cyclin-dependent kinases (Cdks) [114]. However, three major types of Cdk inhibitor, Cip/Waf, Kip and Ink4 family proteins, are important for the exit from the cell cycle [114]. In the vertebrate retina, cyclin D1 promotes the entry into the S phase [115, 116], while the Kip family Cdk inhibitor, p27, plays a central role in the exit from the cell cycle by suppressing cyclin D1 functions [117, 118, 54].

Wnt and Notch are the cell-extrinsic factors of the cell cycle, which functions upstream of cyclin D1 and p27 [119, 120].

In (R)-9-HSA treated retina and *add*[rw399] mutant retina, *cyclin D1* and *p27b* expressions are up- and down- regulated, respectively (Fig.12).

Yamaguchi et all (2005) demonstrated that HDAC1 functions upstream of the interaction between *cyclinD1* and *p27*, their data suggest that HDAC1 antagonizes Wnt signaling to suppress the transcription of cyclinD1 in the zebrafish retina. Our data on *cyclinD1* and *p27b* expression confirmed the HDAC1 inhibition resulting from (R)-9-HSA treatment, suggesting that this effect could be mediated by a stimulation of Wnt signaling pathway.

Finally it was examined the expression of the differentiation marker *Islet1*. After the treatment with (R)-9-HSA and in the *add*[rw399] mutant retina Islet1 is still detectable in a delimited region of the central retina differently from the DMSO treated embryos where it spreads in the entire retina (Fig.13).

These data suggest that (R)-9-HSA affects cell proliferation in a tissue specific manner, stimulating proliferation in the retina, and inhibiting it in the hindbrain.

The observations on the retina suggest that the molecule acts by forcing the cells in reentering the cell cycle, causing and impairment in the consequent differentiation of the different retinal subtypes.

In situ hybridization is a powerful and versatile tool for the localization of specific mRNAs in cells or tissues, but doesn't provide quantitative information. For this reason qRT-PCR analysis were performed to validate the data obtained from the *in situ* for each gene.

The qRT-PCR results don't confirmed all the data from in situ hybridization assays. This would be a consequence of the tissue specific activity of (R)-9-HSA and HDAC1. In this work the analysis was focused for the most part on zebrafish retina and not on the entire embryo. Data resulting from qRT-PCR represent the quantification of gene expression in whole embryos, while for many of the analyzed genes we observed severe changes in transcription just in the retina. This could explain the difference in the results observed in the two experiments.

The retina area more interested by (R)-9-HSA effects on cell proliferation is the CMZ, the final part of this work has been focused on the study of the oxidative state of retinal stem cells located in the CMZ of zebrafish retina. Since (R)-9-HSA is an endogenous lipid peroxidation product, the results on cell proliferation suggest that the effect of the molecule on zebrafish retina could be correlated with the perturbation of the oxidative state of stem cells present in the CMZ.

Previous studies reported the impact of oxidative state balance in stem cells quiescence and proliferation. It has been shown that an increase in ROS, which are mostly produced from mitochondrial respiration, results in the loss of stem cells maintenance and quiescence. [27]

The endogenous production of ROS was analyzed in the retina of wild-type zebrafish embryos at 72 hpf using the radical sensor H_2DCFDA. The

analysis showed that the presence of ROS is localized is limited to the CMZ.

Subsequently, since (R)-9-HSA is an endogenous lipid peroxidation by-product, was examined the expression of one of the major lipid peroxidation products in zebrafish retina, the 4-Hydroxynonenal (HNE), at 72 hpf. HNE like H_2DCFDA is expressed specifically in the CMZ suggesting an involvement of stem cell oxidative state regulation in the mechanism of action of (R)-9-HSA in the zebrafish retina. The effect of the molecule on retinal stem cell niche could results in the loss of their quiescence with the hyperproliferation observed at 72 hpi. The hyperproliferative stem cells are therefore unable to self-renewal and to add new cells to the retina in concentric rings for as long as the eye is growing as they normally do [121].

This hypothesis will have to be proved with further experiments but promises to be an exciting area in the future.

7 Bibliography

1. Finkel T, Holbrook NJ. (2000) Oxidants, oxidative stress and the biology of ageing. Nature 408(6809):239-47.

2. Bayani Uttara, Ajay V. Singh, Paolo Zamboni and R.T Mahajan (2009) Oxidative Stress and Neurodegenerative Diseases: A Review of Upstream and Downstream Antioxidant Therapeutic Options. Curr Neuropharmacol 7(1): 65–74.

3. Chiara Gorrini, Isaac S. Harris and Tak W. Mak (2013) Modulation of oxidative stress as an anticancer strategy. Nature Reviews Drug Discovery 12, 931-947.

4. L. Bigarella, Raymond Liang, Saghi Ghaffari. (2014) Stem cells and the impact of ROS signalling. Development 141, 4206-4218

5. Toledano MB, Leonard WJ. (1991) Modulation of transcription factor NF-kappa B binding activity by oxidation-reduction in vitro. Proc Natl Acad Sci U S A. 88(10):4328-32.

6. Salmeen A, Andersen JN, Myers MP, Meng TC, Hinks JA, Tonks NK, Barford D. (2003) Redox regulation of protein tyrosine phosphatase 1B involves a sulphenyl-amide intermediate. Nature. 423(6941):769-73.

7. Ray PD, Huang BW, Tsuji Y. (2012) Reactive oxygen species (ROS) homeostasis and redox regulation in cellular signaling. Cell Signal 24(5):981-90

8. Jira W, Spiteller G, Carson W, Schramm. (1998) Strong increase in hydroxy fatty acids derived from linoic acid in human lo density lipoproteins of atherosclerotic patients. Chem Phys Lipids 91(1):1-11

9. Barry Halliwell and Susanna Chirico (1993) Lipid peroxidation: its mechanism, measurement, and significance. Am J Clin Nutr May vol. 57 no. 5 715S-724S.

10. Oberley TD. (1997) Antioxidatn enzyme levels in cancer. Histology and Histopathology 12(2):525-535

11. M. Parola, G. Bellomo, G. Robino, G. Barrera, and M. U. Dianzani. (1999) 4-Hydroxynonenal as a biological signal: molecular basis and pathophysiological implications. Antioxidants & Redox Signaling, vol. 1, no. 3, pp. 255–284.

12. Boonstra J, Post JA. (2004) Molecular events associated with reactive oxygen species and cell cycle progression in mammalian cells. Gene 337:1-13.

13. Chow E, Thirlwell C, Macrae F, Lipton L. (2004) Colorectal cancer and inherited mutations in base excision repair. Lancet Oncology 5(19):600-606.

14. Bae YS, Sung JY, Kim OS, et al. Platelet-derived growth factor-induced H_2O_2 production requires the activation of phosphatidylinositol 3-kinase. *Journal of Biological Chemistry*. 2000;275(14):10527–10531.

15. Liou GY, Storz P. Reactive oxygen species in cancer. *Free Radical Research*. 2010;44(5):479–496.

16. Balkwill F. Tumour necrosis factor and cancer. *Nature Reviews Cancer*. 2009;9(5):361–371.

17. C. Mart`ınez Munoz, L. A. van Meeteren, J. A. Post, A. J. ˜ Verkleij, C. T. Verrips, and J. Boonstra. (2002) Hydrogen peroxide inhibits cell cycle progression by inhibition of the spreading of mitotic CHO cells. Free Radical Biology and Medicine, vol. 33, no. 8, pp. 1061–1072.

18. C. E. Helt, R. C. Rancourt, R. J. Staversky, and M. A. O'Reilly. (2001) p53-dependent induction of p21Cip1/WAF1/Sdi1 protects

against oxygen-induced toxicity. Toxicological Sciences, vol. 63, no. 2, pp. 214–222.

19. P. Storz. (2005) Reactive oxygen species in tumor progression. Frontiers in Bioscience, vol. 10, no. 2, pp. 1881–1896.

20. Takubo K, Nagamatsu G, Kobayashi CI, Nakamura-Ishizu A, Kobayashi H, Ikeda E, Goda N, Rahimi Y, Johnson RS, Soga T, Hirao A, Suematsu M,Suda T. (2013) Regulation of glycolysis by Pdk functions as a metabolic checkpoint for cell cycle quiescence in hematopoietic stem cells. Cell Stem Cell. 12(1):49-61.

21. Yan-Lin Guo, Samujjwal Chakraborty, Suja S. Rajan, Rouxing Wang, and Faqing Huang (2010) Effects of Oxidative Stress on Mouse Embryonic Stem Cell Proliferation, Apoptosis, Senescence, and Self-Renewal. Stem Cells Dev. 19(9): 1321–1331.

22. Ward, P.S., J.R. Cross, C. Lu, O. Weigert, O. Abel-Wahab, R.L. Levine, D.M. Weinstock,K.A. Sharp, C.B. Thompson (2012). Identification of additional IDH mutations associated with oncometabolite R(-)-2-hydroxyglutarate production. Oncogene. 31:2491–2498.

23. Folmes CD, Dzeja PP, Nelson TJ, Terzic A. (2012) Metabolic plasticity in stem cell homeostasis and differentiation. Cell Stem Cell. 11(5):596-606

24. Ng Shyh-Chang, Yuxiang Zheng, Jason W Locasale, and Lewis C Cantley .(2011) Human pluripotent stem cells decouple respiration from energy production. EMBO J. 30(24): 4851–4852.

25. Berasain C, Castillo J, Perugorria MJ, Latasa MU, Prieto J, Avila MA. (2009) Inflammation and liver cancer: new molecular links. *Annals of the New York Academy of Sciences*. 1155:206–221.

26. Norddahl, G. L., Pronk, C. J., Wahlestedt, M., Sten, G., Nygren, J. M., Ugale, A., Sigvardsson, M. and Bryder, D.(2011). Accumulating mitochondrial DNA mutations drive premature hematopoietic aging phenotypes distinct from physiological stem cell aging. Cell Stem Cell **8**, 499-510.doi:10.1016/j.stem.2011.03.009

27.Kunisaki, Y., Bruns, I., Scheiermann, C., Ahmed, J., Pinho, S., Zhang,.,Mizoguchi, T.,Wei, Q., Lucas, D., Ito, K. et al. (2013). Arteriolar niches maintain haematopoietic stem cell quiescence. Nature **502**, 637-643.doi:10.1038/nature12612

28.G. Cavalli, E. Casali, A. Spisni, L. Masotti, Identification of the peroxidation product hydroxystearic acid in Lewis lung carcinoma cells, Biochem. Biophys. Res. Commun. 3 (1991) 1260–1265.

29.C. Bertucci, M. Hudaib, C. Boga, N. Calonghi, C. Cappadone, L. Masotti, Gas chromatography/mass spectrometric assay of endogenous cellular lipid peroxidation products: quantitative anal- ysis of 9- and 10-hydroxystearic acids, Rapid Commun. Mass Spectrom. 16 (2002) 859–864.

30.L. Masotti, E. Casali, N. Gesmundo, Influence of hydroxystearic acid on in vitro cell proliferation, Mol. Aspects Med. 14 (1993) 209–215.

31. N. Gesmundo, E. Casali, G. Farruggia, A. Spisni, L. Masotti, In vitro effects of hydroxystearic acid on the proliferation of HT29 and I407 cells, Biochem. Mol. Biol. Int. 33 (1994) 704–711.

32.Parolin C, Calonghi N, Presta E, Boga C, Caruana P, Naldi M, Andrisano V, Masotti L, Sartor G. (2012) Mechanism and stereoselectivity of HDAC1 inhibition by (R)-9-hydroxystearic acid in colon cancer. Biochim Biophys Acta.1821(10):1334-40

33. Calonghi N, Cappadone C, Pagnotta E, Boga C, Bertucci C, Fiori J, Tasco G, Casadio R, Masotti L. (2005) Histone deacetylase 1: a

target of 9-hydroxystearic acid in the inhibition of cell growth in human colon cancer, calonghi. J Lipid Res. 46(8):1596-60

34. Michael Haberland, Rusty L. Montgomery, and Eric N. Olson (2009) The many roles of histone deacetylases in development and physiology: implications for disease and therapy. Nat Rev Genet (1): 32-42

35. Annemieke J. M. De Ruijter, Albert H. Van Gennip, Huib N. Caron, Stephan Kemp and Andre B. P. Van Kuilenburg (2003) Histone deacetylases (HDACs): characterization of the classical HDAC family, Biochem. J. 370, 737–749

36. Bertos NR, Wang AH, Yang XJ (2001) Class II histone deacetylases: structure, function, and regulation. Biochem Cell Biol. 79(3):243-52.

37. K. Halkidou, L. Gaughan, S. Cook, H.Y. Leung, D.E. Neal, C.N. Robson, K. Halkidou (2004) Upregulation and nuclear recruitment of HDAC1 in hormone refractory prostate cancer. Prostate 59, pp. 177–189

38. A.J. Wilson, D.S. Byun, N. Popova, L.B. Murray, K. L'Italien, Y. Sowa, D. Arango, A. Velcich, L.H. Augenlicht, J.M. Mariadason (2006) Histone deacetylase 3 (HDAC3) and other class I HDACs regulate colon cell maturation and p21 expression and are deregulated in human colon cancer. J. Biol. Chem. 281, pp. 13548–13558

39. Z. Zhang, et al. (2005) Quantitation of HDAC1 mRNA expression in invasive carcinoma of the breast. Breast Cancer Res. Treat. 94, pp. 11–16

40. C.Y. Gui, L. Ngo, W.S. Xu, V.M. Richon, P.A. Marks. (2004) Histone deacetylase (HDAC) inhibitor activation of p21WAF1

involves changes in promoter-associated proteins, including HDAC1. Proc. Natl. Acad. Sci. USA, 101 pp. 1241–1246

41. L.J. Juan, W.J. Shia, M.H. Chen, W.M. Yang, E. Seto, Y.S. Lin, C.W. Wu (2000). Histone deacetylases specifically down-regulate p53-dependent gene activation. J. Biol. Chem., 275 pp. 20436–20443

42. Vincent T. Cunliffe (2004). Histone deacetylase 1 is required to repress Notch target gene expression during zebrafish neurogenesis and to maintain the production of motoneurones in response to hedgehog signalling. Development 131, 2983-2995

43. Saverio Minucci and Pier Giuseppe Pelicci (2006). Histone deacetylase inhibitors and the promise of epigenetic (and more) treatments for cancer. *Nature Reviews Cancer* **6**, 38-51

44. Mario Federico and Luigi Bagella (2011) Histone Deacetylase Inhibitors in the Treatment of Hematological Malignancies and Solid Tumors. Journal of Biomedicine and Biotechnology Volume 2011, Article ID 475641,

45. Lane AA, Chabner BA (2009) Histone Deacetylase Inhibitors in Cancer Therapy. J Clin Oncol. 27(32):5459-68

46. Dokmanovic M, Clarke C, Marks PA. (2007) Histone deacetylase inhibitors: overview and perspectives. Mol Cancer Res. 5(10):981-9.

47. Walker and Streisinger. (1983) Induction of Mutations by gamma-Rays in Pregonial Germ Cells of Zebrafish Embryos. Genetics.103(1):125-36.

48. Pillai R, Coverdale LE, Dubey G, Martin CC (2004) Histone deacetylase 1 (HDAC-1) required for the normal formation of craniofacial cartilage and pectoral fins of the zebrafish. Dev Dyn 231(3):647-54.

49. Harrison MR, Georgiou AS, Spaink HP, Cunliffe VT. (2011) The epigenetic regulator Histone Deacetylase 1 promotes transcription of a core neurogenic programme in zebrafish embryos. BMC Genomics. 12:24. doi: 10.1186/1471-2164-12-24.

50. Noël ES[1], Casal-Sueiro A, Busch-Nentwich E, Verkade H, Dong PD, Stemple DL, Ober EA. (2008) Organ-specific requirements for Hdac1 in liver and pancreas formation. Dev Biol. 322(2):237-50. doi: 10.1016/j.ydbio.2008.06.040.

51. Muhammad Farooq, K.N. Sulochana, Xiufang Pan, Jiawei To, Donglai Sheng, Zhiyuan Gong, Ruowen Ge (2008) Histone deacetylase 3 (*hdac3*) is specifically required for liver development in zebrafish. Dev Biol vol 317, Issue 1,336–353.

52. Vincent T. Cunliffe (2004). Histone deacetylase 1 is required to repress Notch target gene expression during zebrafish neurogenesis and to maintain the production of motoneurones in response to hedgehog signalling. Development 131, 2983-2995.

53. Stadler JA, Shkumatava A, Norton WH, Rau MJ, Geisler R, Fischer S, Neumann CJ. (2005) Histone deacetylase 1 is required for cell cycle exit and differentiation in the zebrafish retina. Dev Dyn. 233(3):883-9.

54. Yamaguchi M, Tonou-Fujimori N, Komori A, Maeda R, Nojima Y, Li H, Okamoto H, Masai I. (2005) Histone deacetylase 1 regulates retinal neurogenesis in zebrafish by suppressing Wnt and Notch signaling pathways. Development. 132(13):3027-43

55. Dooley K, Zon LI. (2000) Zebrafish: a model system for the study of human disease. Curr Opin Genet Dev. 10(3):252-6.

56. Chaoyong Ma, Chuenlei Parng, Wen Lin Seng, Chaojie Zhang, Chaterine Willet and Patricia McGrath (2003). Zebrafish - an in vivo model for drug screening.

57. Froese, Rainer and Pauly, Daniel, eds. (2007). "*Danio rerio*" inFishBase

58. Spence, Rowena; Gerlach, Gabriele; Lawrence, Christian; Smith, Carl (2007). The behaviour and ecology of the zebrafish, Danio rerio. *Biological Reviews* **83** (1): 13–34.

59. Brian A. Link PhD, Sean G. Megason PhD (2008) Zebrafish as a Model for Development. Sourcebook of Models for Biomedical Research pp 103-112.

60. Dahm, Ralf (2006). The Zebrafish Exposed. *American Scientist* 94(5): 446–53.

61. Cau, E. and Wilson, S. W. (2002). Ash1a and neurogenin function downstream of Floating head to regulate epiphysial neurogenesis. *Development* 130,2455 -2466.

62. Feitsma H, Cuppen E. (2008). Zebrafish as a cancer model. Mol Cancer Res. 6(5):685-94.

63. Amatruda JF, Shepard JL, Stern HM, Zon LI. (2002) Zebrafish as a cancer model system. Cancer Cell. 1(3):229-31.

64. Mione MC, Trede NS. (2010) The zebrafish as a model for cancer. Dis Model Mech. 3(9-10):517-23.

65. Jijun Hao, Charles H. Williams, Morgan E. Webb, and Charles C. Hong (2010). Large Scale Zebrafish-Based *In vivo* Small Molecule Screen. J Vis Exp. (46): 2243.

66. Kimmel CB, Ballard WW, Kimmel SR, Ullmann B, Schilling TF. (1995) Stages of embryonic development of the zebrafish. Dev Dyn. 203(3):253-310.

67. Cornell, R. A. and Eisen, J. S. (2002). Delta/Notch signaling promotes formation of zebrafish neural crest by repressing Neurogenin 1 function. *Development* 129,2639 -2648.

68. Andermann, P., Ungos, J. and Raible, D. W. (2002). Neurogenin 1 defines zebrafish cranial sensory ganglia precursors. *Dev. Biol.* 251, 45-58.

69. Cau, E., Gradwohl, G., Casarosa, S., Kageyama, R. and Guillemot, F. (2000). *Hes*genes regulate sequential stages of neurogenesis in the olfactory epithelium. *Development*127,2323 -2332.

70. Takke, C., Dornseifer, P., von Weiszacker, E. and Campos-Ortega, J. (1999). *Her4*, a zebrafish homologue of the *Drosophila* neurogenic gene *E(spl)*, is a target of notch signalling. *Development* 126,1811 - 1821

71. Neumann, C. J. and Nuesslein-Volhard, C. (2000). Patterning of the zebrafish retina by a wave of *Sonic Hedgehog* activity. *Science* 289,2137 -2139.

72. Masai, I., Stemple, D. L., Okamoto, H. and Wilson, S. W. (2000). Midline signals regulate retinal neurogenesis in zebrafish. *Neuron* 27,251 -263.

73. Masai, I., Yamaguchi, M., Tonou-Fujimori, N., Komori, A. and Okamoto, H. (2005). Hedgehog-PKA pathway regulates two distinct steps of the differentiation of retinal ganglion cells: the cell-cycle exit of retinoblasts and their neuronal maturation. *Development*132,1539 -1553.

74. Malicki J[1], Neuhauss SC, Schier AF, Solnica-Krezel L, Stemple DL, Stainier DY, Abdelilah S, Zwartkruis F, Rangini Z, Driever W. (1996) Mutations affecting development of the zebrafish retina. Development. 123:263-73.

75. Branchek and Bremiller. (1984) The development of photoreceptors in the zebrafish, *Brachydanio rerio*. Journal of Comparative Neurology. Volume 224, Issue 1, pages 107–115

76. Menke AL, Spitsbergen JM, Wolterbeek AP, Woutersen RA. (2011) Normal anatomy and histology of the adult zebrafish. Toxicol Pathol. 39(5):759-75.

77. Tsujikawa M[1], Malicki J. (2004) Genetics of photoreceptor development and function in zebrafish. Int J Dev Biol. 48(8-9):925-34.

78. Mangel SC, Dowling JE. (1987) The interplexiform-horizontal cell system of the fish retina: effects of dopamine, light stimulation and time in the dark. Proc R Soc Lond B Biol Sci. 1987 Jun 22;231(1262):91-121.

79. Li YN, Tsujimura T, Kawamura S, Dowling JE. (2012) Bipolar cell-photoreceptor connectivity in the zebrafish (Danio rerio) retina. J Comp Neurol. 520(16):3786-802

80. Godinho L, Mumm JS, Williams PR, Schroeter EH, Koerber A, Park SW, Leach SD, Wong RO. (2005) Targeting of amacrine cell neurites to appropriate synaptic laminae in the developing zebrafish retina. Development. 132(22):5069-79.

81. Dowling JE. (2012). The retina: an approachable part of the brain, revised ed. Cambridge, MA: Belknap Press of Harvard University Press.

82. Umino O, Dowling JE. (1991) Dopamine release from interplexiform cells in the retina: effects of GnRH, FMRFamide, bicuculline, and enkephalin on horizontal cell activity. J Neurosci. 11(10):3034-46.

83. Ning Tian. Development of Retinal Ganglion Cell Dendritic Structure and Synaptic Connections by Ning Tian. Webvision

84. Amsterdam A, Nissen RM, Sun Z, Swindell EC, Farrington S, Hopkins N 8 (2004) Identification of 315 genes essential for early zebrafish development. Proc Natl Acad Sci U S A. 101(35):12792-7.

85. Burns CE, Galloway JL, Smith AC, Keefe MD, Cashman TJ, Paik EJ, Mayhall EA, Amsterdam AH, Zon LI. (2009) A genetic screen in zebrafish defines a hierarchical network of pathways required for hematopoietic stem cell emergence. Blood.113(23):5776-82. doi: 10.1182/blood-2008-12-193607.

86. Nambiar RM, Ignatius MS, Henion PD. (2007) Zebrafish colgate/hdac1 functions in the non-canonical Wnt pathway during axial extension and in Wnt-independent branchiomotor neuron migration. Mech Dev. 124(9-10):682-98.

87. Wehman AM, Staub W, Meyers JR, Raymond PA, Baier H. (2005) Genetic dissection of the zebrafish retinal stem-cell compartment. Dev Biol. 281(1):53-65.

88. Raymond PA, Rivlin PK. (1987) Germinal cells in the goldfish retina that produce rod photoreceptors. Dev Biol. 122(1):120-38.

89. Pamela A Raymond, Linda K Barthel, Rebecca L Bernardos, and John J Perkowski (2006) Molecular characterization of retinal stem cells and their niches in adult zebrafish. BMC Dev Biol. 6: 36

90. Bernardos RL, Lentz SI, Wolfe MS, Raymond PA. (2005) Notch-Delta signaling is required for spatial patterning and Müller glia differentiation in the zebrafish retina. Dev Biol. 278(2):381-95.

91. CS Ho, CWK Lam,[*] MHM Chan, RCK Cheung, LK Law, LCW Lit, KF Ng, MWM Suen, and HL Tai (2003). Electrospray Ionisation

Mass Spectrometry: Principles and Clinical Applications. Clin Biochem Rev. 24(1): 3–12.

92. Wojciech Strzalka and Alicja Ziemienowicz (2010) Proliferating cell nuclear antigen (PCNA): a key factor in DNA replication and cell cycle regulation. Annals of Botany Page 1 of 14.

93. Tan, C. K., Castillo, C, SO, A. G. and Downey, K. M. (1986). An auxiliary protein for DNA polymerase-delta from fetal calf thymus. J. biol. Chem. 261, 12310-12 316.

94. BRAVO, R., FRANK, R., BLUNDELL, P A. AND MACDONALD-BRAVO, H. (1987) Cyclin/PCNA is the auxiliary protein of DNA polymerasedelta. Nature 328, 515-517.

95. PREUCH, G., KOSTURA, M., MARSHAK, K. D. R., MATHEWS, M. B. AND SrnxMAN, B. (1987). The cell-cycle regulated proliferating cell nuclear antigen is required for SV40 DNA replication in vitro. Nature 328, 471-475.

96. Maga G, Hubscher U. (2003) Proliferating cell nuclear antigen (PCNA): a dancer with many partners. J Cell Sci. 116(Pt 15):3051-60.

97. G. Morstyn, T. Kinsella, C.S. Shan, J. Whang-Peng, A. Russo, J.B. Mitchell (1985) In vivo incorporation of bromodeoxyuridine into proliferating cells in the marrow and its effects on granulocyte-macrophage progenitor cells. Exp. Hematol., 13 pp. 289–294.

98. Kuebbing D, Werner R. (1975) A model for compartmentation of de novo and salvage thymidine nucleotide pools in mammalian cells. Proc Natl Acad Sci U S A. 72(9):3333–3336.

99. Wlkramaslnghe, S.N. (1981). The deoxyuridine suppression test: a review of its clinical and research applications. Clin Lab Haemat 3, 1-18.

100.Zupanc, G. K. H. and Horschke, I. (1996). Salvage pathway of pyrimidine synthesis: divergence of substrate specificity in two related species of teleostean fish. Comp. Biochem. Physiol. 114B, 269–274.

101. Kyrylkova K, Kyryachenko S, Leid M, Kioussi C. (2012) Detection of apoptosis by TUNEL assay. Kyrylkova K, Kyryachenko S, Leid M, Kioussi C. Methods Mol Biol. 2012;887:41-7.

102.Cathcart, R., Schwiers, E. & Ames, B.N. (1983). Detection of picomole levels of hydroperoxides using a fluorescent dichlorofluorescein assay. *Anal Biochem* **134**, 111-6.

103.Esterbauer H, Schaur RJ, Zollner H. (1991) Chemistry and biochemistry of 4-hydroxynonenal, malonaldehyde and related aldehydes. Free Radic Biol Med. 11:81–128.

104.Schneider C, Tallman KA, Porter NA, Brash AR. (2001) Two distinct pathways of formation of 4-hydroxynonenal. Mechanisms of nonenzymatic transformation of the 9- and 13-hydroperoxides of linoleic acid to 4-hydroxyalkenals. J Biol Chem. 276(24):20831-8.

105.Carini M, Aldini G, Facino RM. (2004) Mass spectrometry for detection of 4-hydroxy-trans-2-nonenal (HNE) adducts with peptides and proteins. Mass Spectrom Rev. 23:281–305.

106.Blader P, Fischer N, Gradwohl G, Guillemot F, Strähle U. (1997) The activity of neurogenin1 is controlled by local cues in the zebrafish embryo. Development. 124(22):4557-69.

107. A, Henrique D, Wilkinson DG. (2001) The zebrafish Hairy/Enhancer-of-split-related gene her6 is segmentally expressed during the early development of hindbrain and somites Mech Dev. 100(2):317-21.

108.Stenkamp DL. (2007) Neurogenesis in the fish retina. Int Rev Cytol. 259:173-224.

109. Ishibashi, M., Moriyoshi, K, Sasai, Y., Shiota, K., Nakanishi, S. and Kageyama, R.(1994). Persistent expression of helix-loop-helix factor HES-1 prevents mammalian neural differentiation in the central nervous system. *EMBO J.* 13,1799 -1805.

110. Ishibashi, M., Ang, S.-L., Shiota, K., Nakanishi, S., Kageyama, R. and Guillemot, F.(1995). Targeted disruption of mammalian *hairy* and *Enhancer of split* homolog-1 (*HES-1*) leads to up-regulation of neural helix-loop-helix factors, premature neurogenesis and severe neural tube defects. *Genes Dev.* 9,3136 - 3148.

111. Pelengaris S A and Khan M (2003) 'The many faces of c-Myc', *Archives Of Biochemistry And Biophysics,* **416** 129 - 136 (0003-9861)

112. Schreiber-Agus, N., Horner, J., Torres, R., Chiu, F.C., and DePinho, R.A. (1993) Zebrafish myc family and max genes: differential expression and oncogenic activity throughout vertebrate evolution. Mol. Cell. Biol. 13(5):2765-2775.

113. Yarden, A., Salomon, D., and Geiger, B. (1995) Zebrafish cyclin D1 is differentially expressed during early embryogenesis. Biochim. Biophys. Acta Gene Struct. Exp. 27:257-260.

114. Galderisi U, Jori FP, Giordano A. (2003) Cell cycle regulation and neural differentiation. Oncogene 22: 5208–5219.

115. V Fantl, G Stamp, A Andrews, I Rosewell, and C Dickson (1995) Mice lacking cyclin D1 are small and show defects in eye and mammary gland development. Genes & Dev. 9: 2364-2372.

116. Sicinski P, Donaher JL, Parker SB, Li T, Fazeli A, Gardner H, Haslam SZ, Bronson RT, Elledge SJ & Weinberg RA. (1995) *Cell* 82: 621−630.

117. Nakayama K, Ishida N, Shirane M, Inomata A, Inoue T, Shishido N, Horii I, Loh DY & Nakayama K. (1996) Mice Lacking p27^{Kip1} Display Increased Body Size, Multiple Organ Hyperplasia, Retinal Dysplasia, and Pituitary Tumors. *Cell* 85: 707−720.

118. Geng Y, Yu Q, Sicinska E, Das M, Bronson RT, Sicinski P. (2001) Deletion of the p27Kip1 gene restores normal development in cyclin D1-deficient mice. Proc Natl Acad Sci U S A. 98(1):194-9.

119. Kubo, F., Takeichi, M. and Nakagawa, S. (2003). Wnt2b controls retinal cell differentiation at the ciliary marginal zone. Development 130, 587-598.

120. Ohnuma, S., Hopper, S., Wang, K. C., Philpott, A. and Harris, W. A. (2002). Co-ordinating retinal histogenesis: early cell cycle exit enhances early cell fate determination in the Xenopus retina. Development 129, 2435- 2446.

121. Ann M. Wehman, Wendy Staub, Jason R. Meyers, Pamela A. Raymond, Herwig Baier (2005) Genetic dissection of the zebrafish retinal stem-cell compartment. Dev Biol Volume 281, Issue 1, Pages 53–65.

122. Neda Mimica-Dukić, Nataša Simin, Emilija Svirčev, Dejan Orčić, Ivana Beara, Marija Lesjak and Biljana Božin. The Effect of Plant Secondary Metabolites on Lipid Peroxidation and Eicosanoid Pathway.

123. Dunyaporn Trachootham, Jerome Alexandre & Peng Huang. (2009) Targeting cancer cells by ROS-mediated mechanisms: a radical therapeutic approach? *Nature Reviews Drug Discovery* **8**, 579-591.

124. Ken Garber (2004) Purchase of Aton spotlights HDAC inhibitors. *Nature Biotechnology* 22, 364 – 365.